MICROBIOLOGICAL REVIEWS, Sept. 1984, p. 222–271
0146-0749/84/030222-50$02.00/0

Vol. 48, No. 3

The Respiratory Chains of *Escherichia coli*

W. JOHN INGLEDEW[1] AND ROBERT K. POOLE[2]*

Department of Biochemistry and Microbiology, University of St. Andrews, St. Andrews KY16 9AL, Scotland,[1] and Department of Microbiology, Queen Elizabeth College (University of London), London W8 7AH, England[2]

* Corresponding author.

INTRODUCTION

Ecological Considerations

Escherichia coli was long considered to be a dominant organism of the human large intestine. However, the development of rigorously anaerobic techniques by Hungate and others led to the discovery of large numbers of obligate anaerobes in feces and so, apart from its occasional pathogenicity, the ecological significance of *E. coli* has received less attention (436). In numerical terms, its population [between 10^5 and 10^8 cells g of feces^{-1}] is only a small proportion of a total fecal bacterial population in excess of 10^{11} g^{-1} (319). However, even ignoring the pathogenic strains, which attach to the wall of the small intestine, the population has a considerable effect upon humans from shortly after birth, when *E. coli* populations become established, to death.

As one of the major groups of facultative anaerobes, it is responsible in part for maintaining the conditions that allow the strict anaerobes to thrive. These anaerobes themselves partially displace the newly established *E. coli* from the gut in the early weeks of life. Like all indigenous bacteria of the gut, *E. coli* must be able to grow anaerobically. However, the ability to utilize oxygen as terminal electron acceptor may afford ecological advantages, for example, close to epithelial cells where oxygen may pass from the blood through the epithelium to the microbial populations attached to it (for references, see reference 436). The avidity with which *E. coli* consumes oxygen is well known and, indeed, has been exploited in the laboratory, where, before inoculation with, say, methane bacteria, final traces of oxygen in a culture tube may be removed by *E. coli* (460). In addition to the advantages accruing to the host and other gut bacteria from the facultative nature of *E. coli*, it (and only a few other bacterial species) is responsible for synthesizing vitamin K (menaquinone), a component of the respiratory chain and a precursor of prothrombin in the liver of the host (71).

The persistence of *E. coli* in the gut must reflect the efficiency with which the bacterium exploits the opportunities offered by this environmental niche. Koch (280) has argued that *E. coli* is extremely well adapted to its environment, being able to survive on a relatively limited number of low-molecular-weight compounds, available only transiently and at low concentration. Success in this scavenging role is assured by powerful active transport systems (281, 282) which can be energized by oxidoreduction reactions, using a wide variety of electron donors and acceptors.

Specific information on the substrates and oxidants used by *E. coli* in its natural environment (where the mean generation time is about 12 h [49]) is scanty, but it is certain that conditions used in laboratory culture seldom approximate those in the gut. Organic materials enter the colon in the form of mucus, desquamated cells, enzyme secretions of the upper digestive tract, and incompletely digested food residues. Much of the carbohydrate, fat, and protein has been previously absorbed (104); in adults, especially, there is very little free carbohydrate. The sources of nitrogen for intestinal *E. coli* are also a subject for conjecture. The species has no exoproteolytic activity and presumably relies on the activities of other members of the microbial consortium for its nitrogen sources. Thus, *E. coli* populations are limited in part by nutritional competition with other microbes. They are also limited by the presence of toxic substances, e.g., fatty acids and H_2S, produced by neighboring anaerobes (436). *E. coli* and other "enteric bacteria are forced by their environment to grow slowly much of the time" (280). During rapid growth in laboratory conditions on a single substrate such as succinate (which is unlikely to be present at high concentrations in the gut), it is not surprising that the kinetic limitation on even faster growth is imposed by the capacity of the respiratory chain to transport electrons to excess oxygen (14, 52).

Several of the characteristics used by microbiologists in identifying *E. coli* reflect features of its respiratory metabolism (89). Thus, the organism is "cyanide sensitive" in that it fails to grow in the presence of ≈1 mM KCN (339), although the composition of the test medium affects the growth response (396). *E. coli* is also "oxidase negative." This test measures the ability of an organism to catalyze the oxidation of di- or tetramethyl-*p*-phenylenediamine plus α-naphthol to indophenol blue. A positive reaction within ≈30 s generally reflects the presence of a membrane-bound high-potential cytochrome *c* linked to an active cytochrome oxidase (253) and is frequently also indicative of the presence of "energy coupling site 3" (238). Jones (237) has suggested that the lack of cytochrome *c* and "site 3" reflects the relative abundance of energy and reducing power in those environments where the oxidase-negative species (e.g., *Enterobacteriaceae*, many pathogens, and some *Bacillus* spp.) are found.

Scope of the Review

This review deals with the diverse respiratory electron transport chains found in *E. coli* growing in laboratory culture. Since this field was last reviewed (42, 43, 198), there have been major developments in understanding the structure, function, membrane organization, and molecular biology of the components of these respiratory chains. It is the purpose of this review to update earlier accounts and to deal in more detail with topics previously neglected. As such, it can be neither comprehensive nor exhaustive, but we hope to illustrate the thrust of current work and draw attention to the approaches being used. Notable omissions are studies of the biosynthesis of certain components, especially quinones and nitrate reductase, the details of coupling of respiration to solute transport, and the proton-translocating ATPase; for the last, the reader is referred to reference 116. The literature survey was completed in September 1983, although we were fortunate in obtaining preprints of then-unpublished work from colleagues.

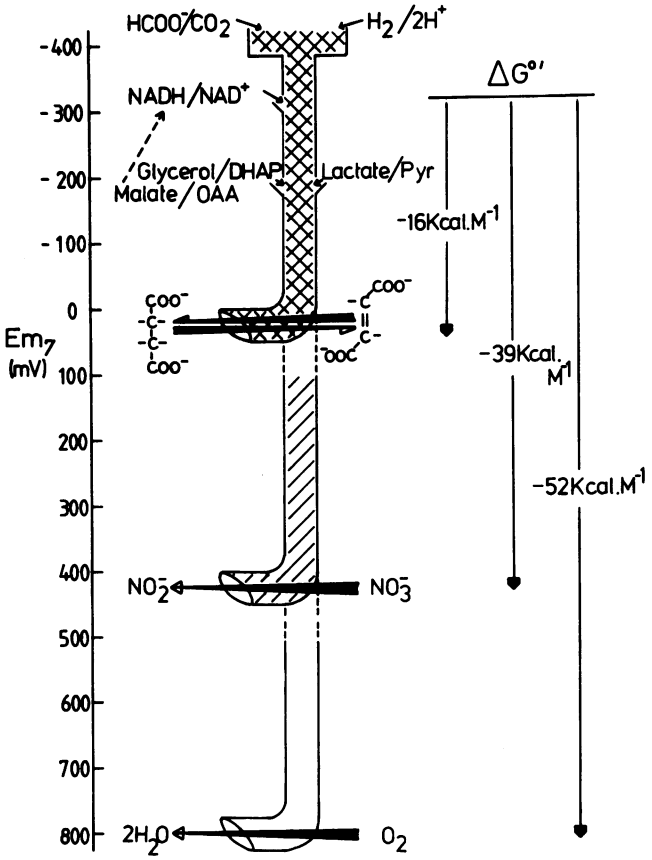

FIG. 1. Thermodynamic profile of *E. coli* respiratory pathways, illustrating the three principal respiratory chains of *E. coli*, fumarate, nitrate, and oxygen based. Major catabolic dehydrogenases, both primary and NAD^+ linked, are also illustrated. The midpoint potentials (Em_7) of the various couples (left) and the standard Gibbs free energies ($\Delta G^{0'}$) for the oxidation of NADH by each of the three oxidants (right) are shown. DHAP, Dihydroxy-acetone phosphate, OAA, oxalacetic acid.

OVERVIEW OF THE RESPIRATORY CHAIN PHENOTYPES

Major changes in cellular protein composition accompany the transition from aerobiosis to anaerobiosis by *E. coli* (458, 459). With respect to respiratory pathways, the most readily observed changes are those resulting in modified cytochrome content dependent on the presence of oxygen or the alternative respiratory chain oxidants fumarate and nitrate (the thermodynamics of which are shown in Fig. 1), nitrite, dimethyl sulfoxide, or trimethylammonium oxide. This review deals with the respiratory chain terminated by each oxidant. Figure 2 illustrates the diversity of cytochrome patterns in membranes prepared from variously grown cells. Similar spectra have been published from other laboratories (e.g., see references 404, 416, 442, 447).

Cells grown with high levels of oxygen as sole respiratory chain oxidant contain relatively low concentrations of cytochromes, mostly of the *b* type, which form a split α-band (556 to 563 nm) in reduced-minus-oxidized difference spectra. (Here and elsewhere, the wavelengths given are the positions of the optical absorption maxima at 77°K.) One *b*-type cytochrome of the three or more detected (cytochrome *o*) binds CO and acts as the major terminal oxidase. As the availability of oxygen decreases (e.g., by experimental manipulation of the entering gas concentration or as a result of attainment of the latter stages of growth in batch culture), cytochromes *d* (a terminal oxidase) and "a_1" (of unknown function) are seen at about 630 and 595 nm, respectively, in reduced-minus-oxidized difference spectra, and additional *b*-type cytochromes appear at 555 and 558 nm (484, 485). The latter is believed to be the immediate reductant of cytochrome *d*. Under oxygen-limited conditions, cytochrome *o* persists but with modified spectral properties. Anaerobic growth with fumarate also results in this cytochrome pattern (b_{555}, b_{558}, a_1, and *d*). Anaerobic growth with nitrate as oxidant leads to the suppression or spectral modification of cytochrome *d* and the appearance of cytochrome *b* (λ_{max}, 555 nm) associated with nitrate reductase and formate dehy-

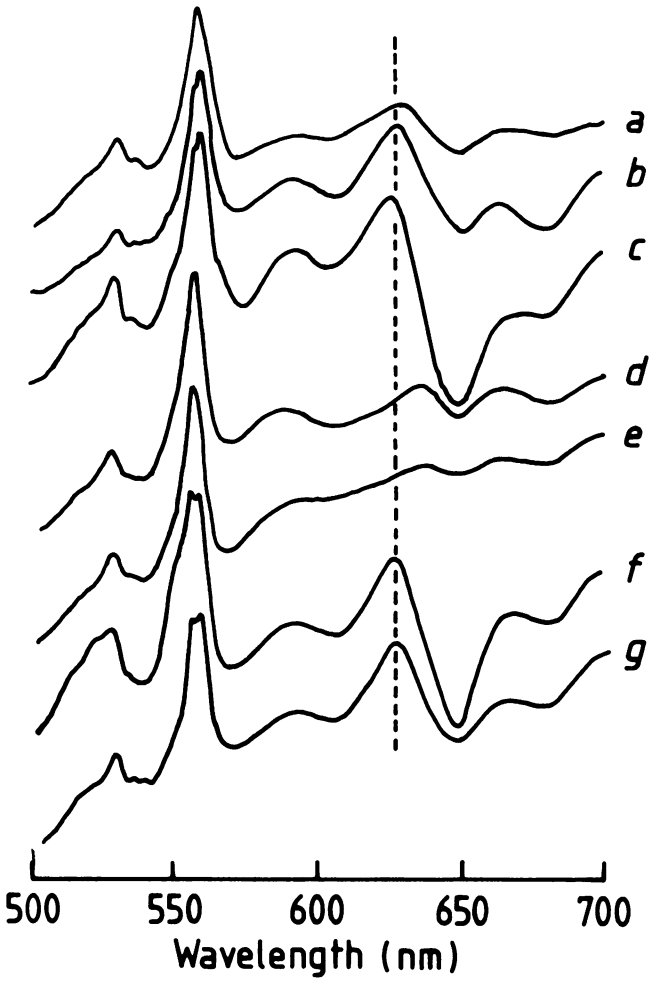

FIG. 2. Reduced-minus-oxidized difference spectra of membranes from *E. coli* grown under various conditions. Cells of strain EMG2 were grown under the conditions described in the text and broken in a French pressure cell; membrane particles were prepared by differential centrifugation. Difference spectra were recorded at 77°K:; they are presented for qualitative comparison only. Growth was to the midlogarithmic phase in the following media: (a) aerobically on glycerol with high aeration; (b) aerobically on glycerol with modest aeration; (c) anaerobically on glycerol with fumarate as oxidant; (d) anaerobically on glycerol with nitrate as oxidant; (e) anaerobically in rich medium supplemented with nitrite; (f) anaerobically on glycerol with dimethyl sulfoxide as oxidant; (g) anaerobically on nutrient broth.

drogenase. The existence of cytochrome *o* in nitrate-grown cells is uncertain (95, 190, 416).

There is some evidence that expression of all of these anaerobic systems is under the positive control of the *fnr* gene product (69, 443, 444).

Accompanying these changes in cytochrome composition are modifications in the quinones and some dehydrogenases as described in later sections of this review. Ubiquinone-8 predominates in cells grown with high aeration but, with alternative oxidants, menaquinone-8 is synthesized. Specificity of some of the dehydrogenases and terminal enzymes for a particular quinone has been suggested (Fig. 3). Some dehydrogenases can exist in more than one form, depending on the growth conditions.

In addition to phenotypic changes arising from changes in the terminal electron acceptor, variations in respiratory chain composition and function can be elicited by varying the nature of the growth-limiting nutrient (193, 198, 383, 406).

The electron transport complexes are organized in the cytoplasmic membrane such that they generate a proton motive force (Δp) across the membrane. The mechanism of the proton translocation is not known. There are two alternatives: (i) the sequence, redox chemistry, and vectorial organization of the respiratory chain components are such that proton translocation is an inevitable consequence of electron transport (the loop mechanism of Mitchell [337]); (ii) the respiratory complexes pump protons via conformational changes. Only (i) is verifiable by direct experimentation, and *E. coli*, with its phenotypically and genotypically modifiable respiratory chains (summarized in Fig. 3), probably offers the greatest potential among experimental systems for resolving these important outstanding questions.

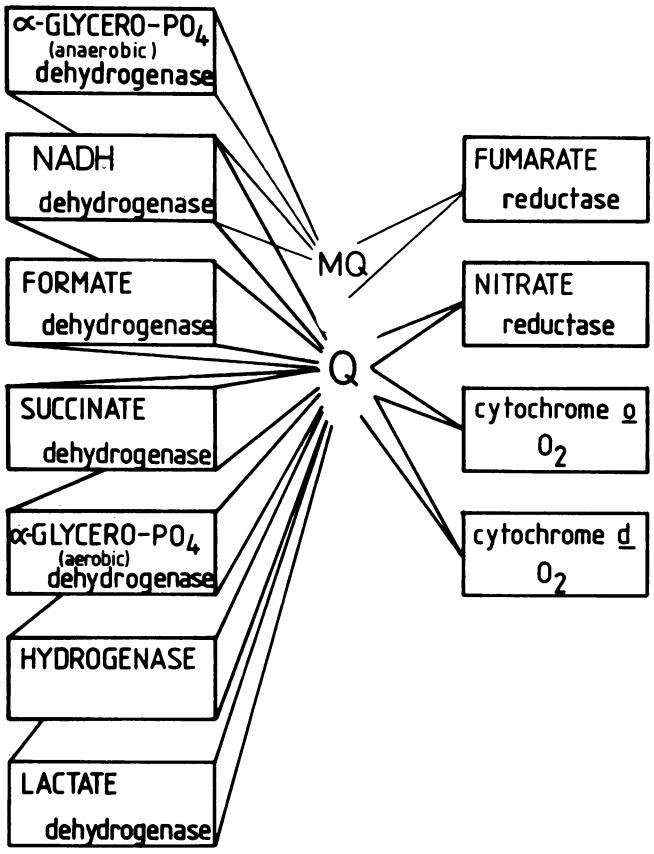

FIG. 3. Overview of the *E. coli* respiratory systems. The major primary dehydrogenases are shown in blocks on the left side and the major oxidases are shown on the right. The two are linked, for the purposes of electron transport, by a quinone, in most cases ubiquinone (Q), but in some cases menaquinone (MQ) (see appropriate sections in text). One potential oxidase, hydrogenase, is also a dehydrogenase, which functions with formate dehydrogenase to give formate:H_2-lyase activity. Each block in this diagram may contain a number of individual respiratory chain components (flavins, iron-sulfur centers, cytochromes, or molybdenum). Not all systems will be present in any one cell type; the presence and concentrations of the different respiratory complexes are regulated by the growth conditions.

FUMARATE REDUCTASE AND ITS ASSOCIATED RESPIRATORY CHAIN

Introduction

E. coli, like many other bacteria as well as a few eucaryotic microorganisms (291), is capable of anaerobic growth on a nonfermentable carbon source when fumarate is added to the medium as a respiratory chain oxidant. A typical medium for such growth would be mineral salts (74) with 1% glycerol, 0.1% Casamino Acids, and 20 to 100 mM potassium fumarate, giving a doubling time of approximately 2.5 h at 37°C. Fumarate serves as an oxidant for anaerobic respiration by being the oxidized half of the succinate-fumarate couple, which has a midpoint potential at pH 7.0 (Em_7) of +30 mV. The midpoint potential is pH dependent by 59 mV per pH unit (Em_6 = +89 mV; Em_8 = −29 mV), and the reaction is a two-electron transfer (n = 2).

Fumarate, like oxygen, acts as a sink for reducing equivalents derived from catabolism, allowing reoxidation of reduced pyridine nucleotides and hence continued turnover of metabolites. In addition, if the electron transfer chain is so designed, the redox energy available between the substrate couples and the succinate-fumarate couple can be conserved in the form of chemical energy in the terminal pyrophosphate bond of ATP, via the process of oxidative phosphorylation. The experimental evidence as to whether or not, and under what circumstances, electron transport to fumarate from metabolites is coupled to ATP synthesis is considered in detail in a later section. The potential contribution of oxidative phosphorylation, utilizing fumarate as oxidant, is quite significant (Fig. 1). If we consider growth on glycerol, a nonfermentable growth substrate, the presence of an oxidant allows for the net gain of 1 ATP/glycerol from substrate-level phosphorylation when fumarate (a Krebs cycle intermediate) is oxidant (Table 1). Substrate-level phosphorylation can give 2 ATP/glycerol when oxygen or nitrate is used. An ATPase-deficient (*uncA*) mutant of *E. coli* incapable of making ATP via oxidative phosphorylation can grow on glycerol with oxygen but not on glycerol with fumarate (330), indicating that 2, but not 1, ATP/glycerol is sufficient for growth. This is confirmed by the observation (185) that a related mutant (*uncB*) can grow on fumarate as oxidant when the carbon source is glycerol-3-phosphate. These ATP yields for oxidative growth, with and without coupling to oxidative phosphorylation, are summarized in Table 1, which shows that growth with oxygen as terminal acceptor gives a more efficient use of glycerol than does fumarate.

Additional proof of the ability of fumarate respiration to support oxidative phosphorylation comes from the work of Macy et al. (316). These authors grew *E. coli* on hydrogen with malate anaerobically; the product was succinate. They determined that growth was by electron transport from

TABLE 1. ATP yields from glycerol oxidation

Phosphorylation	ATP yield in given growth couple (reductant-oxidant)		
	Glycerol-fumarate	Glycerol-3-phosphate–fumarate	Glycerol-oxygen
Substrate level (probable situation in *unc* mutants; 185, 330)	1[a,b]	2[c]	2[d]
Oxidative	2.3[e,f]	2.3[e,c]	8.64[g,h]

[a] *unc* mutants do not grow in this condition.
[b] Diphosphoglycerate kinase (EC 2.7.2.-), pyruvate kinase (EC 2.7.1.41), minus glycerokinase (EC 2.7.1.-).
[c] As for glycerol-fumarate but no glycerokinase.
[d] As for glycerol-fumarate but plus succinate thiokinase.
[e] Using ATP/fumarate ratio of 0.66.
[f] Glycerol-3-phosphate dehydrogenase (EC 1.1.-.-), triose phosphate dehydrogenase (EC 1.2.1.12), formate oxidase, (half) malate dehydrogenase (EC 1.1.1.37).
[g] Using ATP/O ratio of 1.33 except for succinate, where 0.66 was used.
[h] Glycerol-3-phosphate dehydrogenase, triosephosphate dehydrogenase, formate oxidase, isocitrate dehydrogenase (EC 1.1.1.42), oxoglutarate dehydrogenase (EC 1.2.1.-), succinate dehydrogenase (EC 1.3.99.1), malate dehydrogenase (EC 1.1.1.37).

hydrogen to fumarate and, as there can be no substrate-level phosphorylation, hydrogen must be coupled to oxidative phosphorylation when fumarate is the oxidant. The value of 0.66 ATP/fumarate used in Table 1 is assumed from a knowledge of the redox energy available, the phosphorylation potential ($\Delta G_P = \Delta G^{0'} + RT \log [ADP][P_i]/[ATP]$) likely to be found in the cells, and actual measurements of stoichiometries involved in coupling the two processes together. These problems are considered in greater detail later.

Uniqueness of Fumarate Reductase and Succinate Dehydrogenase

In *E. coli* the succinate-fumarate couple may be utilized as either oxidant or reductant for the respiratory chain (Fig. 1). These two reactions are catalyzed by two different enzymes, succinate dehydrogenase and fumarate reductase, which have striking structural similarities (Table 2). The genetic independence of the two enzymes was first suggested by variation of the two activities in a nonparallel manner (217). Thus, succinate dehydrogenase is induced aerobically and repressed anaerobically, whereas fumarate reductase is repressed in the presence of oxygen or nitrate but expressed anaerobically and in the presence of fumarate (217, 462). A mutant incapable of aerobic growth on succinate was capable of anaerobic growth on glycerol with fumarate as terminal oxidant (217). Although the fumarate reductase had both succinate-oxidizing and fumarate-reducing activities under appropriate conditions in vitro (as did the succinate dehydrogenase), the K_m and V_{max} values of the enzymes for the two substrates were substantially different in dye-linked assays (Table 2). The fumarate reductase had a K_m of 17 μM for fumarate, whereas the succinate dehydrogenase had a K_m of 450 μM for fumarate. The apparent K_m values for succinate were 1,000 and 260 μM, respectively. Further studies (94, 182, 462) with mutants have confirmed and extended these observations on the individuality and interrelationships of fumarate reductase and succinate dehydrogenase in *E. coli*. Because the enzymes catalyze the same reaction, it is not surprising that a condition has been obtained in which fumarate reductase can functionally substitute for succinate dehydrogenase (84, 182). The aerobic repression of fumarate reductase can be obviated by multiplication of the fumarate reductase gene. This substitution is

TABLE 2. Comparison of fumarate reductase and succinate dehydrogenase from *E. coli*

Property	Fumarate reductase	Succinate dehydrogenase	Notes	References
Subunit structure				
Flavoprotein	1 × 66,052	64,300	Fumarate reductase values from sequences; fumarate reductase can be isolated as a two-subunit enzyme	84, 162, 251, 299; Guest, personal communication
Iron-sulfur protein	1 × 27,092	26,600		
Anchor protein	1 × 15,000	14,200		
Anchor protein	1 × 14,000	12,800		
Prosthetic groups				
Flavin	[8α-*N*(3)-histidyl]-FAD	[8α-*N*(3)-histidyl]-FAD	The succinate dehydrogenase information refers to the ox heart enzyme; the polypeptide sequences adjacent to the flavin are identical	79, 267, 494
Ferredoxin (mV)	Em_7 (g = 1.94), −45	Em_7 (g = 1.94), −20	The observations on the iron-sulfur centers were made in situ and the assignments for succinate dehydrogenase are tentative	Simpkin et al., unpublished data; 220, 222
Ferredoxin (mV)	Em_7 (g = 1.94), −275	Em_7 (g = 1.94), −220		
HiPIP type (mV)	Em_7, −60	Em_7, +100		
Genetic loci (min)	*frdA-D*, 92.8	*sdhCDAB*, 16		84, 464; Guest, personal communication
Control repressors	Aerobiosis, NO_3^-	Anaerobiosis		See 84
Control inducers	Anaerobiosis	Aerobiosis		
Kinetic parameters (μM)				
K_m for fumarate	17 (470 μM)	450		217, but see also 111
K_m for succinate	1,000	260		111, 422

probably allowed by titration of a repressor; when this was done in a mutant defective in succinate dehydrogenase, complementation with an *sdh* lesion could be observed. It seems a reasonable hypothesis that the *sdh* and *frd* genes arose from duplication of a precursor gene and that these duplicates came under the control of different regulators to serve different functions. A certain amount of "fine tuning" of the genes, so that the enzymes better fit their respective roles, would be expected over time. The sequences of the fumarate reductase genes and polypeptides are known (79, 80). The sequences have a great degree of homology with known segments of succinate dehydrogenases from other sources. The full extent of homology and the modifications attributable to slightly different functions must await the determination of the sequences of *E. coli* succinate dehydrogenase polypeptides.

Structure of Fumarate Reductase

The *E. coli* fumarate reductase, a membrane-bound enzyme, was first isolated by Dickie and Weiner (111). The enzyme consists of two polypeptides, in a 1:1 molar ratio, of M_r 70,000 and 24,000 measured by sodium dodecyl sulfate (SDS) gel electrophoresis. The native enzyme has an M_r of approximately 100,000, indicating that it is a dimer. A small (non-stoichiometric) amount of cytochrome *b* (M_r = 19,000) appears to be associated with the preparation, but there is no indication of any functional significance for it. Many membrane proteins isolated from *E. coli* have at some time been reported to have a *b*-type cytochrome in the preparation. This fumarate reductase preparation has been further analyzed (494) and the flavin has been identified as FAD, covalently linked through its 8α-position to the *N*-3 position on a histidine residue, [8α-*N*(3)-histidyl]-FAD, the same linkage that has been found in mammalian succinate dehydrogenase.

The gene coding for fumarate reductase has been cloned and amplified by linkage to the *ampC* gene (β-lactamase), thus linking copy number to penicillin resistance. Overproduction of fumarate reductase caused accumulation of a soluble form of the enzyme after membrane sites were saturated (81, 82). The soluble form of the enzyme appeared similar in structure to that isolated by Dickie and Weiner (111), consisting of two subunits of M_r 72,000 and 26,500. Both the membrane-bound form of the enzyme and the soluble form are enzymatically active, but the soluble form is the more labile. Amplification of fumarate reductase (see also reference 165) has now been achieved by (i) using gene dosage effects obtained with chromosomal duplication mutants (81, 82), (ii) replicating λ *frd* phages (83), and (iii) using multicopy hybrid plasmids (182, 305). Recent work on fumarate reductase from strains with amplified levels of the enzyme has revealed two additional hydrophobic polypeptides (M_r = 15,000 and 14,000) which are necessary for the soluble two-subunit form of fumarate reductase to become associated with the membrane (299). These two polypeptides are coded for by genes in the fumarate reductase operon, designated *frdC* and *frdD*. The purification procedure for this four-subunit form of the enzyme (the holoenzyme; Table 2) uses Triton X-100 solubilization of the membrane, followed by sucrose density gradient centrifugation. The resulting four-subunit form of the enzyme is more stable than the two-subunit form and resembles more closely the membrane-bound activity. It follows that, in the work of Cole and Guest (81, 82) on the relationship between the extent of overproduction of fumarate reductase and its membrane association, either (i) these anchor polypeptides are not amplified to the same extent as the two large subunits or (ii) the membrane sites for fumarate reductase come under a separate, additional limitation which the anchor proteins cannot overcome when fumarate reductase is extensively overproduced.

The fumarate reductase genes are arranged as an operon, which consists of a promoter-operator region, four cistrons (*frdA*, *-B*, *-C*, and *-D*), and a transcriptional terminator. The complete nucleotide sequence of this operon has been determined (76, 80, 119, 180), and the DNA sequence has been used to predict the primary structures of the subunits. The flavin-containing subunit, the product of *frdA*, consists of 602 amino acid residues (M_r = 66,052) and has, near the amino terminus, a nine-residue sequence identical to the sequence around the FAD-binding site of ox heart succinate dehydrogenase (79, 267). The iron-sulfur protein-containing subunit (product of *frdB*), consists of 244 amino acid residues (M_r = 27,082).

The nonheme iron and acid-labile sulfide content of fumarate reductase appears to be 4 to 5 mol of each mol of enzyme^{-1} (80). It should be noted, however, that due to the lability of some iron-sulfur centers, these estimates may be erroneously low as was the case with studies on ox heart succinate dehydrogenase (354, 355). From the primary protein sequence, it has been suggested that there may be two iron-sulfur centers of the two iron–two sulfur (2Fe-2S) cluster type (Fig. 4 gives a diagrammatic representation of these structures) located in the 27,082 M_r subunit. This polypeptide contains 11 cysteinyl residues in three separate sections of the amino acid sequence. Two of the 2Fe-2S clusters would involve eight of these cysteinyl side chains. On the other hand, the flavoprotein subunit (M_r = 66,052) contains 10 randomly distributed cysteinyl residues and it is difficult to see how 8 of these could be arranged to ligand with two 2Fe-2S iron-sulfur clusters. It is possible, however, that four of these residues align to ligand one 4Fe-4S cluster, or it may also be in the 27,082 M_r subunit. Some clarification may be gained by a comparison of what is known of the iron-sulfur centers of fumarate reductase with those of ox heart succinate dehydrogenase. This enzyme contains eight acid-labile sulfides (the sulfides shown in the structures in Fig. 4, but not the sulfur atoms of the cysteinyl side chains, are liberated as H_2S on acidification). In the intact enzyme, four are thought to come from each subunit. In addition, succinate dehydrogenase has three iron-sulfur centers as detected by electron-paramagnetic resonance (EPR); these are two iron centers of the ferredoxin type (paramagnetic and EPR detectable in the reduced state) and one four-iron high-potential iron protein [HiPIP]-type center (paramagnetic and EPR detectable in the oxidized state) (354, 355). Studies on fumarate reductase in situ (220; D. Simpkin, W. J. Ingledew, J. R. Guest, unpublished data) indicate that this enzyme also contains two ferredoxin type and one HiPIP type of iron-sulfur centers. These iron-sulfur centers have EPR properties very similar to those of the membrane-bound succinate dehydrogenase of eucaryotic mitochondria (353) and of *E. coli* (222). Thus, from the sequence analysis of the fumarate reductase, a comparison with succinate dehydrogenases, and a study of the iron-sulfur centers, the tentative assignment of two ferredoxin-type two-iron clusters to the B (smaller) subunit seems a reasonable working hypothesis (Fig. 4). The 4Fe-4S cluster may be in either subunit.

Robinson and Weiner (422, 423) have reported the effects of a range of anions and reducing agents on the isolated fumarate reductase. Generally, these agents increase the

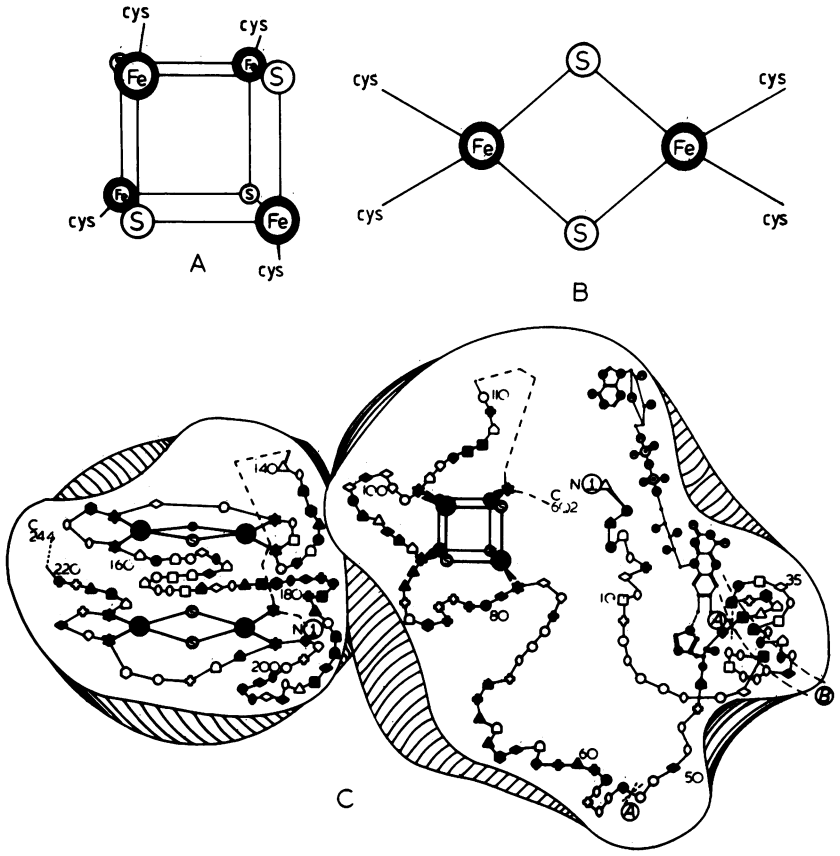

FIG. 4. Structure and arrangement of the prosthetic groups of fumarate reductase. (A) Structure of a 4Fe-4S cluster. This cluster is completed and held by four cysteine residues of the protein. (B) Structure of a 2Fe-2S cluster. This cluster also requires four cysteinyl side chains for completion. (C) Model of fumarate reductase showing the "flavin-containing" subunit (right), with a 4Fe-4S cluster and the "iron-sulfur" subunit (left) with two 2Fe-2S centers. In the flavin subunit, the primary amino acid sequence between 1 and 110 is shown. The flavin is attached to histidine-45. The sequence between the two points marked (A) is homologous with the comparable position in mammalian succinate dehydrogenase. The region marked (B) contains only positively charged amino acid residues, which are connected by neutral amino acid residues. This positive sequence close to the flavin may form the fumarate-binding site. The structure around the 4Fe-4S center is conjectural. In the iron-sulfur subunit, the sequence between amino acids 140 and 220 is shown. The two clusters are shown attached to the cysteines as suggested by Cole et al. (80). Symbols—in the flavin moiety: (⊕) nitrogen, (◑) oxygen, (⊙) phosphorous; in the protein (solid symbols, polar, open symbols, nonpolar): (✱) cystine, (✚) aspartate, (⬮) asparagine, (◆) glutamate, (●) glutamine, (■) arginine, (▲) histidine, (⬢) lysine, (⬣) serine, (⬟) threonine, (□) tyrosine, (○) glycine, (⬯) alanine, (⬦) valine, (◇) leucine, (□) isoleucine, (△) methionine, (⬠) phenylalanine, (○) tryptophan, (⬠) proline.

V_{max} of the enzyme without affecting the K_m. Thermal stability and conformation, as monitored by circular dichroism and the susceptibility to a thiol reagent, are also affected by the anions. The succinate dehydrogenase activity of the enzyme is also anion dependent, but the K_m is affected rather than the V_{max}. The membrane-bound enzyme is not affected by the anionic composition of the media, but the authors conclude that appropriate anions alter the properties of the isolated enzyme so that it more closely resembles the membrane-bound form.

Organization in the Cytoplasmic Membrane

The two-subunit form of fumarate reductase is associated with the membrane but located in the cytoplasmic compartment of the cell. The evidence for this location is threefold.

First, saturation of membrane-binding sites for fumarate reductase by overproduction of the enzyme leads to the two-subunit form of the enzyme accumulating in the cytoplasm (81, 82). Since this form of the enzyme contains the prosthetic groups so far identified, the organization of groups is unlikely to be transmembranous, even though the two small, hydrophobic anchor proteins may confer a degree of "integral membrane protein" status on the holoenzyme.

Second, whole cells cannot use fumarate to oxidize rapidly membrane-impermeable oxidation-reduction dyes, whereas broken cells can oxidize these dyes (246). Membrane-permeable dyes can be rapidly oxidized by both whole and disrupted cells, indicating that the dyes can feed reducing equivalents to fumarate reductase only from the cytoplasmic aspect of the membrane. Although this work is suggestive of a cytoplasmic location for fumarate reductase, it does not rule out the possibility that membrane-bound fumarate reductase does not directly react with the dyes but with another component of the electron transport chain located on the cytoplasmic aspect of the membrane, which reacts and passes the reducing equivalents on to the fumarate reductase.

Third, Van der Plas et al. (483) have used crossed-immunoelectrophoresis and immunoabsorption techniques to show that at least some part of the fumarate reductase enzyme is located on the cytoplasmic aspect of the mem-

brane and that there are no antigenic determinants of this enzyme located on the outer aspect of the cytoplasmic membrane. Furthermore, electron microscopy of negatively stained preparations (298) reveals knobs (4-nm diameter) on the cytoplasmic aspect of the membrane. Although attributed to fumarate reductase, confusion with the F_1 ATPase or other proteins cannot be ruled out at present.

The weight of evidence from these approaches places the fumarate reductase on the cytoplasmic aspect of the cell membrane. The consequences of this location are that (i) it implies the need for a dicarboxylate carrier and (ii) it fixes the site of the terminal reaction of the fumarate-supported electron transport sequence; any scheme to explain respiratory chain-driven proton transport must take this location into account (as discussed in detail below). Kay and Kornberg (264) have shown the presence of a dicarboxylate porter in *E. coli* that allows a range of dicarboxylic acids (including succinate and fumarate) to cross the membrane. Gutowski and Rosenberg (185) have suggested that these dicarboxylic acids enter by proton symport. If this were the case, cells growing on fumarate could not tolerate a significantly more alkaline cytoplasm than that of the external medium as, for each pH unit of transmembrane pH difference, the dicarboxylic acids will be accumulated 100-fold.

Coupling of Electron Transport to the Generation of Δp and ATP Synthesis

There have been a number of studies on the coupling of solute accumulation in the cell (β-galactosides, lactose, phosphate, amino acids, and fluorescent probes) to fumarate-supported electron transport (35, 36, 199, 285, 330, 424, 455, 456). Fumarate-dependent ATP synthesis via oxidative phosphorylation has also been reported (330). All of these processes are, however, secondary to the generation of a Δp ($\Delta p = \Delta\Psi - Z\,\Delta pH$, where $\Delta\Psi$ is the membrane potential and Z is 2.3 RT/F [337]).

To establish a Δp, it is necessary for respiration (or ATP hydrolysis) to move protons from one side of the membrane of a closed compartment to the other. Respiration-driven proton translocation has been demonstrated in *E. coli* for all three major oxidants, oxygen, nitrate, and fumarate, by the technique of oxidant pulse. This technique involves adding a small amount of the oxidant to a resting, anaerobic suspension of cells or vesicles and observing transient pH changes during consumption of the oxidant. Brice et al. (48) obtained a ratio of 1.15 ± 0.16 protons translocated per fumarate reduced for oxidation of endogenous substrates by whole cells (H^+/fumarate or $H^+/2e^-$). The use of endogenous respiration left open the possibility that some of the proton translocation could be due to hydrolysis of ATP derived from oxidant-dependent substrate-level phosphorylation. Gutowski and Rosenberg (185, 186), however, confirmed these observations, using an *uncB* mutant, thus proving that fumarate reduction can support proton translocation. In both cells and inverted vesicles, proton pumping coupled to glycerol-3-phosphate oxidation by fumarate (assayed by the production of dihydroxyacetone-phosphate from glycerol-3-phosphate oxidation) has been measured (330, 333). Stoichiometries of approximately $2H^+$/dihydroxyacetone phosphate ($2H^+/2e^-$) were presented. However, the direct stoichiometry from the experimental data gave a much lower ratio. Unfortunately, with fumarate pulses, the stoichiometry will be underestimated because the K_m for fumarate is not very low and because the product (succinate) will compete at the level of the reductase (217) and at the level of the porter (264). In addition, Gutowski and Rosenberg (186) have shown that dicarboxylic acids enter by proton symport, thus causing a further underestimation of these ratios.

The reduction of fumarate by either NADH or formate in inverted membrane vesicles leads to the generation of a transmembrane ΔpH as measured by atebrin (quinacrine) fluorescence. Atebrin is a fluorescent weak base which distributes according to the transmembrane ΔpH, its accumulation giving rise to quenching of fluorescence (Fig. 5). Lactate (with fumarate) could not support a ΔpH, and the ability of glycerol-3-phosphate to do so was variable. The slow decrease in fluorescence quenching, as the effect of the fumarate pulse decays, is possibly due to kinetic problems associated with fumarate consumption and succinate inhibition. The extent of the fluorescence quenching for fumarate respiration is less than that for oxygen respiration, indicating that the ΔpH is less. This difference could be due to a number of reasons which do not necessarily reflect a functionally lower Δp in fumarate-supported respiration. These include the following: (i) atebrin measures ΔpH and not Δp; and (ii) the membrane vesicles may be leaky to protons. An attempt to quantify the Δp generated by fumarate-linked oxidations has been made by Hellingwerf et al. (210), who measured the ΔΨ by the distribution of radioactively labeled electrophoretic probes and ΔpH by the distribution of labeled weak acids and bases. Values of +105 mV (whole cells) and +103 mV (inverted vesicles) were obtained for Δp. These values are surprisingly low. There is, however, an unusual facet of these results that requires further study, which is that no significant ΔpH was measured in whole cells, even when the external pH was as low as 5.2. However, *E. coli*, like other bacteria, is thought to maintain its cytoplasmic pH close to neutrality (367). In some of the fumarate experiments (210), maintenance of the internal pH would have greatly increased the size of the Δp. This problem requires some clarification but could be due to the collapsing of the ΔpH by fumarate-proton symport through the dicarboxylate porter.

That fumarate respiration must support oxidative phosphorylation has been discussed in a previous section (see

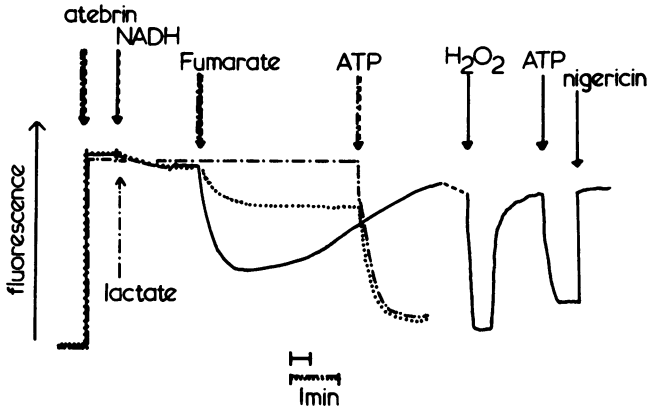

FIG. 5. Quenching of atebrin fluorescence. Quenching of atebrin fluorescence in inverted membrane vesicles, when driven by electron transport or ATP hydrolysis, is taken as a measure of the "energized state" of the membrane. The solid line represents data, redrawn from Haddock and Kendall-Tobias (199), for NADH oxidation by a wild-type membrane preparation. The dotted line shows data, replotted from Singh and Bragg (455), for NADH oxidation by a membrane preparation from a hemeless mutant (no cytochrome *b*). Both sets of authors reported no energization for lactate oxidation by fumarate (·····).

also Table 1). Direct measurement of this phenomenon has only been reported in one publication (330) where ATP synthesis was observed concomitant with electron transfer from glycerol-3-phosphate to fumarate. The measured stoichiometry of 0.1 ATP/fumarate is rather low, but, as the authors point out, ATP synthesis requires sealed vesicles, and electron microscopic examination of their preparation revealed a mixture of unsealed and sealed membrane fragments. The unsealed membranes would add to the rate of fumarate consumption without adding to ATP production and they might also serve to hydrolyze some of the ATP before it is trapped. The possibility remains that the ATP generated in this experiment came not from oxidative phosphorylation but from adenylate kinase acting on the added ADP. It is also noteworthy that Haddock and Kendall-Tobias (199) reported variability in the atebrin quenching accompanying glycerol-3-phosphate oxidation by fumarate. Better evidence for fumarate-supported oxidative phosphorylation has come from other bacteria (25, 291).

In summary, there is poor correlation between the experimentally determined energetic parameters. Proton translocation, the generation of a Δp, and oxidative phosphorylation have all been demonstrated in fumarate respiration, but the stoichiometries and magnitudes of these parameters do not agree with the thermodynamic interrelationships between them. This is probably because some of the values are experimental underestimates. Earlier in this section, a stoichiometry of 0.66 ATP/fumarate was assumed. This value was attained by using a value of $2H^+$ translocated per fumate reduced ($2H^+$/fumarate) and $3H^+$/ATP synthesized. The former value is derived from the data; the latter is derived from measurements of the stoichiometry of proton pumping by the ATP synthetase/hydrolase in other bacteria (346). This value would represent an efficiency of 50% for NADH oxidation if the phosphorylation potential (ΔG_P; see Fig. 1) were -12 kcal (ca. -50 kJ) mol^{-1} (187). These values are derived for NADH oxidation, whereas formate or hydrogen oxidation by fumarate is a more thermodynamically favorable process ($\Delta G^{0'} = -21$ kcal [ca. -88 kJ] mol^{-1}) and has the potential to make more ATP by translocating more protons per oxidation. It is assumed in Table 1 that all of the dehydrogenases have the same ATP/fumarate (and hence H^+/fumarate) ratios. This is probably an oversimplification. Some, like hydrogenase and formate dehydrogenase, which have more redox energy available, could in principle have higher stoichiometries; others may not be coupled at all, e.g., from lactate dehydrogenase to fumarate reductase (199).

Energy-dependent solute transport linked to fumarate reduction has been reported. Lactose and some amino acids can be accumulated by right-side-out membrane vesicles in a process driven by fumarate-dependent oxidation of glycerol-3-phosphate (285, 330). It has also been shown that *uncA* mutants are able to drive active transport of serine and phosphate by fumarate reduction (424).

The work of Bragg and colleagues has highlighted a possible specific function of cytochrome *b* in fumarate-dependent energy conservation. Although a heme-deficient mutant can grow anaerobically on glycerol or glycerol-3-phosphate with fumarate (455), indicating that cytochromes are not involved in electron transport to fumarate, fumarate-dependent active transport processes could not be demonstrated in the cytochrome-deficient cells. By using atebrin fluorescence in inverted membrane vesicles, no "energization" could be observed during fumarate reduction by glycerol-3-phosphate or lactate and only slight (piericidin A-sensitive) energization was observed with NADH (Fig. 5), i.e., about 15 to 25% of the ATP-induced change (456). From this observation and others in which solute transport was measured, these authors suggest that cytochrome *b* is required for coupling electron transport to proton translocation. Nonetheless, that ATP synthetase mutants can grow on glycerol-3-phosphate, but not on glycerol with fumarate (see Table 1), and that this hemeless mutant is able to grow on glycerol with fumarate suggest that it can derive at least one ATP from the three and a half pairs of reducing equivalents derived from glycerol.

In summary, the role of this cytochrome *b* (presumably b_{555}) in energy conservation is not proven. In both the hemeless mutant and the wild type, atebrin quenching was not consistently observed with lactate or glycerol-3-phosphate. Quenching was observed with NADH in both cases, and although the extent of the quenching was less in the hemeless mutant, this can be explained by the lower specific activity of the electron transport reaction in these membranes. These observations are taken into account in the scheme presented in Fig. 6.

Other Electron Transport Chain Components Associated with Growth on Fumarate as Terminal Oxidant

So far, we have discussed the properties and function of fumarate reductase. In this subsection, we consider the other components of the electron transport chain which it serves.

The fumarate reductase-terminated respiratory chain utilizes menaquinone to link the dehydrogenases with the cytochromes, including cytochrome *d*. A number of dehydrogenases have been identified in membranes from cells grown with glycerol and fumarate (Table 3). The major membrane-bound dehydrogenases are those for formate, NADH, and lactate. The succinate oxidase activity is probably due to the fumarate reductase operating in reverse, although a very small amount of succinate dehydrogenase has been detected in these membranes by immunochemical methods (483). The glycerol-3-phosphate oxidase activity is surprisingly low for glycerol-grown cells, but the dye-linked and fumarate-linked activities are much higher, implying that the glycerol-3-phosphate dehydrogenase does not readily react with the pathway to oxygen. Such a compartmentation, if confirmed, complicates schemes describing the electron transport chain (e.g., Fig. 3). The glycerol-3-phosphate dehydrogenase induced under these conditions will be the anaerobic type [see "*sn*-Glycerol-3-Phosphate (L-Glycerol-3-Phosphate) Dehydrogenases"], which has been reported to be a soluble enzyme (274), although later reports (329, 330) describe a functional complex between glycerol-3-phosphate dehydrogenase and a fumarate reductase-containing membrane. The apparent solubility of the enzyme in the earlier case may arise from the lack of fumarate reductase in such membranes. This membranous glycerol-3-phosphate dehydrogenase-fumarate reductase "complex" gives a fairly rapid rate of electron transfer from glycerol-3-phosphate to fumarate, which is very sensitive to small amounts of detergent, indicating the importance of membrane integrity in the relationship. In conclusion, it seems that the anaerobic glycerol-3-phosphate dehydrogenase is a soluble enzyme that can become membrane associated when coinduced with fumarate reductase. The low activities of glycerol-3-phosphate oxidase (Table 3) need clarification. This pattern of activities is specific for growth on glycerol with fumarate. Other carbon sources would be expected to give different dehydrogenase activities. Omission of molybdenum from the

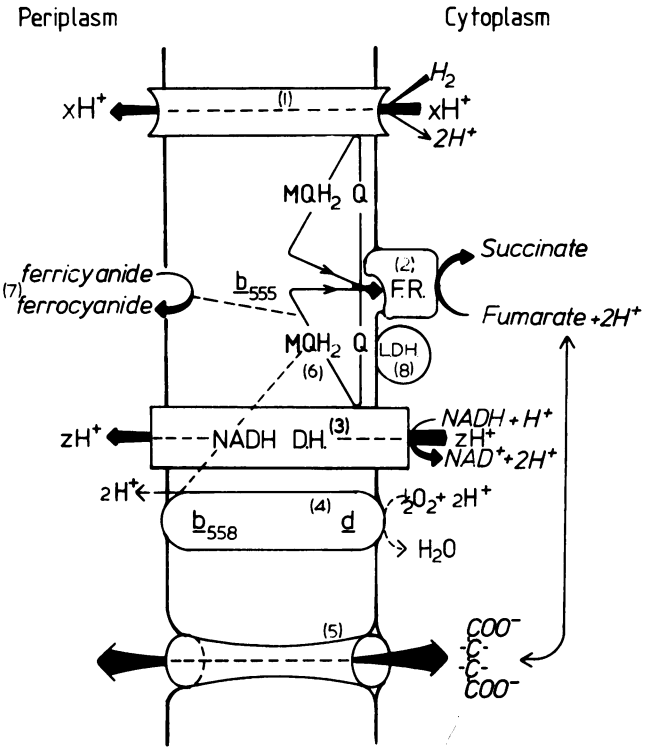

FIG. 6. Fumarate reductase-based electron transport chain, a model to explain the observed phenomena relating proton translocation to electron transfer reactions. The scheme attempts to incorporate the following features: (i) that lactate oxidation cannot pump protons when fumarate is the oxidant, but can when oxygen is the oxidant; (ii) that there is a periplasmic site for ferricyanide reduction, which can support energy-driven processes; (iii) an internal location for the fumarate reductase site; (iv) the nonrequirement of cytochrome *b* for electron transport to fumarate (but see text). It is possible, if the requirement for cytochrome *b* for energy coupling to certain dehydrogenases is confirmed, that the scheme shown represents the electron transport pathway in the hemeless mutant. (1) Hydrogenase; (2) fumarate reductase; (3) NADH dehydrogenase; (4) cytochrome *b-d* oxidase complex (oxidation of the quinol at the periplasmic side will result in proton translocation); (5) the dicarboxylate porter (proton support); (6) quinone and quinol diffusing in the membrane and cycling between reductant and oxidant; (7) ferricyanide reduction site which can support the generation of a $\Delta\mu_{H^+}$ (on ferricyanide reduction by a quinol, a proton will be released); (8) lactate dehydrogenase; this enzyme activity cannot generate a Δp when the oxidant is fumarate but it can when oxygen is the oxidant.

medium also changes the activities (W. J. Ingledew, unpublished data).

Table 4 lists the potentiometric and spectral properties of the oxidation-reduction centers of the fumarate-terminated respiratory chain. Some of these centers are assignable to specific functions or enzyme complexes, although in the case of formate dehydrogenase these assignments are speculative. Figure 7 shows the components ordered with respect to midpoint potential. Details of the flavins are given in the sections on the appropriate dehydrogenases.

There have been relatively few studies on the function of these components. The kinetics of cytochrome oxidation have been studied by Haddock et al. (196) and are described below. In addition to a rapidly oxidized cytochrome (either cytochrome *o* [196] or the cytochrome b_{558} associated with cytochrome *d*), kinetically heterogeneous *b*-type cytochromes were observed. The oxidation of a slower-reacting species occurred with a half-time ($t_{1/2}$) of 150 ms (≈25% of the total) and was followed by a third phase (50% of the total change) with a $t_{1/2}$ of 2 s. This last phase is especially difficult to interpret as the electron transport chain should be in a steady state by this time. The use of intact whole cells in this study introduces additional complications: (i) the kinetics will be confused by the setting up of a Δp, which will exert respiratory control after a few turnovers; (ii) soluble cytochromes, which are known to be present but which are not normally associated with the main electron transport chain (not included in Table 4), may contribute to some of the observed changes. There has been no work published on the steady-state behavior of the cytochromes or membranes from cells grown on glycerol and fumarate. An EPR study of the oxidation-reduction state of Fe-S centers (with oxygen as terminal acceptor) has been published (220). During substrate oxidation by oxygen, a single Fe-S center (designated center 1; Em_7, −20 mV) is extensively reduced when NADH is the substrate. Succinate and lactate also reduce this center, but to a lesser extent, and they also reduce other centers. Lactate reduces a small amount of a second "*g* = 1.94" ferredoxin and succinate gives extensive reduction of

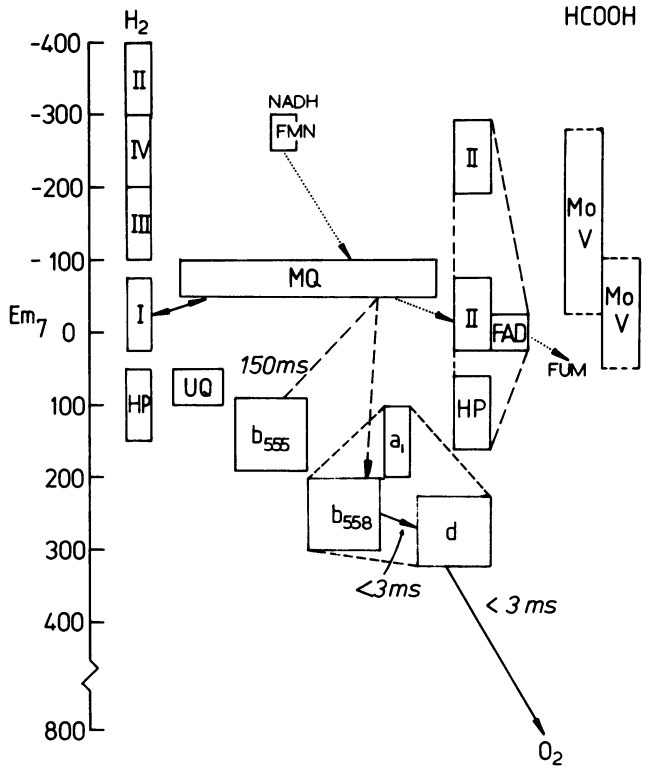

FIG. 7. Oxidation-reduction components in membranes from *E. coli* grown with glycerol and fumarate. Each component is centered on the ordinate at its midpoint potential (pH 7). The size of the component's box on the ordinate is determined by whether an $n = 1$ (120 mV) or an $n = 2$ (60 mV) midpoint is represented. The span of each component on the abscissa approximately indicates relative abundance in the membrane. Components are linked into larger boxes where data are available on their functional complexes. Possible electron transfer sequences are shown. The presence of cytochrome *o* in these cells requires further investigation. MQ, Menaquinone; UQ, ubiquinone; Mo, molybdenum; Fum, fumarate; HP, HiPIP.

TABLE 3. Activities of membrane particles from glycerol-fumarate-grown cells

Enzyme	Immunochemical detection	Activity (nmol min^{-1} mg of $protein^{-1}$)		
		Oxidase	Dye linked	Fumarate linked
NADH dehydrogenase	+	520		73
Formate dehydrogenase		1,140		Hemeless, 0
D-Lactate dehydrogenase	+	124		
L-Lactate dehydrogenase		27		
Glycerol-3-phosphate dehydrogenase	+	10	114	206
Malate dehydrogenase	+	>10		
Hydrogenase	+	930		
6-Phosphogluconate dehydrogenase	+			
Dihydroorotate dehydrogenase	+			
Succinate dehydrogenase	+	280		
Fumarate reductase	+		560	
Nitrate reductase	+		0.35	
Nitrite reductase			34.6	
Reference(s)	483	220	246, 329; Simpkin and Ingledew, unpublished data	38, 329

two additional ferredoxins. These observations are summarized in Fig. 7.

NITRATE REDUCTASE AND ITS ASSOCIATED RESPIRATORY CHAIN

Introduction

E. coli is able to utilize nitrate as terminal electron acceptor for the respiratory chain by virtue of a respiratory (dissimilatory) nitrate reductase, which is induced when nitrate is provided in the medium. A typical medium (196) consists of mineral salts (74), 0.5% glycerol, and 1% potassium nitrate (approximately 100 mM) supplemented with 1 μM ammonium molybdate (required for nitrate reductase and formate dehydrogenase). Nitrate reductase expression is under the control of the *nirR* gene and is repressed by oxygen except in certain mutants (156, 158, 161). The literature on this enzyme has been reviewed in reference 198, and information on molybdenum and molybdenum-containing enzymes, including nitrate reductase, may be found in Coughlan (88). This section focuses on some recent advances in the understanding of this enzyme. Work on its biosynthesis and turnover (70, 157, 188, 260, 266, 310) falls outside the scope of this review.

In *E. coli*, the terminal reaction of nitrate-supported respiration reduces nitrate to nitrite. The nitrite, which is potentially toxic, accumulates in the medium and appears not to be extensively utilized. The reaction

$$NO_3^- + 2e^- + 2H^+ \leftrightharpoons NO_2^- + H_2O \quad (1)$$

has a midpoint potential of +420 mV at pH 7, giving a $\Delta G^{0'}$ for nitrate reduction by NADH of −38,744 cal (ca. 163 kJ) mol^{-1} (Fig. 2), a large enough standard free energy for the reaction to be coupled to the synthesis of more than 1 ATP/$2e^-$ and still leave the reaction highly favorable. The utilization of nitrate as terminal oxidant does not incur the

TABLE 4. Electron transport chain components in membranes derived from cells grown on glycerol and fumarate

Component	Em_7 (mV)	*n* value	Spectral characteristics		Notes	Reference(s)
			α band (λ_{max}, nm) or *g* value	Observation temp (°K)		
Menaquinone	−74	2				291
Ubiquinone	−70	2				291, 419
Ferredoxin F1	−50	1	2.022, 1.927	30	Fumarate reductase	220
Ferredoxin F2	−240	1	2.022, 1.927	10	Fumarate reductase	220
HiPIP F3	+120	1	2.023, 2.011	20	Fumarate reductase	220
Cytochrome *d*	+280	1	630		Dioxygen reductase	416
Cytochrome *b*	+140	1	555	77		416
Cytochrome *b*	+250	1	558	77		416
Cytochrome a_1	+160	1	593	77		R. B. Gennis, unpublished data
Molybdenum I	−20	1	1.978	100	Formate linked	220
	−270	1				
Molybdenum II	+50		1.978	9	Formate linked	220
	−100	<1				
Ferredoxin center I	−20	1	2.037, 1.937, 1.923	150		220
HiPIP b	+120		2.017, 1.976	9		220
Ferredoxin center IIb	−240	1	2.022, 1.927	12		220
Ferredoxin center III	−150	1	2.045, 1.89	12		220
Ferredoxin center IV	−250	1	2.07, 1.875	12		220

metabolic consequences that accompany use of fumarate, so a full oxidation of the carbon source (say glycerol) may ensue and, assuming similar stochiometries for oxidative phosphorylation with oxygen, the ATP yields will be the same as with oxygen (Table 1). A note of caution, however, comes from Yamamoto and Ishimoto (502), who showed that when *E. coli* was grown on lactate plus nitrate 58% of the carbon source was liberated as CO_2 but the remainder accumulated as acetate and formate. When grown on glucose and nitrate, no oxidative phosphorylation occurred; i.e., the tricarboxylic acid pathway was not used. Thermodynamic and metabolic considerations make growth on nitrate more favorable than on fumarate, although less favorable than on oxygen (Fig. 1).

Structure of Nitrate Reductase

Nitrate reductase has been isolated from the cytoplasmic membrane of *E. coli* by a number of detergent-based, alkaline heat treatment or solvent extraction procedures (72, 122, 128, 309, 315). The enzyme contains molybdenum, nonheme iron, and acid-labile sulfide. Although there is some variation in the reported subunit composition of the enzyme under nondissociating conditions, three subunits, designated α, β, and γ, are reported as constituents of nitrate reductase. The γ-subunit, however, is absent in some preparations and a β′-subunit, which runs very close to the β-subunit in denaturing electrophoretic gels, is often present in variable quantities. The M_r values reported for the native enzyme also vary from 800,000 (4α, 4β, 0γ) to 220,000 (1α, 1β, 0γ). The latter appears to be the minimal functional unit for nitrate reduction by artificial electron donors. Recent work has clarified some of these early controversies. There do appear to be three subunits in the "holoenzyme," the α-subunit ($M_r \approx 150{,}000$), the β-subunit (M_r of 60,000), and the γ-subunit ($M_r \approx 20{,}000$). This holoenzyme comprises 2α, 2β, and 4γ subunits ($M_r \approx 500{,}000$). The enzyme can also be isolated in a form in which the β-subunit is modified and the γ-subunit is not present $(\alpha\beta')_n$, where n is 1 (alkaline heat treatment [315]) or 4 (some detergent-solubilized preparations [72]). In membrane-bound respiratory chain assemblies, the distinction between a subunit and an associatable protein is often difficult to make, but the functional significance of the γ-subunit of nitrate reductase is well defined. The γ-subunit is a *b*-type cytochrome (cytochrome ^{nr}b), whose structural gene is part of the nitrate reductase operon and which is necessary for the oxidation of quinol by nitrate but not for the oxidation of reduced benzyl viologen (309). The α-subunit has been reported to be the catalytic subunit on the basis that, when the α-subunit is cleaved by proteolysis, the enzyme activity (benzyl viologen to nitrate) is lost. However, the β-subunit can undergo proteolysis, to become substoichiometric, without loss of activity with benzyl viologen. The role of the β-subunit in the oxidation-reduction process is not known, but it is involved in membrane attachment.

The β-subunit has two forms, β and β′. The subunit can be obtained in different ways and may not be a single species. The β- and β′-subunits migrate electrophoretically in denaturing gels with apparent M_r values of 60,000 and 58,000, respectively. At one time it was suggested that the β′-subunit was a degradation product of the α-subunit (72), but later work using radiolabel pulse-chase studies has indicated that the β′-subunit can be a precursor of the β-subunit and that the two subunits have similar antigenic determinants (313). These observations apparently contradict the contention that the β-subunit is converted into the β′-subunit by a membrane-bound protease (107, 315). Recent work by Chaudhry et al. (65) has indicated that the modification of the β-subunit to β′ is a reversible (non-proteolytic) process and is due to the removal of one or more nonprotein moieties (e.g., by reversible phosphorylation or glycosylation). However, there may also be a form of the β′-subunit that is a proteolysis product. Forget and Rimassa (130) have presented evidence for the presence of carbohydrate moieties in the enzyme. Glucose and glucosamine were identified but the subunit to which they are attached was not reported. It is noteworthy that some glycosylated peptides appear anomalously small in denaturing gels.

The enzyme-catalyzed (65) interconversion of β- and β′-subunits may have a role in regulating the turnover of the nitrate reductase. The quantity of the β′-subunit present in a preparation correlates inversely with the amount of the γ-subunit present, and this form predominates in either the soluble, nondetergent (alkaline heat treatment) or cytoplasmic precursor form of the enzyme. Thus, if the β′-subunit is present, the preparation does not bind the γ-subunit nor does it bind to the membrane. Conversely, the presence of a functional γ-subunit is necessary for the membranous assembly of the holoenzyme (17). If the γ-subunit is absent or nonfunctional (as in *chlI* mutants, which are defective in the structural gene for the γ-subunit, or hemeless mutants, which lack the prosthetic group for the *b*-type cytochrome), the nitrate reductase accumulates in the cytoplasm as the αβ′ form. The γ-subunit has been isolated and purified (65). The cytochrome has 44.8% of its residues of a hydrophobic type and an isoelectric point of greater than pH 9.5.

A unique claim for the structure of nitrate reductase has been made (129). Nitrate reductase, purified after acetone treatment (128), was treated sequentially with alkali and acid, resulting in 70% of the protein being recovered as an apparently homogeneous polypeptide of M_r 15,000. It was suggested (129) that the enzyme is composed of 10 repeating units of this peptide, linked not to peptide bonds but through FeS centers or sugar molecules, thus explaining the behavior of the α-subunit on SDS gel where it migrates with an apparent M_r at 150,000. However, the peptide bonds of arginine, an amino acid expected predominantly in the hydrophilic regions of the protein, can be hydrolyzed by such treatments and so an alternative explanation is possible: the protein may be one polypeptide with transmembranous hydrophobic sections (M_r = 15,000) linked by arginine-containing sequences.

In summary (Fig. 8), there have been disputes over the molecular weight and subunit stoichiometries of the assembled "holo"-nitrate reductase, the functional significance of the γ-subunit, and the source and significance of the β′-subunit. However, the γ-subunit appears to be a true, functional component, and the β′-subunit seems to be a reversibly and physiologically modified form of the β-subunit. Other forms also designated β′ may not fall into this category. The native enzyme, as isolated, has a composition of 2α:2β:4γ, a dimer of the minimum stoichiometry, giving an M_r of approximately 500,000. The genes coding for the enzyme subunits have now been cloned (Table 5), and so significant developments in our understanding of the structure of the nitrate reductase should soon emerge.

The purified nitrate reductase (of minimum stoichiometry 1α, 1β, 2γ subunits) contains between 12 and 28 acid-labile sulfides and nonheme iron atoms, in addition to the two hemes of the γ subunits (67, 198). This indicates the presence of 3 to 14 FeS clusters (3 × [4F3 − 4S] to 14 × [2Fe − 2S]).

Molybdenum is thought to be associated with pterin (235;

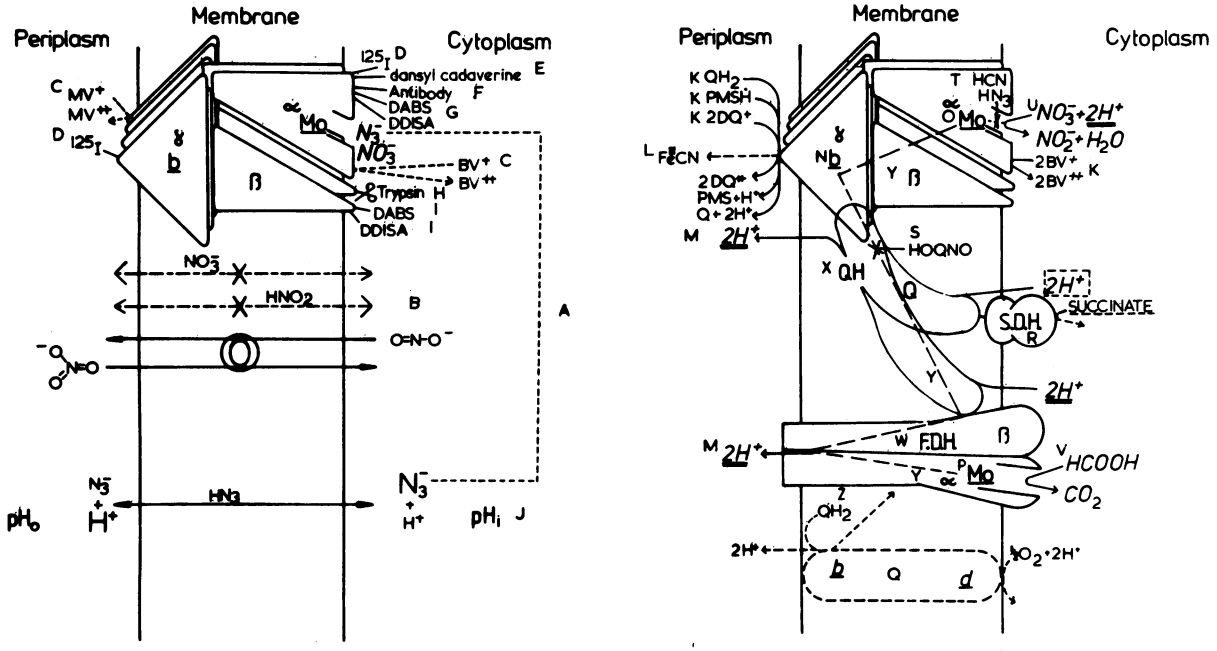

FIG. 8. Spatial organization of the *E. coli* nitrate reductase and its associated electron transport chain. (Left) Organization of the nitrate reductase in the membrane; (right) proton-translocating electron transport chain. (Left) A, Localization of the site of nitrate reduction by azide (250); B, required antiporter and passive permeability barriers for nitrite and nitrate; C, external electron donation site for diquat and cytoplasmic site for the membrane-permeable benzyl viologen (150); D, ^{125}I radioiodination of exposed tyrosines to locate subunits (39); E, radiolabeled dansyl cadaverine attachment to exposed glutamine residues (312); F, detection of the α-subunit on the cytoplasmic aspect by antibody attachment (171); H, trypsin cleavage of the β-subunit from the cytoplasmic side of the membrane (106, 170); I, diazobenzanesulfonate and diiodosulfanilic acid radiolabeling of the β-subunit from the cytoplasmic side (170). J, The pH_i (cytoplasmic pH) is thought to be maintained at about pH 7.5 (367); the difference between the pH_o (external pH) and pH_i determines the accumulation ratio of the azide ion (221). (Right) K, Conclusion of oxidant and reductant pulse experiments linking these dyes to nitrate reduction for the location of the electron donation site and the absence of proton pumping by the nitrate reductase (249, 250); L, ferricyanide reduction supporting proton translocation (one of the sites is shown; the other site is closer to formate dehydrogenase [38]); M, proton translocation—$2H^+/2e^-$ for succinate, lactate, and glycerol-3-phosphate and $4H^+/2e$ for formate and NADH (only formate and succinate dehydrogenases are shown [148]); N, γ-subunit is cytochrome ^{nr}b; O, α-subunit is the catalytic subunit and probably contains the molybdenum cofactor (66, 169, 309); P, As for (O) but the enzyme is formate dehydrogenase (40); Q, hypothetical arrangement for the cytochrome b_{558}-*d* complex (this complex can sustain proton translocation with the same stoichiometries as can nitrate reductase [148] and is not, therefore, required to be a proton pump [see text]; R, succinate dehydrogenase; S, main site for HOQNO (2-*N*-heptyl-4-hydroxyquinoline-*N*-oxide) inhibition (428); T, sites for cyanide and azide inhibition of nitrate reductase; U, nitrate reductase reaction and sites; V, formate dehydrogenase reaction and site (40); W, formate dehydrogenase (the α- and β-subunits are transmembranous; little is known of the γ-subunit; enzyme contains molybdenum, selenium, iron-sulfur, and a *b*-type cytochrome [not shown; 40]; X, quinone loop, necessary for proton translocation; Y, path of flow for reducing equivalents from formate to nitrate; Z, quinol acting as electron donor to the cytochrome *b-d* complex with consequent release of protons.

K. V. Rajagopalan, *in* J. R. Dilworth and M. F. Lappert, ed., *Some Recent Developments in the Chemistry of Chromium, Molybdenum, and Tungsten*, abstr. L8, R. Soc. Chem., Dalton Div., London, 1983) (Fig. 9) in a range of molybdoproteins, including *E. coli* nitrate reductase, although X-ray absorption studies (S. P. Cramer, *in* J. R. Dilworth and M. F. Lappert, ed., *Some Recent Developments in the Chemistry of Chromium, Molybdenum, and Tungsten*, abstr. L27, R. Soc. Chem., Dalton, Div., London, 1983) suggest a greater structural diversity of molybdenum-containing cofactors. The synthesis of molybdenum-containing cofactors is complex. Early work implicated five genetic loci in *Aspergillus nidulans* (369) and four in *Neurospora crassa* (480). The functions of these loci are not understood. Some of the *E. coli* strains isolated, lacking nitrate reductase activity, appear to be defective in the processing of the molybdenum-containing cofactor, although not in the synthesis of the demolybdo cofactor itself. The lesions appear to be in the insertion of the molybdenum into the cofactor and insertion of the assembled cofactor into the protein (see Table 5). The molybdenum is probably associated with the catalytic subunit (α-subunit).

EPR studies of *E. coli* nitrate reductase (47, 487, 488) have identified signals from an HiPIP-type FeS center and at least two ferredoxin-type centers, in addition to a signal attributable to molybdenum V. The molybdenum V species was observed as an interconvertible (high or low pH) form, the latter differing through the presence of proton hyperfine splittings. The pK_a for proton binding is pH 8.2, and the enzyme activity in the pH range 6 to 10 may be controlled by this pK_a, the unprotonated form being active. More recent work has shown that this proton hyperfine interaction is to an extent anion dependent (F. F. Morpeth, D. H. Boxer, R. C. Bray, and G. N. George, *in* J. R. Dilworth and M. S. Lappert, ed., *Some Recent Developments in the Chemistry of Chromium, Molybdenum, and Tungsten*, abstr. P10, R. Soc. Chem., Dalton Div., London, 1983). The binding of nitrate and nitrite ions also modifies the molybdenum EPR signal. Blum and Poole (31) have reported that the orientation of the molybdenum V and HiPIP centers in the mem-

TABLE 5. Genes involved in the processing and synthesis of nitrate reductase and formate dehydrogenase

Gene	Map position (min)	Mutant phenotype	Reference(s)	Alternative designation
chlA	17	Pleiotropic; lesion in molybdenum cofactor processing; defective incorporation of formate dehydrogenase into membrane; gene product of M_r 82,000	155, 334, 405, 477	*narA bisA*
chlB	85	Pleiotropic molybdenum cofactor processing lesion; defective in inserting the cofactor into the enzyme and incorporating formate dehydrogenase into membrane; gene product of M_r 35,000	334, 477	*narB*
chlC	27	Structural gene for the α and β subunits	21, 121, 126, 127, 309, 334, 405	*narG,H,I,K,L*
chlD	18	Pleiotropic; molybdate transport?	163, 334, 486	*narD*
chlE	18	Pleiotropic; function unknown; results in deficiency of cytochromes ^{nr}b and ^{fdh}b but not their structural gene; processing of molybdenum cofactor?	190, 309, 314, 334, 466	*bisB*
chlF	26	Unknown	163	
chlG	0	Synthesis or insertion of molybdenum cofactor	163, 234, 334, 466	*bisD*
chlI	27	Structural gene for γ subunit (cytochrome *b*)	359	*narI*
fdhA	80	Available as temperature-sensitive mutants; thought to be a structural gene	317	
fdhB	38	Possibly involved in governing the synthesis of an activator for the control of formate dehydrogenase synthesis	200	
fdhC	82		200	
fdhD	87		200	
fdhE	87	Only characterized mutant to lack PMS reductase while retaining BV reductase; could be same gene as *fdhD*?	200	
nirA	29	Regulating gene for anaerobic electron transport systems, including nitrate reductase, nitrite reductase, and fumarate reductase	69, 156, 158, 294, 465, 497	*fnr, nirR*

brane is nonrandom. Membranes derived from cells grown on glycerol plus nitrate, however, also contain formate dehydrogenase (molybdenum V and HiPIP) and succinate dehydrogenase (HiPIP) which overlap spectrally and frustrate a more detailed analysis.

The molybdenum IV to molybdenum V transition has a midpoint of +180 mV, and the molybdenum V to molybdenum VI transition has a midpoint of +220 mV (pH 7.14) (487). The HiPIP-type Fe-S center has a midpoint of +80 mV, and one ferredoxin has a midpoint of +50 mV (g_z = 2.003; g_y = 1.888; g_x = 1.870); a value for the other spectrally distinguishable ferredoxin (g_z = 2.041; g_y = 1.945; g_x = 1.921) was not reported. Cytochrome ^{nr}b of the γ-subunit titrates with an Em_7 of +10 mV in membrane preparations (416). More recently, this component has been resolved (189) into components with values of +10 and +125 mV, respectively, in partially purified nitrate reductase. These latter studies require extension to pure preparations.

Organization in the Cytoplasmic Membrane

To understand how electron transport through nitrate reductase is coupled to the generation of a Δp, it is necessary to have a detailed knowledge of the organization of the enzyme in the membrane. Relatively little is known about the position and redox chemistry of the prosthetic groups,

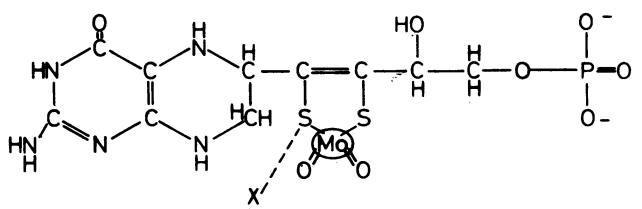

FIG. 9. Proposed structure of the molybdenum-containing cofactor of nitrate reductase.

but the sidedness of the catalytic sites and the subunits of the enzyme have been extensively studied.

The aspect of the cytoplasmic membrane at which nitrate is reduced is of crucial importance in any model of the respiratory chain. Garland et al. (148) reported that the rate of passive entry of nitrate into spheroplasts, as measured by consequent osmotic swelling at relatively high concentrations of nitrate, would, if extrapolated to lower nitrate concentrations, fail to support the measured activities of nitrate reductase. Thus, the site of nitrate reduction was thought not to be cytoplasmic. This group conceded that their approach had two limitations: (i) the transport rate for nitrate would be underestimated if a permease with a low K_m for nitrate were operating, and (ii) their method would not detect nitrate entry if it were a strict exchange process with the product (i.e., a nitrite/nitrate antiport). An alternative method of determining sidedness of nitrate reduction is to utilize the fact that the azide ion, a weak acid, is a competitive inhibitor of nitrate reduction and that the concentration of the anion in the cytoplasm is determined by the ΔpH (Fig. 8). Thus, by comparing the sensitivities of nitrate reductase activity to azide in intact cells, inverted vesicles, and isolated enzyme preparations, it has been concluded that the site of nitrate reduction is cytoplasmic (221, 249, 250), a conclusion supported by the pH profile of the enzyme activity in the different preparations. The activity of nitrate reductase in whole cells was relatively insensitive to the pH of the suspending medium. Kristjansson and Hollocher (290) also concluded that the site of nitrate reduction is on the inner aspect of the membrane from their study of the latency of chlorate reductase activity in cells when compared with inverted vesicles (chlorate is an analog of nitrate which nitrate reductase can reduce to chlorite).

The implications of a cytoplasmic location for the active site of nitrate reductase are that (i) the scalar proton consumption of the terminal respiratory reaction is cytoplasmic and (ii) there is a need for porter systems for nitrate and presumably for nitrite. The nitrate ion is generally considered to be membrane permeable, although this nonspecific process is slow (148). Nitrate is unlikely to enter the cells via a uniporter as any membrane potential across the cytoplasmic membrane would tend to exclude nitrate. The extent of exclusion of nitrate would increase 10-fold for a rise in membrane potential of 59 mV and would give a much higher apparent K_m for nitrate in cells than in inverted vesicles (a phenomenon that is not observed). A suitable mechanism for entry would be an electroneutral nitrate/nitrite antiporter with low nonspecific electrophoretic movement of either species and no significant redistribution of nitrite acting as a weak acid (Fig. 8). Such a nitrite/nitrate antiporter system has recently been described in *Paracoccus denitrificans* (34).

Although the catalytic site of nitrate reductase is on the cytoplasmic aspect of the membrane, the enzyme itself is transmembranous. The γ-subunit, cytochrome *b*, has been found by direct covalent labeling of spheroplasts, using lactoperoxidase-catalyzed radioiodination, to have amino acid residues exposed at the periplasmic surface (39). No labeling method yet used has shown that the γ-subunit has any residues on the cytoplasmic side of the membrane. The lactoperoxidase method iodinates tyrosine residues, which are normally found in the hydrophobic region of a protein. This method also indicated a cytoplasmic location for the α-subunit, but could not label the β-subunit from either side of the membrane. An alternative method (dansyl-cadaverine labeling catalyzed by transglutaminase), which labels exposed glutamine residues, has been used (312) to show labeling of the α (A)-subunit only from the cytoplasmic aspect of the membrane. The β- and γ-subunits were unlabeled. Both the α- and β-subunits can be labeled from the cytoplasmic side of the membrane (inverted membrane vesicles), using the membrane-impermeable reagents [^{35}S]diazobenzanesulfonate, which reacts with exposed carboxyl groups, and [^{125}I]diiodosulfanilic acid, which reacts with exposed nucleophilic residues. The location of the α-subunit has been confirmed by immunofluorescence studies, using antibodies specific for the α-subunit (168, 175). By using fluoroscein isothiocyanate coupled to goat antirabbit immunoglobulin, only the α-subunit was detected on the cytoplasmic aspect of the membrane. A study using trypsin as a probe for sidedness located the β-subunit exclusively on the cytoplasmic aspect of the membrane (170, 171). The results of these studies are summarized in Fig. 8. The site on nitrate reductase that oxidizes $FMNH_2$ is located on the cytoplasmic aspect of the membrane (266).

Genetics of Nitrate Reductase

A range of mutants lacking nitrate reductase activity have been isolated by virtue of their ability to grow anaerobically in the presence of chlorate (e.g., reference 430). This resistance is conferred upon these mutants because a functional nitrate reductase is necessary to reduce the chlorate to the toxic species, chlorite. These mutants are usually designated *chl*. Data on these strains are compiled in Table 5. Some of these mutants (*chlA*, *chlB*, *chlD*, *chlE*, and *chlG*) are pleiotropic for both nitrate reductase and formate dehydrogenase, apparently being defective in the processing of the molybdenum cofactor into both enzymes. *chlA*, *-D*, and *-E* map closely together at 17, 17, and 18 min, respectively, and may form an operon. The *chlD* gene product is thought to be required for molybdate transport and for ensuring that the molybdenum is in the correct chemical state for insertion into the cofactor or protein. These lesions can be circumvented by adding high concentrations of molybdate (159, 168). The *chlA* and *chlB* mutants also accumulate demolybdo forms of nitrate reductase and formate dehydrogenase, but these lesions cannot be circumvented by high concentrations of molybdate. Active forms of the enzymes in these strains can be produced by mixing cell-free extracts derived from the two mutants with the defective membrane preparations, indicating that the products of *chlA* and *chlB* are required for insertion of the molybdenum into the demolybdo forms of both enzymes. The *chlA* gene, coding for a protein of M_r 82,000, maps at 17 min and has been cloned. A protein of similar M_r (isolated from a *chlB* mutant) has been shown to reconstitute nitrate reductase activity in cell-free extracts of a *chlA* mutant. The *chlB* gene maps at 85 min and is thought to code for a protein of M_r 35,000 (420). The work of Amy (13) suggests that the *chlA* gene product inserts molybdenum into the molybdenum-containing cofactor or that mutations in *chlA* produce defective cofactors. The lesion in the *chlB* mutant seems to be in the specific insertion of the molybdenum-containing cofactor into nitrate reductase and formate dehydrogenase. The *chlE* gene product also appears to be required for insertion of the cofactor.

The structural genes for nitrate reductase (α-, β-, and γ-subunits; see Table 5) are organized in an operon at 27 min (33). The operon appears to be under the control of a regulatory gene, designated *nirR* and mapping at 29 min, which controls the expression of various anaerobic respiratory chain components (Table 5).

Coupling of Electron Transport to the Generation of Δp and ATP Synthesis

In the nitrate-terminated electron transport chain, respiratory proton translocation has been studied at the level of the nitrate reductase alone and over the whole electron transport chain. Net proton consumption of the terminal (scalar) reaction (equation 1) occurs in the cell matrix and does not have superimposed upon it any vectorial movement of protons by the nitrate reductase (150, 236, 247, 249, 252). The production of protons in the bulk phase is dependent on the chemistry of the artificial electron donor used (Fig. 8). Although there is no vectorial proton movement associated with the nitrate reductase, the scalar consumption of protons in the cytoplasm does contribute to the generation of Δp. Proton pumping has also been observed during electron transfer from physiological substrates to nitrate. For endogenous substrates (48), L-malate and formate, stoichiometries of approximately $4H^+/NO_3^-$ were obtained after correction for pH changes attributable to sources other than direct proton translocation, whereas for succinate, D-lactate, and glycerol, a stoichiometry of $2H^+/NO_3^-$ was measured (148). Similar values were obtained when oxygen was substituted as oxidant. Since the nitrate reductase is not a proton pump, it follows that the oxygen reductase is not one either. That this nitrate-dependent proton translocation generates a transmembrane Δp has been demonstrated qualitatively for formate, NADH, D-lactate, and glycerol-3-phosphate oxidation in inverted membrane vesicles, using atebrin fluorescence quenching to detect ΔpH (199), and quantitatively by lipophilic cation (triphenyl methyl phosphonium) and weak acid (acetate) distribution (37). Values of up to −165 mV for the Δp were obtained; these measurements are slightly higher than those reported for fumarate respiration but comparable to those for oxygen respiration (210, 408).

From studies of molar growth yields, there is evidence that approximately 1 ATP is synthesized by oxidative phosphorylation per nitrate reduced (500). Direct measurement of ATP synthesis supported by electron transport from the substrates NADH, glutamate, and citrate to nitrate, in a cell-free preparation which probably contained inverted vesicles, gave ATP/NO_3^- ratios of 0.55, 0.65, and 1.1, respectively (360). The use of a cell-free preparation, although necessary, will probably lead to an underestimate of the ATP synthesized.

In summary, nitrate respiration can support ATP synthesis through oxidative phosphorylation. Measurements have been made of the important chemiosmotic parameters, H^+/NO_3^- and ATP/NO_3^- ratios, and Δp, although values of H^+/ATP and ΔG_{ATP} are not directly available. In addition to being used for ATP synthesis, the Δp generated by nitrate respiration can be used to drive solute transport (286). Oxidation of glycerol-3-phosphate and formate by nitrate can support the transport of amino acids and lactose.

Other Electron Transport Chain Components Associated with Growth on Nitrate as Terminal Oxidant

In addition to the major inducible components nitrate reductase and formate dehydrogenases, membranes from nitrate-grown cells contain diverse cytochromes and dehydrogenases. By crossed-immunoelectrophoresis of solubilized membranes, from cells grown with glucose plus nitrate, Van der Plas et al. (483) detected 6-phosphogluconate, NADH, formate, dihydroorotate, and D-lactate dehydrogenases. G. Cummings and W. J. Ingledew (unpublished data) have shown that the specific oxidase activities induced by nitrate are dependent on the carbon source and have, with membrane derived from cells grown on glycerol plus nitrate, detected NADH, formate, lactate, succinate, and glycerol-3-phosphate oxidase activities. There is no evidence that the membrane-bound lactate, NADH, and succinate dehydrogenases in these cells differ from those described for aerobic growth. However, the homogeneity or otherwise of the formate and glycerol-3-phosphate dehydrogenases is more complex (see below).

Cytochromes *b*, *d*, and a_1 (Fig. 1) are present in membranes from nitrate-grown cells. One of the several *b*-type cytochromes (189–191, 485) is specifically associated with nitrate reductase (^{nr}b) and another is associated with formate dehydrogenase (^{fdh}b) (428). The *b*-type cytochromes of cells grown on glycerol plus nitrate were first resolved potentiometrically by Reid and Ingledew (416) who reported three *b*-type cytochromes with EM_7 values as follows: $^{nr}b_{556}$, +10 mV; b_{555}, +140 mV; and b_{558}, +250 mV). Later work (190, 191) also resolved cytochrome ^{fdh}b (Em_7 = −113 mV) in membranes from cells grown with glucose and nitrate. As with the *b*-type cytochromes of aerobically grown cells, there is some disagreement on precise values for the midpoint potentials. Hackett and Bragg (190, 191) confirmed the designations of ^{nr}b and ^{fdh}b by their studies on mutants lacking these activities.

There is also some controversy over the presence of one or both of the oxidase pathways in these membranes. Reid and Ingledew (416) detected only one oxidase pathway ($b_{555} \rightarrow b_{558} \rightarrow d \rightarrow O_2$), which was also the only oxidase pathway found in membranes from cells grown with glycerol plus fumarate. Crispin et al. (95) also concluded that cytochrome *d* is the main oxidase in these membranes, but they detected a small amount of cytochrome *o*. In contrast, Hackett and Bragg (190, 191) detected only the cytochrome *o*-terminated pathway in most of their strains and under their growth conditions (cytochrome *d* was present in some strains). It is known that in membranes from nitrate-grown cells the spectral α band of cytochrome *d* is shifted and is smaller in amplitude than in membranes from cells grown under other conditions. Whereas some authors speak of repression and derepression of the cytochrome *d* pathway, others have suggested that the changes in this α region in nitrate-grown cells are due to the formation of a heme · NO (or related) compound, the NO being derived from nitrate and nitrite reductase activities (W. J. Ingledew, J. A. M. Hubbard, M. N. Hughes, and R. K. Poole, unpublished data). In this context, it is interesting to note that the mutant strains reported by Hackett and Bragg (190) as containing cytochrome *d* lack both nitrate and nitrite reductase activities.

Pre-steady-state (196) and steady-state (95, 196) studies on the *b*-type cytochromes of *E. coli* have been reported. In the pre-steady-state (stopped-flow) analysis, the cytochrome *b* pool behaved as a single component on rapid mixing with either nitrate or oxygen. With nitrate as oxidant, about one-third of the oxidizable total of cytochrome *b* was oxidized, with a t½ of 300 ms. With oxygen as oxidant, two-thirds of the oxidizable cytochrome *b* was oxidized, with a t½ of 50 ms. These two processes were additive when both oxygen and nitrate were added together. The faster (t½ ≈ 50 ms) phase was sensitive to CO and the slower phase was sensitive to azide. Nitrate caused extensive oxidation of a cytochrome b_{556}, presumably ^{nr}b. Oxygen, but not nitrate, oxidized cytochrome *d*. Cytochromes absorbing at 558, 556, and 555 nm and constituting two-thirds of the oxidizable cytochrome *b* (and presumably lacking $^{nr}b_{556}$) were oxidized as a single pool by oxygen. The kinetics of cytochrome *d*

oxidation (α band) were very complex; initial oxidation was followed by apparent re-reduction and a second phase attributed to oxidation was followed by a second reductive phase, all these processes being relatively slow. It is possible that these curious kinetics are related to the spectral modification of cytochrome *d* in such membranes (see above) or inappropriate choice of wavelength pairs (see later). During steady-state substrate oxidation, all of the oxidizable cytochromes were oxidized by oxygen (part of the change being quite slow). Addition of both oxygen and nitrate together did not further oxidize the *b*-cytochromes and addition of nitrate alone oxidized about two-thirds of the total. That part which was not oxidizable by nitrate contained some b_{558}, b_{556}, and b_{555}. Thus, in the steady state, it seems that ^{nr}b can be oxidized by oxygen, although its oxidation to a steady state appears slow (cf. traces a and b in Fig. 4 of reference 196). Cytochrome b_{558} is known to be closely associated with cytochrome *d* and so it is not surprising that it was also not oxidized by nitrate (95, 335, 417). The rate of oxidation of cytochrome *d* and its associated cytochrome *b* was much faster in membranes from fumarate-grown cells ($t_{1/2} < 3$ ms) and so the $t_{1/2}$ (50 ms) for the whole *b* pool in the "nitrate membranes" may be imposed by a rate limitation on the modified cytochrome *d*.

A detailed steady-state analysis (95), using the quinone analog HOQNO as an inhibitor, extended earlier work (428) and showed that, in addition to inhibiting between cytochrome ^{nr}b and ^{fdh}b, the compound could inhibit between cytochrome b_{558} and *d* and between ^{nr}b and nitrate (molybdenum). By analogy with other systems, this may imply a role for quinones in these regions of the electron transport chain. Such complex HOQNO effects have been considered in other systems as evidence for a Q-cycle (338). A Q-cycle is thus a possibility in *E. coli*, but we do not invoke it because an analysis of the relevant chemiosmotic parameters leads to the conclusion that the simpler schemes shown adequately explain the data.

OXYGEN-DEPENDENT RESPIRATORY CHAINS

This section deals with those cytochromes and other components that are believed to function in respiratory electron transfer to oxygen as terminal acceptor. There is some justification for this approach, rather than discussing in turn those cytochromes synthesized "aerobically" and "anaerobically." Regrettably, growth conditions are frequently poorly controlled or described or both, and it is far from certain that the concentration of oxygen in the medium is the predominant factor in regulating the composition of the chains.

Three cytochrome types (*o*, *d*, and a_1) are known, or believed by some, to react with oxygen and to function as terminal oxidases. More extensive reviews of these cytochromes are by Poole (376, 377).

Cytochrome *o*

Photodissociation spectra demonstrated the light sensitivity of the CO complex of a *b*-type cytochrome (for references, see reference 377), and action spectra (58, 59) showed that a protohemin enzyme acted as a major functional oxidase in *E. coli* and several other bacteria. The enzyme was called cytochrome *o* (59) (for oxidase). Establishment of its presence under all growth conditions requires confirmation by action spectra, even though its synthesis is sometimes regarded as constitutive (177, 198). Synthesis is clearly regulated as a function of growth conditions (190), but there is no report of a cytochrome *o*-deficient strain.

In *E. coli*, the presence of cytochrome *o* is generally determined from spectral changes in spectra of the difference between a reduced sample and a similar sample sparged with CO ("reduced plus CO minus reduced"). Peaks corresponding to absorption of the CO adduct are seen at about 416, 535 to 538, and 567 nm. A major trough in the Soret region in such spectra at 430 to 436 nm is attributed to loss in absorbance of the reduced form on binding CO. Photodissociation spectra suggest that the α-band is small or appears to be little affected by CO (380, 381, 392, 393, 441). Attempts, by higher-derivative analysis, to determine which of the α-bands attributable to *b*-type cytochromes is due to cytochrome *o* were unsuccessful (442). Potentiometric analysis (416) suggested that the α-peak was at 557 nm (at 77°K) and titrated with a midpoint potential of +80 mV (see, however, K. Miki, Fed. Proc. **34**:577, 1975). The weight of current evidence suggests that cytochrome *o* is of relatively high potential and may have a split α-band. Such a *b*-type cytochrome has been resolved with a midpoint potential of +250 mV (416).

A CO-binding pigment spectrally resembling cytochrome *o* has been purified from *E. coli* incubated with excess δ-aminolevulinic acid (223). This pigment deserves further study.

Cytochrome *o* from *E. coli* has recently been purified (275, 277), after Sarkosyl and cholate solubilization. On reconstitution into liposomes (276), the oxidase complex generated a membrane potential (−145 mV) on addition of ubiquinol-1 or ascorbate plus phenazine methosulfate (PMS); this does not necessarily indicate that any proton translocation occurs. The later preparation of Matsushita et al. (323) involved initial treatment of membranes with urea and cholate, the residue from which was solubilized with octyl-β-D-glucopyranoside (see also reference 482). Four silver-stainable bands of M_r 55,000, 34,000, 21,000, and 14,000 were observed on SDS-polyacrylamide gels. The M_r of the largest subunit was reassessed as 68,000. Two *b*-type cytochromes were present. CO bound to the reduced enzyme, but it is not clear whether both or only one of the spectrally distinguishable cytochromes bound the ligand. The heme *b* content (19 to 20 nmol mg of protein^{-1}) was slightly higher than in the earlier preparation by Kita et al. (275–277).

Matsushita et al. (323) described the formation of proteoliposomes by detergent dilution of the oxidase and purified *lac* carrier protein, followed by freeze-thawing and sonication. The system was found to generate a Δp (interior negative and alkaline) with ubiquinol as electron donor. The magnitude of the potential was dependent upon cytochrome *o* concentration. The extent of "uphill" lactose transport was in turn dependent on the magnitude of Δp.

Complementary results have been obtained by preparation of monospecific antibodies against cytochrome *o* and their use to purify the oxidase (289). The antiserum was capable of quantitatively precipitating ubiquinol-1 oxidase activity in Triton X-100 extracts of membranes from a cytochrome *d*-deficient mutant (see below). Four subunits (M_r = 51,000, 28,500, 18,000 and 12,700, respectively) were found in approximately equal stoichiometry; 77°K spectroscopy of the immunoprecipitate showed peaks at 555 and 562 nm.

The characteristic binding of CO by cytochrome *o* has been studied after flash photolysis of the CO compound at subzero temperatures. The technique (60) requires that the sample be prepared in 30% ethylene glycol to allow oxygen to be introduced while the sample is still fluid at about −25°C. Flash photolysis of the CO-liganded, substrate-reduced cytochrome *o* in intact cells of aerobically grown *E.*

coli, and comparison with the prephotolysis state, yields the photodissociation difference spectrum of the oxidase (392, 393, 441). At temperatures below about 90°C, and in the absence of O_2, recombination of CO is immeasurably slow, although at this temperature oxygen reacts to form an early reaction intermediate. At higher temperatures, repetitive wavelength scanning or multiwavelength time-sharing spectrophotometry show pseudo-first-order kinetics (392, 393). In cells from oxygen-limited cultures, the low-temperature photodissociation spectrum (381) gives a peak due to the γ-absorption maximum of unliganded cytochromes at 436 nm rather than 432 nm. Thus, in these cells, cytochrome *o* may be modified spectrally and kinetically (see below); it remains to be seen whether the two forms can be distinguished structurally.

There is little information on the reaction of other ligands with *o*-type cytochromes. Cytochrome *o* is more sensitive to cyanide than is cytochrome *d* (401).

E. coli is one of the relatively small number of bacteria in which cytochrome *o* has been unequivocally established as a functional terminal oxidase (59, 120). The low apparent K_m values (95, 418) are consistent with this role, as are direct observations of the oxygen-binding reactions at subzero temperatures. Multiwavelength kinetic recordings after flash photolysis of CO-liganded cells in the presence of oxygen reveal heterogeneous oxidation of *b*-type cytochromes between −79 and −102°C (393), with no evidence for the involvement of cytochrome *d*. Below about −100°C, only cytochrome *o* is oxidized and the reaction proceeds via formation of an intermediate with spectral properties similar to the CO compound, but which is light insensitive. The reaction affords an interesting comparison with the analogous formation of "compound A" by mitochondrial cytochrome a_3 (61, 377). The formation of the cytochrome *o* intermediate proceeds virtually irreversibly at about −100°C and may be regarded as an effective, oxygen-trapping strategy (376). This intermediate is believed to be an "oxy" or "oxygenated" species (i.e., $Fe^{2+} \cdot O_2$ or $Fe^{3+} \cdot O_2^-$; 478), on the basis of its optical absorbance properties and by analogy with the oxygen compounds of other hemoproteins.

The CO-binding pigment with a γ-absorption band at 436 nm, seen in cells from oxygen-limited cultures, has been shown (381) to be an *o*-type cytochrome, and not cytochrome *d* (see reference 418), on the basis of the insensitivity of its CO complex to laser irradiation at 633 nm. This cytochrome o_{436} reacts with oxygen at subzero temperatures approximately 10-fold faster than does cytochrome *o* in cells grown aerobically, suggesting that its synthesis represents an adaptation to lowered oxygen availability.

The subsequent reactions of the oxygenated intermediate of cytochrome *o* are poorly understood, due largely to the spectral similarity of the various *b*-type cytochromes that constitute the cytochrome *o*-terminated electron transport chain. Some success has been obtained by forming a mixed-valence respiratory chain (cf. reference 62) in which all *b*-type cytochromes, except the CO-liganded cytochrome *o*, are oxidized by ferricyanide before photolysis (R. K. Poole, unpublished data).

The product of oxygen reduction by cytochrome *o* has not been established. However, preliminary experiments have failed to detect peroxide as a product or as a free intermediate. Both rate and stoichiometric considerations of the NADH-dependent oxygen uptake suggest that four electrons are transferred to oxygen, generating water (R. K. Poole and D. O'Hara, unpublished data). In addition, Matsushita et al. (323) noted that proteoliposomes containing high ratios (5:1) of cytochrome *o* to the *lac* carrier exhibited depressed capacity for transport, an effect that could be largely prevented by adding superoxide dismutase but not peroxidase or catalase. Superoxide anion, therefore, must be one product of either ubiquinol oxidation or oxygen reduction.

Cytochrome *d*

Cytochrome *d* (previously called cytochrome a_2) is the alternative major oxidase of *E. coli* and appears to be synthesized coordinately with cytochrome a_1 and cytochrome b_{558}. Cytochrome *o* persists under some of the conditions that favor synthesis of cytochrome *d* and which include the following: low oxygen tension (225, 288, 340, 418, 442); attainment of the stationary phase of growth on nonfermentable carbon sources (288, 402, 447); aerobic growth with glucose (201); anaerobic growth (196, 201; see, however, reference 224); growth in the presence of cyanide (16); growth under sulfate-limited conditions (383; see, however, reference 125); in certain *chl* mutants, which lack both *b*-type cytochromes involved in the formate dehydrogenase/nitrate pathway (191); in mutants defective in cyclic AMP or catabolite-gene activator protein (103); and in "gradostat" cultures (opposing gradients of glucose and of oxygen plus nitrate [306]). Strains carrying apparently unrelated mutations in respiratory metabolism sometimes have elevated levels of cytochrome *d* (90).

The enhanced synthesis of cytochrome *d* may have deleterious effects on the efficiency of oxidative phosphorylation in *E. coli* (328) and in *Enterobacter aerogenes* (395). Despite this, growth competition experiments (236) show that, under oxygen-limited conditions, organisms containing cytochrome *d* displace potential competitors having cytochrome oxidase *o* or aa_3. This can be rationalized by the higher oxygen affinity of cytochrome *d* (418; see below).

The spectral properties of cytochrome *d* are quite distinctive and arise from the presence of the chlorin heme (22). Reduced preparations show an absorbance maximum at 628 to 632 nm, which is shifted by approximately 5 nm further to the red in the presence of CO. Aeration of cell or membrane suspensions containing cytochrome *d* results in a further shift of the peak to 648 to 652 nm. It has been widely assumed that this latter narrow band arises from the ferric form (265), but more recent evidence (384, 386) suggests that it should be attributed to a stable oxygenated compound of cytochrome *d* (379, 403). Early evidence that the Soret band is weak and diffuse has been supported by: (i) photodissociation spectra at 4°K (390); (ii) selective photolysis by a He-Ne laser of the CO complex of cytochrome *d* (381); (iii) lack of correlation between the intensities of the α-band and putative Soret bands in photodissociation spectra in the absence or presence of oxygen (381); (iv) the assignment of a band at 448 nm to cytochrome a_1, not *d* (389). These lines of evidence are discussed at greater length in reference 377. A further absorption band at 675 to 680 nm is possibly also attributable to cytochrome *d*. This has also been detected in *Azotobacter* spp. (262) and appears during the course of oxidation of *E. coli* "cytochrome d_{650}" at subzero temperatures (386). Its origin is unknown.

The EPR spectrum of cytochrome *d* in *E. coli* has not been described in detail. In *Azotobacter* spp., ferric heme resonances at $g = 6.20$, 5.80, and 5.48 (108) have been resolved into axial and rhombic components and attributed to cytochrome *d*. Ingledew (unpublished data) has found that cytochrome *d* is high spin, as is cytochrome b_{558}. The former is axial and the latter is rhombic, but there are complex relationships between these species.

Only recently has cytochrome *d* from *E. coli* been purified, although its solubilization with deoxycholate was reported (213) and a "green band" attributed to cytochrome oxidase in sucrose gradient centrifugation of deoxycholate-solubilized material (412) was active in reconstitution from soluble components of electron transfer from succinate to oxygen. Reid and Ingledew (417) partially purified an oxidase complex, but this contained at least three or four cytochrome types, namely, cytochrome *d*, cytochrome a_1 (trace), and two *b*-type cytochromes. A stoichiometry of equimolar amounts of two *b*-type cytochromes and 2 mol of cytochrome *d* was proposed. Recently, Miller and Gennis (335) have solubilized a cytochrome *d*-containing complex, using a zwitterionic detergent, and accomplished purification by chromatography with DEAE-Sepharose and hydroxyapatite. The complex contains cytochromes b_{558}, a_1, and *d* (288), yet consists of only two subunits with molecular weights of about 57,000 and 43,000. Only one type of cytochrome *b* was detected, but a small shoulder at 547 to 550 nm was observed which, it was suggested, could be an optical transition related to cytochrome a_1. CO bound to cytochrome *d*, perhaps to cytochrome a_1, and also to part of the cytochrome *b*. Binding to a *b*-type cytochrome could reflect the presence of some cytochrome *o* or perhaps denaturation of cytochrome *b*. Interestingly, CO also perturbed the spectrum of an air-oxidized sample, shifting the α-peak of the cytochrome *d* from 646.5 to 636 nm. This observation has previously been made with the membrane-bound "oxidized" cytochrome *d* of *Azotobacter vinelandii* (263). This unexpected finding is consistent with the designation (384) of the 646.5- to 652-nm form as an oxy (i.e., $Fe^{2+} \cdot O_2$) species. In the presence of detergents, the complex oxidized ubiquinol, tetramethyl-*p*-phenylenediamine, and diaminodurol. Protoheme IX and iron were detected, but not nonheme iron or copper. The inability to detect copper in the purified preparation, consistent with the previously observed absence of signals near 840 nm during cytochrome *d* oxidation in vivo (386) and with an early EPR study (307), precludes a role for copper in the oxygen reduction mechanism.

Reid et al. (415) have suggested that part of the cytochrome *d*-containing oxidase complex is assembled into the membrane in the absence of heme synthesis. Thus, the apoprotein of cytochrome b_{558}, but not of the other *b*-cytochromes once thought to be included in the complex (417), is detectable after reconstitution of membranes from a δ-aminolevulinic acid-requiring mutant with ATP and hematin.

Cytochrome *d* is unusually cyanide resistant and responsible for conferring cyanide insensitivity on *E. coli* and certain other bacteria. Indeed, its synthesis is induced by growth on a nonfermentable substrate in the presence of 0.15 mM KCN (16). In the presence of oxygen, cyanide binds to the reduced form of cytochrome *d*, eliminating its α-band (401). The report that a Soret band at 442 nm also disappears may suggest that cytochrome a_1 also binds cyanide, since there is substantial evidence (see above) that the so-called cytochrome a_1 is the main contributor to this Soret band. Cyanide reacts with the form of cytochrome *d* that absorbs around 650 nm, without the formation of the reduced form (401). The original interpretation was that the 650-nm (oxidized) form reacted with cyanide to give cyanocytochrome *d* which had little or no absorbance in the α-band region. However, only under turnover conditions was the rate constant for disappearance of the oxidized form (0.58 M s^{-1}) close to that obtained from cyanide inhibition of NADH oxidase activity (401, 402). These and other data led to the proposal (401) that there exists an "invisible" form of cytochrome *d*, intermediate between the oxidized (648 to 650 nm) and reduced (628 to 630 nm) species, that was termed *d** and was the cyanide-binding form:

$$\begin{array}{c} {d_{648}}^{ox} \rightleftharpoons d^* \rightleftharpoons {d_{648}}^{red} \\ \text{HCN} \downarrow \\ d^* - \text{HCN} \end{array} \qquad (2)$$

Similar intermediates have been proposed for cytochrome *d* of other bacteria (377).

In addition to cyanide, cytochrome *d* binds CO and perhaps other ligands. The reaction with CO is unusual in that the CO liberated from photolysis of the CO complex at subzero temperatures immediately recombines with the reduced enzyme unless the photolysis is conducted at temperatures close to that of liquid He (390). This feature, unique among cytochrome oxidases, may be due to the absence in cytochrome *d* of copper, which, in cytochrome aa_3, is believed to be the binding site for the photodissociated CO (9). However, other oxidases widely believed to lack copper, e.g., *E. coli* cytochrome *o*, exhibit ligand recombination kinetics at low temperatures (see above) similar to those of mitochondrial cytochrome oxidase aa_3 (61).

Meyer (327) reported that nitrite, when added to reduced membrane particles, gave a difference spectrum that was indistinguishable from that produced by NO in the 610- to 720-nm region. Differences below 610 nm and especially in the Soret, however, indicated reaction with cytochrome *o* or a_1 or both. Recently we (J. A. M. Hubbard, M. N. Hughes, and R. K. Poole, unpublished data) have confirmed and extended these findings. NO_3^-, NO_2^-, $N_2O_3^{2-}$ (trioxodinitrate), and NO all react with reduced membrane particles causing diminution and shifting of the 630-nm peak to 641 to 645 nm. The rapid reduction of trioxodinitrate is of special interest, since this compound has long been postulated as an intermediate in microbial denitrification; reaction probably occurs between cytochrome *d* nitroxyl ion, produced in the self-decomposition

$$HN_2O_3^- \rightarrow HNO + NO_2^- \qquad (3)$$

Thus, it seems likely that all four compounds result, albeit at different rates, in formation of the nitrosyl species. In contrast, Bragg and Rainnie (46) found that $AgNO_3$, but not $NaNO_3$, reacted with cytochrome *d*; the discrepancy is unresolved.

The midpoint potential of cytochrome *d*, measured at the absorbance maximum of the reduced form, is +260 to +280 mV ($n = 1$) (404, 416) and does not appear to be affected by the conditions of growth (49). Even at potentials as high as +440 mV the 650-nm form does not appear unless oxygen is present (404) or unless the sample is cycled through a preliminary phase of air oxidation, followed by substrate reduction. Under the latter conditions (215), the absorption bands at about 630 and 650 nm exhibit very unusual and complex behavior which to date has been interpreted only by invoking concerted four-electron transport by cytochrome(s) *d*.

Cytochrome *d* has been identified as a functional terminal oxidase (59, 196). Unusual multiphasic reaction kinetics, however, were observed when cells grown anaerobically with glycerol and nitrate were mixed with oxygen and monitored at 655 to 630 nm (196; see above). These studies require reexamination in view of the suggestion that the

component absorbing at about 655 nm is an oxygenated intermediate and not a direct oxidation product of the reduced form absorbing at 630 nm. In addition, the absorption maximum of the reduced species in such cells has an α-band at 634 nm, displaced ≈10 nm to the red from the form synthesized under other anaerobic conditions (196, 416). An explanation may lie in the affinity of cytochrome *d* for nitrite or other nitrogen compounds, which also shift the α-band further towards the red (see above). The reported K_m for cytochromes *d* of *E. coli* is 0.024 μM (418).

In contradiction to the view that cytochrome *d* is a high-affinity oxidase, Crispin et al. (95) have described kinetic experiments in which cytochrome *d* reduction was monitored at 630 minus 615 nm after addition of formate to an aerobic suspension of membranes from cells grown anaerobically with nitrate. Reduction of cytochrome *d* commenced after 1 min, during which time oxygen tension fell from 240 to 30 μM, and was accompanied by an almost instantaneous reduction of one cytochrome *b* pool and the subsequent slower reduction of a second. When dissolved oxygen became undetectable and cytochrome *d* reduction was complete, a phase of cytochrome *d* reduction was still extant and was attributed to "reduction of a cytochrome having a great affinity for oxygen," tentatively identified as cytochrome *o*. A K_m of 32 μM was attributed to cytochrome *d*. Although these results tend to support the conclusion (196) that cytochrome *d* in nitrate-grown cells exhibits curious reaction kinetics with oxygen, it would be desirable to make independent measurements of the oxygen affinities of the oxidase in such cells with a more conventional approach.

Low-temperature trapping and ligand exchange techniques and consideration of the curious behavior of cytochrome *d* in kinetic and potentiometric experiments have recently led to the hypothesis that an early product of the reaction with oxygen is a relatively stable intermediate, absorbing at about 650 nm and probably erroneously described previously as the oxidized form. The argument is advanced in detail elsewhere (377, 379, 384, 386, 403, 404).

The interpretation of the optical, EPR, and resonance Raman spectra favored by Poole and his collaborators is that cytochrome d_{650} is an oxygenated form and an intermediate in the oxidoreduction of cytochrome *d*, whereas the oxidized ferric form should be equated with the "invisible species" described by others.

$$d_{630}^{red} \overset{+\,O_2}{\rightleftharpoons} d_{650} \rightleftharpoons d^{ox} \overset{HCN}{\rightleftharpoons} d\text{-CN} \quad (4)$$

("invisible")

A more detailed scheme is presented in references 377 and 384.

Since the heme of d_{650} is formally in the ferrous state (478), CO might be expected to displace O_2 and form carbonmonoxycytochrome *d*. This has indeed been observed for both the *Azotobacter* sp. (263) and *E. coli* (335) enzymes.

The implications of designating cytochrome d_{650} as an oxygenated form are far-reaching. It casts doubt on all measurements of the extent of oxidation or reduction of cytochrome *d* where redox state has been quantified from peak-trough differences (i.e., approximately 630 minus 650 nm) and permits the reinterpretation of many experiments (384).

An additional previously unexplained finding is that the wavelength of the absorbance maximum of cytochrome *d* appears to vary with protein concentration of the sample, i.e., the magnitude of the difference in absorbance between the cytochrome *d* spectral peak and trough (448). During a study of gene dosage effects on cytochrome levels, it was noted that peak height was proportional to protein concentration, provided that the peak height was measured at its maximum, irrespective of its position. The peak shifted from 633 nm at low concentrations to 626.5 nm at high protein concentrations. Inspection of the spectra (448), however, reveals that the trough depth in the latter, concentrated samples was more prominent, relative to the peak height, than in the dilute samples. This is inconsistent with the trough being the oxidized form, but can be explained by proposing that the oxygenated form is stabilized at high protein concentrations and that its spectrum, centered at about 650 nm, interferes with that of the reduced form in difference spectra and shifts this maximum to the blue.

The extreme stability of the presumptive oxy form is notable by comparison with the elusive oxygen intermediates formed by cytochromes aa_3, but not unprecedented. A similarly stable oxygenated intermediate has been described for the cytochrome *o* of *Vitreoscilla* spp. (for a review, see reference 166).

Until recently, there were no published accounts of the isolation of cytochrome *d*-deficient mutants, although such mutants appear to have been found (J. A. Downie, personal communication). Other devices have therefore been used to eliminate cytochrome *d*, allowing the properties of cytochrome *o* as a terminal oxidase to be investigated. These include: (i) exploiting the requirement in the medium of dehydrostreptomycin for synthesis of cytochrome *d* (and a_1) by streptomycin-dependent strains (45); (ii) irradiation of membranes with near-UV light (emission maximum, 360 nm), claimed (41) to destroy cytochrome *d* with little effect on cytochromes *o* and "b_1," although quinones have been proposed as more likely targets (293); (iii) hematin-dependent reconstitution of a heme-deficient mutant, which excludes reconstitution of a functional *d*-type oxidase (415; W. J. Ingledew and B. A. Haddock, unpublished data).

Green and Gennis (179) have used a screening procedure that permits the isolation of cytochrome *d*-deficient mutants by their inability to oxidize tetramethyl-*p*-phenylenediamine. The intrinsic impermeability of cells to this artificial electron donor was overcome by freezing and thawing colonies on agar plates before overlaying with soft agar containing tetramethyl-*p*-phenylenediamine. One such mutant lacked cytochromes a_1, *d*, and b_{558}, supporting the idea that all three cytochromes form part of an alternative oxygen-dependent respiratory complex. The mutant had an increased sensitivity to cyanide, in accordance with the known inhibitor response of cytochrome oxidase *d*. A single lesion in a gene designated *cyd* (at 17 min) and mapping between *tolA* and *sucB* appears to be responsible for the mutant phenotype.

Cytochrome a_1

An α-band, generally weak and lying in the 585- to 595-nm range of reduced-minus-oxidized difference spectra, has been attributed to cytochrome a_1, although other hemoproteins and free protoheme could also be responsible for such a band (377). The γ-band, however, is reminiscent of an *a*-type cytochrome at 440 to 445 nm, although frequently attributed to cytochrome *d* (see above). The role of cytochrome a_1 in *E. coli* is obscure. Photochemical action spectra (59), with one exception (120), and stopped-flow kinetic studies (196) have failed to demonstrate an oxidase function for this hemoprotein (for a discussion, see reference 377). Despite the paucity of knowledge on its composition and ligand-binding proper-

ties and the divergence of published values for its midpoint potential (215, 404, 416), it is frequently depicted in schemes of the respiratory chain (42, 215) and described as an oxidase (253). It is generally assumed to bind CO (196, 481), as does cytochrome a_1, in certain other bacteria such as *Acetobacter* spp. (59, 328). However, a more recent investigation of cytochrome a_1 in *E. coli* (416) described the ineffectiveness of CO in influencing the behavior of this cytochrome in redox titrations and it was suggested that it does not bind CO, ruling out the possibility that this pigment is an oxidase in *E. coli*.

Subsequently, Poole et al. (389) demonstrated that CO decreased the intensity of the α- and γ-bands of a cytochrome a_1-like pigment in intact cells from oxygen-limited cultures. Dual-wavelength scanning spectrophotometry at subzero temperatures revealed a flash-dissociable CO complex with a broad band around 595 nm attributed to a_1. If this cytochrome acts as an oxidase in *E. coli*, it should have been detectable in the photochemical action spectra of Castor and Chance (59). The possibility that CO is binding to inactive or denatured hemoprotein cannot be ruled out, however. "It has been stated that 'there is no known example of a CO-binding pigment that does not also react with oxygen' (265). However, a pigment can function as a terminal oxidase only if it is kinetically and thermodynamically competent to participate in electron flow to oxygen" (219).

Cytochrome a_1 in anaerobically (with fumarate or nitrate) grown or aerobic cells apparently titrated as two components that contributed equally to the total spectral change, with Em_7 values (n = 1) of +260 and +160 mV (416). The former potential, however, may be attributed to interference of the (small) spectral changes in cytochrome a_1 caused by the neighboring (intense) absorption of cytochrome *d*. Much lower values (−9 to −25 mV; n = 1) have also been reported (215). Apart from differences in the growth conditions used and slight inconsistencies in choice of redox mediators, there appears to be no apparent cause for these markedly different results.

No growth conditions are known in which the synthesis of cytochrome a_1 is not accompanied by cytochrome *d* and, probably, characteristic *b*-type cytochromes. Indeed these three components appear to copurify. Since most a_1-type cytochromes described thus far, in *E. coli* and other organisms, bind CO but only a few appear to be oxygen reactive, other ligands that could act as terminal electron acceptors require investigation. There is some evidence that nitrite (or a ligand derived therefrom) binds to cytochrome a_1 in *E. coli* membranes (327); nitrate and nitrite appear to bind to cytochrome a_1 in other bacteria (377). Further consideration should be given to the possibility that other hemoproteins contribute to the optical signals generally attributed to cytochrome a_1 (377), especially since there is no convincing evidence for the presence of heme A in *E. coli*.

Recently, a CO-binding hemoprotein having spectral properties similar to those generally attributed to cytochrome a_1 (maxima in the reduced form at 440 and 590 nm) has been solubilized and purified from anaerobically grown cells (B. S. Baines, H. D. Williams, J. A. M. Hubbard, and R. K. Poole, manuscript in preparation). The preparation lacks copper. The only heme detectable is protoheme, and the preparation has high catalase and cytochrome *c* peroxidase activities. These findings suggest a high-spin b-type cytochrome, perhaps a hydroperoxidase that could be confused with a_1. A membrane-associated hyperoxidase, in association with an oxidase such as cytochrome *d*, could serve to ensure complete reduction of oxygen to water.

b-Type Cytochromes (Excluding Cytochrome *o*)

Fourth-order finite difference analysis of low-temperature spectra has shown that the α-band previously, and still occasionally (42), attributed to cytochrome b_1 is a composite of the bands of five or more different pigments, tentatively assigned to at least two different *c*-type and three *b*-type cytochromes (447). The problems of interpreting such analyses are discussed elsewhere (53, 326, 391). Nevertheless, there is agreement from three independent studies, using these methods (442, 447, 484), that the α-absorption band observed in reduced-minus-oxidized spectra of aerobically grown cells, or membranes derived therefrom, is composite. Table 6 shows that three major components with similar absorption maxima (555.6, 560, and 563.5) were detected in two such numerical analyses (442, 447), albeit using somewhat different differencing intervals. Low-temperature spectroscopy of samples trapped during the course of a redox titration led to a similar conclusion (416) and also provided Em values for the 556-nm (+80, +260 mV), 558-nm (−50 mV), and 563-nm (+260 mV) components. A more sophisticated analytical technique (444), which integrated spectrum deconvolution with potentiometric analysis, revealed four major cytochromes *b*, of which two were separated in their absorption maxima by only 1 nm (555.7, 556.7), yet exhibited discrete midpoint potentials. This is consistent with the description in reference 416 of two components titrating at 556 nm. There is also general agreement between the potentials reported by these two groups for the 558-nm component (low potential) and 563-nm band (high potential). It is possible that the highest-potential component (+260 mV; 416) has a split α-band. Titration of such a component is affected by the presence of CO, suggesting that it may be cytochrome *o* (416). Further heterogeneity of the 555.5-nm band is suggested by the presence of a component that can be removed from the membrane by washing with a buffer of

TABLE 6. Spectral and potentiometric resolution of *b*-type cytochromes in aerobically grown *E. coli*

Shipp (447) (λ_{max} [nm])	Reid and Ingledew (416)		Scott and Poole (442)		Van Wielink et al. (484, 485)		Hackett and Bragg (190)[a]	
	λ_{max} (nm)	Em (mV)	Small intervals (λ_{max} [nm])	Shipp's intervals (λ_{max} [nm])	λ_{max} (nm)	Em (mV)	λ_{max} (nm)	Em (mV)
556	556	+80 +260	555.5	555	555.5–555.7 556.7–556.8	+46–+48 +174–+162	555	+129
560	558	−50	560		558.4–558.6 (560.2)	−75 (+169)[b]	556	−43
565	563	+260	563	563	563.5	+18–+176	562	+196

[a] Solubilized "b_{555}–b_{562} complex."
[b] Minor component described in reference 484.

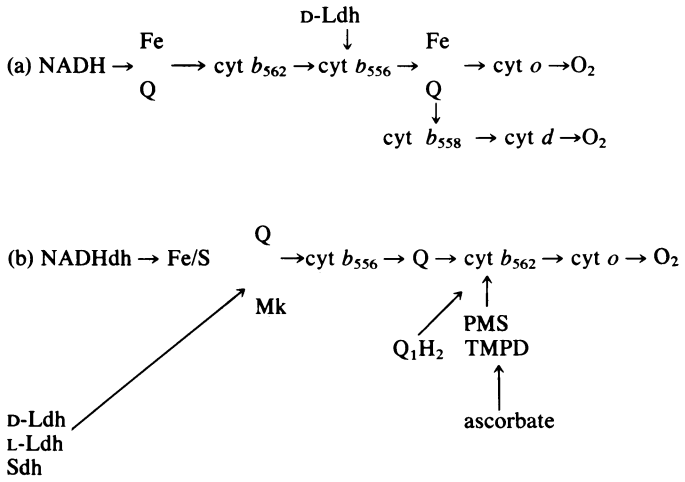

FIG. 10. Sequence of *b*-type cytochromes relative to ubiquinone proposed in references (a) 115 and (b) 275. cyt, Cytochrome; Q, ubiquinone; MK, menaquinone; Ldh, Lactate dehydrogenase; Sdh, succinate dehydrogenase; TMPD, tetramethyl-*p*-phenylenediamine.

low ionic strength (442). It is not clear whether the band observed in "aerobically grown" cells around 558 nm is equivalent to the cytochrome b_{558} associated with cytochrome *d*.

Other potentiometric titrations clearly indicate multiple *b*-type cytochromes, but with conflicting details. Thus, there are reports of three (216) *b*-type cytochromes (−50, +110, and +220 mV) or two (404) with midpoint potentials of +36 and +165 mV. Spectral resolution of the potentiometrically distinct forms was not achieved (cf. Table 6). More recently, Hackett and Bragg (190) have reported three midpoint potentials for *b*-type cytochromes in aerobically grown cells, namely, +195, +69, and −100 mV, corresponding well with the values (+186, +57, and −105 mV) obtained by using automated electrodic potentiometry (211, 215). Kinetic experiments, both at subzero temperatures (393) and using stopped-flow spectrophotometry (196), also reveal multiple *b*-type cytochromes or perhaps kinetically distinct pools.

In summary, membranes from cells grown under aerobic conditions, where the contribution from components of the "low aeration" respiratory chain is minimal, contain cytochrome *o* plus two to four other *b*-type cytochromes distinguishable by their potentiometric and spectral properties. Their individual functions and their sequence in electron transfer from dehydrogenases to oxidases has been the subject of several studies (for a detailed survey, see reference 42) with conflicting results. The more recent schemes recognize that cytochromes *o* and *d* are both oxidases and may be associated with different pools of *b*-type cytochromes (41, 201, 269, 345). Since the publication of Bragg's review (42), Downie and Cox (115) have presented evidence, exploiting a ubiquinone-deficient mutant and assaying steady-state reduction levels of cytochrome, that quinones are involved at two points and that the order of *b*-type cytochromes in the electron transfer chain is as shown in Fig. 10a. These data are consistent with earlier data (90), but are not supported by the majority of published midpoint potentials of these cytochromes (Table 6). Also, a similar approach (275) has yielded different conclusions (Fig. 10b). Support for the scheme in Fig. 10b is that "cytochrome *o*" copurifies with "cytochrome b_{562}" (high potential; see above), indicating their close association as a respiratory oxidase complex. In the presence of a suitable mediator, ascorbate does reduce a cytochrome with an absorption maximum at 556 nm but, on the basis of CO binding studies, this component is believed to be cytochrome *o*. It should be noted that, although the value of the Em_7 for cytochrome b_{556} found in reference 277 is −45 mV and thus different from that in Table 6, there is agreement with Table 6 in that the location of cytochrome b_{562} in the scheme of reference 275 requires that it has a more positive potential than b_{556}. The midpoint potential (+196 mV; Table 6) assigned elsewhere to b_{562} (in a solubilized *o*-containing complex [190]) also favors its location near O_2. This complex also contained b_{555} (+129 mV) and traces of b_{556} (−43 mV); neither of these was thought to be cytochrome *o*, which must, it was felt, have a weak or broad α-band (or both) in the reduced state as suggested previously (441, 442).

Multiple *b*-type cytochromes have been detected kinetically in membranes from *E. coli* anaerobically grown with NO_3^- (95; see above). In addition to cytochrome *o*, a b_{558} component was proposed to function as the immediate electron donor to cytochrome *d* in an oxygen-dependent electron transfer pathway. The coexistence of cytochromes of the aerobic and anaerobic nitrate-reducing pathways has been confirmed recently (190, 191). Shipp (447) found that the same five bands (attributed to two *c*- and three *b*-type cytochromes) were detectable, albeit in different proportions, under all growth conditions examined. In contrast, a similar analysis (442) found only two bands in membranes from oxygen-limited cells at 555.5 and 559 nm. Spectrally similar components were detectable in cells grown anaerobically with glycerol and fumarate with the addition of (probably) *c*-types at 548 and 550.5 nm. Additional evidence for the presence of two cytochromes *b* in oxygen-limited cells and their role in electron transfer to cytochrome *d* has come from observation of the time course of cytochrome oxidation at subzero temperatures (386). Further analysis by spectral deconvolution of variously grown *E. coli* is presented in reference 485.

There have been several attempts to purify the *b*-type cytochromes from *E. coli*. An important caveat in describing this work is that growth conditions have rarely been defined or at least described satisfactorily, so that attribution of the purified preparation to the fully aerobic or oxygen-limited respiratory chain is problematic.

TABLE 7. Cytochromes attributed to the *c* type resolved in *E. coli* membranes (λ_{max} [nanometers])

Shipp (447)		Scott and Poole (442)			Van Wielink et al. (484, 485)
Aerobic	Anaerobic[a]	Aerobic	Oxygen limited	Anaerobic[b]	(aerobic)
548	549	548		548	547 (+67–+71 mV)
		551.5		550.5	
552	553				

[a] Cells were grown with nitrate, in pennasay broth, or with glucose.
[b] Cells were grown with glycerol and fumarate.

Cytochrome b_{556} has been purified (277) from Sarkosyl-solubilized membranes, previously depleted of lactate dehydrogenase. The highly hydrophobic cytochrome is an oligomer composed of idential polypeptides each with M_r of ≈17,500. It contains equimolar amounts of heme and polypeptide. The α-absorption peak is at 556 nm (77°K) and its midpoint potential is −45 mV. It is unclear, therefore, which of the membrane-bound *b*-types in Table 6 corresponds to this purified enzyme. The preparation did not bind CO. Interestingly, the two major peaks elicited from Sephadex G-200 during preparation had α-absorption bands (at 77°K) at 554, 557, and 562 nm, and at 556 and 558 nm, again indicating the complexity of this group of cytochromes and suggesting a strategy for purification of the other components.

A cytochrome b_{562} has been purified from "soluble" subcellular fractions (202) and extensively characterized. It is not clear whether this component is truly soluble or is merely readily lost from membranes, since a cytochrome absorbing at this wavelength is observed in membrane particles (Table 6; also reference 16). It is a small molecule (M_r 12,000; 110 amino acids [228]) and contains a single noncovalently bonded iron protoporphyrin IX as the prosthetic group (220). Its midpoint potential is approximately +113 mV (227), lower than that of the membrane-bound b_{563}, and it has a pI of 7 to 8. Crystalline properties of oxidized cytochrome b_{562} have been reported (99, 100). A later study at 0.25-nm resolution showed the protein to consist of four nearly parallel α-helices with the heme group inserted between the helices at one end and the heme face partially exposed to solvent (322). In confirmation of earlier work (499), the two heme ligands are histidine and methionine. Sophisticated spectroscopic methods have yielded information on the spin states of the heme and conformational properties during redox and pH changes (51, 342). The coordination configurations appear identical to mitochondrial cytochrome *c*.

A component referred to as "cytochrome b_1" has been solubilized from membranes by prolonged sonication to yield a detergent-free, soluble preparation that has been purified and crystallized (105). At pH 7, the M_r is 500,000 and the protein contains 8 mol of iron protoporphyrin IX, giving a minimum monomeric M_r of approximately 60,000. Dissociation of the octomer at high pH into monomeric species is accompanied by a drastic change in midpoint potential from −340 to about 0 mV, a value which is also characteristic of cruder preparations (105, 136). During purification, the b_1 separates from a colorless protein which has been termed "potential-modifying protein." The readdition of this results in a rise of the midpoint potentials to higher values. The reduced form of cytochrome b_1 has absorption maxima at 425, 527.5, and 557.5 nm. The prosthetic group of cytochrome b_1 can be removed with acidified acetone and then reconstituted (136). Reconstitution is accompanied by spectral changes and acquisition of reactivity with CO. It seems probable that cytochrome b_1 corresponds to a low-potential cytochrome *b*, which was removed from the membranes by washing in buffer of low ionic strength (416). This has an α-band centered at 558 nm (77°K). A spectrally and potentiometrically similar component was detected in reference 484, whereas Scott and Poole (442) also described a loosely bound cytochrome *b*.

Cytochrome *c*

The composite α-absorption band of aerobically grown cells contains one or two peaks generally attributed to *c*-type cytochromes (Table 7). These findings, however, which are based on higher-derivative analysis, should be regarded with caution in view of the reservations presented elsewhere regarding this technique (53, 326, 391). These *c*-type cytochromes are partially reduced by NADH, succinate, and ascorbate plus PMS (404), but their function or location in the electron transport chain is unknown.

A cytochrome c_{552} is also found in anaerobically grown *E. coli* (498). The anaerobic enzyme has been purified and extensively studied (see "Nitrite Reductase"; 297). It has a role in anaerobic electron transport, particularly in nitrite reductase activity (302) or possibly formate hydrogenlyase activity (114). In addition, a cytochrome c_{552} was reported in aerated and "microaerobic" cultures (23). Inclusion of NO_3^- depressed its synthesis. The enzyme was partially purified but was observed to alter to a CO-binding form on cell breakage. A role as part of a sulfite-reducing system has been suggested.

Mutants of Heme Biosynthesis

In addition to those mutants defective in specific components of the oxygen-dependent electron transport chain, e.g., in cytochrome *d*, individual dehydrogenases, and quinones, discussed in the relevant sections here and also in references 193 and 194, particularly useful mutants are those affected in the *hemA* gene (mapping at 26 min) and deficient in synthesis of δ-levulinic acid, an intermediate in heme synthesis. Such mutants have been isolated in several laboratories, following the pioneering work of Sasarman et al. (435), and used to probe both the composition and function of the oxygen-dependent respiratory chain and the dependence on it of other presumptive energy-linked reactions (Table 8).

The 503-nm Pigment

Under certain growth conditions, a pigment absorbing at about 503 nm can be observed in reduced-minus-oxidized spectra of *E. coli* cells. Such conditions include growth aerobically in minimal media with glucose, lactate, or succinate as carbon source or anaerobically with glucose (356) and under iron-limited conditions (Hubbard et al., unpublished data). The absence of this pigment in complex media may be due to its repression by amino acids (348, 356). The

TABLE 8. Examples of uses of *hemA* mutants in analysis of the composition and function of the aerobic electron transport chain

Mutant	Inference	Reference(s)
A201	Cytochrome apoproteins are incorporated into membrane in absence of heme synthesis.	192, 201
A1004a	Energy-linked reduction of NAD^+ is independent of cytochrome-mediated electron transport.	302
A1004a	First proton-translocating region (NADH → UQ) is cytochrome independent: second (UQ → O_2) is cytochrome dependent.	197
A1004a	Reconstitution of oxidase activity is associated with formation of functional, H^+-translocating respiratory chain.	195
K207	β-Galactoside transport is driven by cytochrome-mediated respiration or ATP.	110
SASX76	Phenylalanine uptake and hydrogenase are driven by cytochrome-mediated respiration or ATP.	454
SASX76	Site of membrane energization exists between ubiquinone and oxygen.	456
SASX76	α-Methylglucoside uptake is inhibited by respiration-driven membrane energization.	457
SASX76	Heme synthesis is required for flagellum synthesis.	24
AN344	Cytochromes do not act as oxygen sensors in aerobic repression of nitrate reductase activity.	311
AN704	NADH-menadione reductase is unaffected by absence of cytochromes.	50
EB53	Uptake of iron as ferrichrome complex is cytochrome independent.	117
A1004a	Cytochrome synthesis is required for membrane orientation of Fe-S clusters.	32
A1004a	ATP is required for association of heme with apocytochrome *o*.	415

pigment is bleached by cyanide, azide, hydrazine, and dithionite and does not react with CO (356). These authors suggested that the compound was coprotetrahydroporphyrin and, although in kinetic equilibrium with flavoprotein, did not participate in the major electron flux of the respiratory chain. Streptomycin-dependent *E. coli* cells lack, or contain low levels of, the 503-nm pigment (259, 398), attributed by these authors to catabolite repression of protoporphyrinogen oxidase. It remains unclear what role the pigment plays in the electron transport chain, but in air-oxidized cells provided with gluconate as substrate the 503-nm pigment appears before cytochromes become reduced, suggesting that it might act as an electron acceptor from NADH (259).

Iron-Sulfur Centers of Aerobic Respiratory Chains

When grown aerobically, *E. coli* can synthesize a number of primary dehydrogenases, i.e., dehydrogenases directly linked to the respiratory chain without the intermediary of a soluble cofactor (NADH or NADPH). The amount of a specific primary dehydrogenase present is dependent on the carbon source used for growth. The specific activity of the NADH and succinate dehydrogenases is not greatly altered by growth on a range of different nonfermentable carbon sources (glycerol, malate, succinate, Casamino Acids, acetate, and lactate). Formate oxidase activity is lowest in membranes from succinate-grown cells and highest in membranes from Casamino Acid-grown cells. Lactate oxidase activity is greatly amplified in the membranes derived from lactate-grown cells compared with other membranes; similarly, glycerol-3-phosphate oxidase activity is greatest in membranes from glycerol-grown cells (M. C. Kirby and W. J. Ingledew, unpublished data).

Iron-sulfur centers in the respiratory chain are generally associated with specific dehydrogenases. In *E. coli* membranes, a ferredoxin-like EPR signal was first reported by Nicholas et al. (345), and subsequently by others (204, 213, 383). Poole and Haddock (383) reported that sulfate-limited growth had deleterious effects on energy coupling and the iron-sulfur center content of membranes. In a recent study of membranes from succinate-grown cells, Ingledew et al. (222) resolved four iron-sulfur centers, three of which could be assigned to succinate dehydrogenase, by analogy with other succinate dehydrogenases. Kirby and Ingledew (unpublished data) have shown that a greater complexity of iron-sulfur centers exists and that the iron-sulfur centers in membranes alter with growth substrate. Blum et al. (32) have studied, in *E. coli* grown aerobically on succinate, the orientation of the iron-sulfur clusters, specifically the centers attributed to succinate dehydrogenase, and report that the *g*-tensors of these centers have a fixed orientation to the membrane plane. Membranes derived from a hemeless mutant grown anaerobically on glucose contained an additional iron-sulfur center with a g_{xy} at 1.90, which also showed fixed orientation to the membrane plane. The centers attributed to the succinate dehydrogenase were not orientated in the hemeless mutant.

NITRITE REDUCTASE

In the absence of oxygen, *E. coli* can rapidly reduce nitrite to ammonia. At least three separate pathways contribute to this process: a soluble NADPH:sulfite reductase (EC 1.8.12) which also has a measurable activity with nitrite; a soluble NADH:nitrite reductase (EC 1.6.6.4); and a respiratory chain-linked (partially membrane-dependent) nitrite reductase. The respiratory chain-linked enzyme is the main consideration of this section. The others will be considered only briefly. The major product of nitrite reduction is ammonia (76). This is a six-electron reduction:

$$NO_2^- + 6e^- + 8H^+ \rightarrow NH_4^+ + 2H_2O \quad (5)$$

In the case of the NADPH:sulfite and NADH:nitrite reductase, the whole process is catalyzed by one enzyme. It is not known whether the entire reduction is catalyzed by a single terminal enzyme in the case of the respiratory chain system, but it is probable that the terminal enzyme is a periplasmic cytochrome c_{552} that can reduce nitrite to ammonia. The various steps of nitrite reduction will have different redox potentials but, as intermediates are not released or known, the values are unknown. Overall, the midpoint potential for the six-electron transfer reaction is +275 mV, a value between those of fumarate and nitrate couples and enough to support oxidative phosphorylation and give a $\Delta G^{0'}$ for NADH oxidation of −27,350 cal (ca. −113 kJ) mol^{-1}. Although the product of these pathways is ammonia, the control of the processes is such that they do not appear to have an assimilatory function, but rather the removal of catabolic reducing equivalents. The nitrite reductases are induced by nitrite and repressed by oxygen; ammonia is without effect (77, 229).

One common feature of all three pathways is the involvement of heme; no nitrite reduction occurs in *hemA* mutants. Mutants selected for the absence of NADPH:sulfite reduc-

tase and NADH:nitrite reductase have been isolated. One mutation in each case (designated *cysG* and *nirB*, both at 74 min) appeared in early studies to be at the same locus, and it was suggested that the deficiency was in the biosynthesis of the common cofactor, siroheme (78). More recently, the identity of these two genes has become confused by the isolation of two classes of mutation mapping in this region, the *cys nir* class which lacks both activities and the *cys*$^+$ *nir* class which lacks only the NADH:nitrite reductase. It is now thought that the *cysG* gene is involved in siroheme biosynthesis and thus controls both activities but that a second and adjacent gene, *nirB*, controls the NADH:nitrite reductase alone. This latter gene may be the structural gene for the enzyme or be involved in cofactor processing unique to this enzyme.

The sulfite reductase is an extensively characterized enzyme, containing four FMN, four FAD, and four siroheme moieties plus Fe-S centers in a $\alpha_8\beta_4$ enzyme complex. The flavins are associated with the α-subunit, and the siroheme and the Fe-S center are associated with the β-subunit. The enzyme catalyzes the six-electron reduction of sulfite to sulfide or nitrite to ammonia. Genes *cysI* and *cysJ* code for the enzyme and map at 59 min in an "operon" with adenylsulfate reductase in addition to the sulfite reductase subunits (18, 76, 325, 452).

The soluble NADH:nitrite reductase is less well characterized. It has recently been purified (231) and found to contain noncovalently bound FAD, at least one binuclear Fe-S center, and one siroheme per monomer (see also references 55, 229, 230). As isolated, the enzyme is a dimer of two identical monomers of M_r 88,000 (85, 231). In addition to the pleiotrophic defects previously described, the activity is also affected by lesions in *nirB*, *-C*, *-D*, *-E*, *-F*, and *-A* or *-R* genes which map at 74, 26, 74, 50, 53, 29, and 29 min, respectively. The *nirR* gene is identical to the *nirA* and *fnr* genes and is a regulatory gene for nitrate and nitrite reductases, hydrogenase, and fumarate reductase. The functional *fnr* gene has been isolated and its product has been identified as a protein of M_r 31,000 (444). It is probable that the *nirB* and *nirD* genes are the same (2, 76, 229, 231); the structural gene for nitrite reductase has not been identified.

The least well-characterized nitrite reduction pathway in *E. coli* is that which involves the electron transport chain. Only nitrite reductase activity with lactate and formate as reductants has been reported, but this does not imply specificity; other respiratory chain donors may support nitrite reduction. The activity is lost on cell disruption, and so NADH cannot be tested as a possible reductant. However, if generated internally NADH could act through the soluble NADH:nitrite reductase (1, 3). Ascorbate plus PMS cannot support nitrite reduction, perhaps because its electrode potential is too high (0 mV). Abou-Jaoudé et al. (1) found that the highest specific activity for this pathway is obtained by growth on relatively rich media in the presence of low nitrite concentrations; this activity is totally repressed by oxygen. In such cells, competition among nitrite, nitrate, and oxygen is such that oxygen is always the preferred oxidative substrate, nitrite being consumed only when oxygen is depleted. Nitrate is also preferred to nitrite, but a lowered rate (25%) of nitrite reduction occurs concurrently with nitrate reduction. By specifically inhibiting the nitrate reductase with azide, these authors showed that nitrate can directly inhibit the nitrite reductase; thus, competition for reducing equivalents within the respiratory chain (1) is not the sole regulatory parameter. The formate-to-nitrite activity is insensitive to azide, but is inhibited by Cu^{2+} (0.1 mM) and cyanide (1 mM). The soluble NADH:nitrite reductase activity is also sensitive to Cu^{2+} (75); it is not known why both of these rather different nitrite reductases are thus sensitive. Cyanide sensitivity of the overall reaction is not due to the nitrite reductase, but to the inhibition of formate dehydrogenase. The respiratory nitrite- and nitrate-reducing pathways appear to have a common single site for inhibition by HOQNO and similar, but complex, responses to the destruction of quinones (primarily) by UV light (3). The effects of carbon monoxide on this system seem anomalous. Lactate-to-nitrite activity is not sensitive to carbon monoxide, although the formate-to-nitrite pathway is (3). As the formate dehydrogenase itself is not carbon monoxide sensitive, the explanation must be in the slower turnover of the lactate-to-nitrite pathway compared with the formate-to-nitrite activity. Cole has obtained up to 60% inhibition of this nitrite reductase activity by carbon monoxide in strains in which the other pathways are missing (76). *E. coli* contains a carbon monoxide-binding *c*-type cytochrome (23) which is probably c_{552} and involved in nitrite reduction (see below).

Although the formate- or lactate-to-nitrate pathway is strongly dependent on ubiquinone, the formate-to-nitrite pathway has no absolute ubiquinone dependence but is 40% inhibited in the menaquinone-deficient strain or the double (*men ubi*) mutant. The pathway to nitrite is absent in the hemeless mutants but unaffected in the *chlI* mutant, which lacks the cytochrome-*b* associated with nitrate reductase. The *nir-197* strain, which lacks cytochrome c_{552}, does not have this nitrite reductase activity (2). Cytochrome c_{552} is induced by the presence of nitrite and an association with the nitrite reductase has been inferred (135–139). It is a low-potential *c* type (178) and is rapidly oxidized by nitrite (midpoint potential, −194 to −220 mV). Its role in nitrite reduction has been obscured by confusion between the different nitrite reductase pathways (75). It has been purified (302) and shown to reduce nitrite, the product being ammonia with artificial electron donors. The cytochrome c_{552}-dependent nitrite reductase activity was also supported by a soluble NADH oxidase activity (not pure) if FAD was included in the assay (perhaps as mediator). Dye-linked assays yield ammonia as product but could perhaps directly reduce an intermediate (e.g., hydroxylamine); thus, without the physiological electron donor it is not possible to conclude that cytochrome c_{552} produces ammonia. Cytochrome c_{552} is a monomer containing 4 to 6 hemes per peptide (cited in reference 302) and is located in the periplasmic space, explaining why nitrite reduction is lost during spheroplast formation or cell breakage (75, 137–139).

Motteram et al. (341) have demonstrated that the respiratory formate-to-nitrite pathway can support a $\Delta\psi$. Values of up to 150 mV could be maintained and these are wholly attributable to the formate-to-nitrite oxidation process (76, 394). Although the ΔpH was not measured (and thus the Δp is not known), this is nonetheless a very significant observation. It is noteworthy, however, that in the wild-type cells, with all nitrite reductase systems present, only 10 to 20% of the nitrite is consumed by the energy-conserving pathway and the operation of this pathway does not increase the growth yield (76).

TMAO REDUCTASE

Trimethylamine *N*-oxide (TMAO), a constituent of marine fish and invertebrates, is reduced post mortem by bacteria, including *E. coli*, to trimethylamine, which gives rise to the characteristic "off" flavor of decaying fish (475). TMAO stimulates anaerobic growth of *E. coli* on glucose (226) and

also supports anaerobic growth on formate or hydrogen (500, 501). TMAO reductase is an inducible membrane-bound enzyme, which accepts electrons from NADH, NADPH, and formate via *b*- and *c*-type cytochromes or directly from reduced methyl viologen (226, 432, 433). P. D. Bragg and N. R. Hackett (personal communication) have described this respiratory chain in more detail; it consists of cytochromes c_{548}, c_{552}, b_{554} (?), and b_{557} plus the TMAO reductase. The NADH-to-TMAO activity is quinone dependent. In cells grown anaerobically in the presence of TMAO, its reduction is coupled to proton translocation with a stoichiometry of 3- to $4H^+/2e^-$ and the generation of a $\Delta\psi$ (470). In *chlA*, *chlB*, and *chlD* mutants, which lacked the molybdenum cofactor of nitrate reductase, TMAO reductase activity was lost but could be restored by adding molybdate, indicating a requirement for the same molybdenum cofactor as found in nitrate reductase (93). Mutants defective in TMAO reductase (*tor*) have been detected (469) by their formation of acid from lactose; wild-type cells producing trimethylamine maintained a neutral pH. The *tor* mutation lies between the origins of transfer of strains PK3 and KL228, a region devoid of genes coding for nitrate reductase.

QUINONES

Quinones are considered to function in respiratory chains as links between the dehydrogenases and the next protein component in the sequence; in mitochondria this would be the bc_1 complex, but in *E. coli* it can be cytochrome oxidase, nitrate reductase, or fumarate reductase (Fig. 1). *E. coli* is capable of synthesizing two quinones, ubiquinone-8 and menaquinone-8 (also called vitamin K) (372). The ratio of these two components in cells is variable and dependent on the growth conditions. Typically, under conditions of high aeration and in logarithmic phase, approximately 0.55 nmol of ubiquinone mg of bacterial dry weight^{-1} can be produced, with menaquinone present at only 0.025 nmol/mg^{-1}, a ratio of 22:1. An 18-h stationary-phase culture contained 0.17 nmol of ubiquinone and 0.11 nmol of menaquinone mg (dry weight)$^{-1}$, a ratio of only 1.5:1, and a strictly anaerobic 40-h culture did not contain detectable amounts of ubiquinone (<0.0003 nmol mg^{-1}) but did contain 0.25 nmol of menaquinone mg of bacterial dry weight^{-1} (372). The induction of the respective quinones under different growth conditions has been considered by a number of authors (198, 248, 291, 419).

Mutants have been isolated that lack either or both of the quinones, and these have proved to be valuable tools in ascertaining their respective functions (344, 468, 490, 491) and their biosynthesis (10, 11, 91, 181, 183, 241, 445, 505) and in the tentative assignment of an EPR signal around $g = 2.003$ to ubisemiquinone (204). Use of these mutants has confirmed that the quinones function as carriers of reducing equivalents between the dehydrogenases and the various terminal enzyme complexes; some activities can be supported by either quinone but other activities show marked preferences for one species. Wallace and Young (491) studied the role of quinones in electron transport to oxygen and to nitrate by use of mutants. NADH, D-lactate, glycerol-3-phosphate, and succinate dehydrogenases in membranes from the aerobically grown double quinone mutant all required exogenous quinones for oxidase activity. Ubiquinone reconstituted electron transport in all four cases, whereas menaquinone could only fully reconstitute the glycerol-3-phosphate activity and partly support D-lactate oxidation, but was ineffective in supporting succinate and NADH oxidation. Similar findings relating to both oxidase activities and proline transport have been reported by Stroobant and Kaback (468). Growth studies support these observations: the mutant *ubi*$^+$ *menA* grows aerobically on glucose as well as does the wild type, but the *ubiA men*$^+$ strain grows more slowly and has only 30% of the growth yield. The double mutant was even more severely affected. Electron transport in membranes derived from cells grown anaerobically in the presence of nitrate was also quinone dependent. Formate oxidation by nitrate can be fully supported by either menaquinone or ubiquinone, whereas the oxidation of glycerol-3-phosphate, D-lactate, and NADH by nitrate exhibited the same quinone dependencies as they did in the aerobic respiratory chain. Anaerobic growth in the presence of nitrate induces the "aerobic" form of the glycerol-3-phosphate dehydrogenase (see below), and there is no evidence to suggest that a different NADH or D-lactate dehydrogenase functions in these membranes from anaerobic cells. The fumarate reductase is menaquinone selective and in "fumarate membranes" a different glycerol-3-phosphate dehydrogenase is induced (the anaerobic enzyme); this appears to be menaquinone specific. Menaquinone is essential for fermentative growth in the absence of uracil, as it is specifically required to link the dihydroorotate dehydrogenase (of the uracil biosynthetic pathway) with the fumarate reductase (344); ubiquinone cannot substitute.

Utilization of fumarate as a respiratory oxidant is found only in bacteria which contain either menaquinone or its close analog desmethylmenaquinone (291). Two reasons for the specificities of the quinones can be proposed. First, the difference in midpoint oxidation-reduction potential between the species (ubiquinone, +70 mV, and menaquinone, reported as −74 mV, at pH 7.0 [291]) may suit to a greater or lesser degree the redox potentials of the immediate donor and acceptor couples. Alternatively, the functional specificity could be for the purpose of compartmentalization of the respiratory chain reactions. Rich (419) has pointed out that redox equilibration between the two quinone species within the membrane will be rather slow.

THE DEHYDROGENASES

Formate Dehydrogenase

Introduction. The formate dehydrogenase developed by *E. coli* when grown anaerobically on nitrate has been purified and extensively characterized (122, 172). This protein contains Fe-S centers, a molybdenum cofactor, and covalently bound selenium. The presence of molybdenum and selenium in the active enzyme explains the requirements for these metals in the growth media if formate dehydrogenase activity is to be developed; these requirements and their interdependence were studied in detail by Pinsett (371) and have been reviewed recently (303). Tungstate acts as an antagonist to the molybdate, leading to loss of formate dehydrogenase activity.

Although there is evidence for only one formate dehydrogenase in nitrate-grown cells, *E. coli* does utilize different oxidants for formate, e.g., oxygen, nitrate, fumarate, and protons. In the last case (formate:H_2-lyase activity), reducing equivalents are fed through the formate dehydrogenase to a hydrogenase which acts as the terminal enzyme. Formate dehydrogenase is involved in all of these pathways, but is it the same formate dehydrogenase?

The case for multiple formate dehydrogenase rests on three lines of evidence. (i) There is a correlation between the two formate dehydrogenase-linked activities (H_2-lyase and formate oxidase) and two distinct dye reductase activities, H_2-lyase activity correlating with benzyl viologen reductase and the oxidase activity correlating with PMS or methylene

blue reductase activity (122, 177, 370, 426). Peck and Gest (370) reported that the benzyl viologen activity was largely cytoplasmic, whereas the methylene blue activity was exclusively associated with the membrane. In contrast, both activities have been found in each fraction (177) or both membrane bound (427). The formate:H_2-lyase system can reduce benzyl viologen in whole cells, and since oxidized benzyl viologen is not membrane permeable, the enzyme cannot be wholly cytoplasmic. The difference in the dye reductase activities could be attributable to the presence or absence of hydrogenase rather than to any change in the formate dehydrogenases, although it may be necessary to postulate a specific association of hydrogenase with the formate dehydrogenase to modify the latter's dye reductase activity.

(ii) In a series of mutants defective in nitrate reductase, formate:methylene blue (or PMS plus dichloroindophenol) activity was absent in all strains but roughly half retained benzyl viologen-linked activity, concomitant with gas production. One interpretation of this is that all nine strains tested were pleiotropic for nitrate reductase and one of the formate dehydrogenases, but four of the mutants in addition lacked a second formate dehydrogenase. Most lesions pleiotropic for both nitrate reductase and formate dehydrogenase appear defective in the processing of the molybdenum cofactor (see "Nitrate Reductase"). This interpretation suggests that the cofactors in the two formate dehydrogenases are not the same. More recently, however, a series of formate dehydrogenase mutants have been better characterized (200). Of the five strains studied, four lost both activities (*fdhA* to *-D*) and only *fdhE* (87 min) retained the benzyl viologen activity in the absence of the PMS activity. The *fdhE* gene maps close to *fdhD* and *chlB*, mutations in either of which cause loss of both formate dehydrogenase activities.

(iii) Third, Cox et al. (92) have studied the production of peptides covalently labeled with selenium (^{75}Se), a feature of the well-characterized formate dehydrogenase of nitrate-grown cells. Although this work presupposes that any additional formate dehydrogenase would also contain covalently bound selenium, the authors did find the relative concentrations of some of the selenopeptides on SDS gels altered in parallel with the two-dye reductase activities. A selenopeptide of M_r 80,000 was apparently coinducible with the formate:H_2-lyase activity. Although there is no report of such a peptide in hydrogenase, a number of other enzymes will be switched on under these conditions, and the link between the changes in selenopeptides with the changes in metabolism is not necessarily attributable to formate dehydrogenases. Alternatively, the 80,000 selenopeptide could be a derivative (e.g., by glycosylation) of the 110,000 selenopeptide associated with the formate dehydrogenase of nitrate-grown cells. In conclusion, although there is some evidence for multiple formate dehydrogenases, the case is not fully proven and such a resolution may be looked for in further detailed genetic analyses.

Genetics. To date there are five classes of mutants specifically lacking formate dehydrogenase, i.e., that do not lack nitrate reductase (see Table 5). These are in *fdhA* (80 min), *fdhB* (38 min), *fdhC* (82 min), *fdhD* (87 min), and *fdhE* (87 min) (200). The *fdhA* and *fdhB* lesions produce no immunologically detectable formate dehydrogenase polypeptides and may, therefore, be structural lesions (174).

Purification and properties. Formate dehydrogenase was first purified by Enoch and Lester (122). The purified enzyme has much in common with nitrate reductase. It consists of three subunits: A (α), M_r 110,000; B (β), M_r 32,000; and C (γ), M_r 20,000. Selenium is associated with the 110,000 M_r peptide. The enzyme also contains a molybdenum cofactor and a cytochrome b_{555}. Genetic studies indicate that the molybdenum cofactor is the same as that found in nitrate reductase. Cytochrome $^{fdh}b_{555}$ differs from cytochrome $^{nr}b_{555}$ in having a lower midpoint potential, -105 mV at pH 7 (189). By analogy with the nitrate reductase structure, it has been suggested that cytochrome $^{fdh}b_{555}$ is the M_r 20,000 subunit (122). Boxer et al. (40), however, have reported a formate dehydrogenase preparation containing cytochrome b_{555} but lacking the M_r 20,000 subunit.

Organization and function. The organization of the formate dehydrogenase in the membrane has been studied, using approaches similar to those applied to nitrate reductase. Labeling of exposed tyrosine residues by lactoperoxidase and ^{125}I shows that the A subunit is transmembranous. The B subunit is unlabeled by lactoperioxidase (172). By using [^{35}S]diazobenzanesulfonate and [^{125}I]diiodosulfanilic acid as protein modification reagents (see "Nitrate Reductase"), it was demonstrated that the B subunit is also transmembranous. Although not subunit specific, antibody studies also show the transmembranous nature of the formate dehydrogenase (175, 483). To date, there has been no report on the location of the C subunit. These results are summarized in Fig. 8.

There is strong evidence that formate dehydrogenase pumps protons across the cytoplasmic membrane, concomitant with oxidoreduction reactions (148, 245). Stoichiometries for the overall formate-to-oxygen or formate-to-nitrate reaction have been measured at up to 4- and $3H^+/2e^-$, respectively. The use of menadione and ubiquinone-1 as artificial oxidants for formate oxidation by *E. coli* spheroplasts gave stoichiometries of 1.73 and 1.58 $H^+/2e^-$, respectively, suggesting that the formate-to-quinone segment of the respiratory chain translocates $2H^+/2e^-$. This process is inhibited by HOQNO. The site of formate oxidation, with respect to the two surfaces of the cytoplasmic membrane, has not been demonstrated.

NADH Dehydrogenases

The early literature on NADH dehydrogenases in *E. coli* is complex and confused and suggests the presence of multiple enzymes. Interpretation is not helped by the use of a range of artificial electron acceptors in assaying for NADH dehydrogenase activity, e.g., cytochrome *c*, dichlorophenolindophenol, PMS, ferricyanide, and naptho- and benzoquinones. Often, differences in reactivity to these acceptors have been taken to show enzyme multiplicity. The term "diaphorase" is applicable to any enzyme capable of catalyzing the oxidation of NADH or NADPH by any electron acceptor, its use in this context is perhaps appropriate. Detergent solubilization of an electron transport chain containing a single enzyme capable of diaphorase activity could yield a number of different fractions containing that activity. The early work on *E. coli* NADH dehydrogenase (see references 42 and 43) and diaphorase-staining arcs on crossed-immunoelectrophoresis gels (362, 366) should be viewed in this light. The enzyme(s) that concerns us here is that which links with the other components of the electron transport chain to support NADH oxidase (or NADH:nitrate or NADH:fumarate) activity. On detergent fractionation of the electron transport chain, as a preliminary to isolation of the enzyme, its integration with the other components will be dislocated and overall activities will be lost; only diaphorase activity will remain.

Bragg and Hou (44) resolved three fractions with NADH-dye reductase activity from deoxycholate-solubilized membranes; only six- to ninefold purifications were obtained, and one of the fractions seemed to have a complete electron transfer chain. Hendler and Burgess (212, 213) also described three fractions that catalyzed NADH-dye reductase activity, resolved from a deoxycholate solubilization; again, one contained other elements of the electron transport chain, including an oxidase and succinate dehydrogenase. None of these fractions bears much similarity to the enzyme isolated by Gutman et al. (184) from freeze-dried membranes, which contained both FMN and FAD in addition to nonheme iron and acid-labile sulfide.

Crossed-immunoelectrophoretic studies on solubilized membranes from aerobic cells indicated three diaphorase arcs (15, 19, and 27 on Owen and Kaback's numbering system [362–364]), two of which show partial coidentity (19 and 27) so that the number of unrelated activities is possibly only two. Antigen 15 has been shown to derive from the cytoplasmic membrane exclusively, whereas antigen 19/27 is equally distributed between membrane and cytoplasm (363, 364). As the 19/27 antigen appears not to be an integral membrane protein, the principal candidate for the respiratory NADH dehydrogenase must be antigen 15. Antigen 19/27 has subsequently been identified as dihydrolipoyl dehydrogenase (365). The NADH dehydrogenase (antigen 15) cross-reacts with antibodies raised against *Salmonella typhimurium* extracts and contains nonheme iron as shown by ^{59}Fe autoradiography of crossed-immunoelectrophoretic gels (366). Both diaphorase antigens are inaccessible to antibody in right-side-out vesicles, indicating a location on the cytoplasmic aspect of the membrane (362–366). Analysis of the precipitin lines on denaturing gels has not been published, and so correlation of antigen 15 with the reports on purified enzymes is not possible. Crossed-immunoelectrophoretic analysis of membranes from cells grown on glucose and nitrate or glycerol and fumarate also revealed diaphorase-staining arcs. In the "glucose-nitrate extracts" a major and a minor arc were detected; in the "glycerol-fumarate extracts" only one arc was detected. NADH dehydrogenases from the two cell types have different electrophoretic mobilities (483).

Young and Wallace (509) have isolated a number of biochemically identical mutants in which the respiratory NADH oxidase activity is negligible. These mutants (*ndh*) map at 22 min and cotransduce with the *pryC* gene (dihydroorotase). Although NADH oxidase activity was absent in these mutants, some diaphorase activities remain.

There have been three recent reports of a highly purified NADH diaphorase activity claiming to be the respiratory NADH dehydrogenase. One of these purified enzymes certainly is the *ndh* gene product (232); the other two may be derivatives of the same enzyme. The *ndh* gene has been cloned and amplified, leading to overexpression of a membrane-bound NADH dehydrogenase, 60-fold amplification of the dye reductase activity, and a 6-fold amplification of NADH oxidase activity (506). From the strain with amplified levels of enzyme, the NADH dehydrogenase has been extracted and purified (232). It can be reconstituted into membranes of an *ndh* mutant to restore cyanide-sensitive NADH oxidase activity (233). The NADH dehydrogenase has been synthesized in vitro (397) and the nucleotide sequence has been established (508). The enzyme is a single polypeptide of M_r 47,304 with tightly bound FAD, which can be reversibly lost in purification and contains no iron, copper, molybdenum, tungsten, or phosphate. With benzoquinone, a turnover of 500 s^{-1} was measured. The codon UUG, which normally specifies leucine, acts as the translocational initiation codon (*N*-formylmethionine).

The primary amino acid sequence has a polarity of 43.4%, not unusually low overall, but there are hydrophobic regions which may play a part in the membrane assembly of the protein. A hydrophobic sequence preceded by two lysines is present at residues 8 to 18. Young et al. (508) point out that this sequence resembles the "signal" sequences of secreted proteins. As isolated after cholate solubilization, the enzyme is associated with 70% of its own weight of lipid (primarily phosphatidylethanolamine), including approximately one ubiquinone-8 molecule.

There are two other reports in which an NADH dehydrogenase activity from *E. coli* has been extensively purified and characterized. Although isolated from unamplified strains, one of these preparations is probably identical to that of Jaworowski et al. (232), and the other may possibly be a product of it. Dancey and others (101, 102) have isolated and purified to 75% homogeneity, from Triton X-100-solubilized membranes, an NADH dehydrogenase. Extensive kinetic analysis of this protein showed that it had much in common with the membrane-bound NADH oxidase activity. The enzyme required flavin for activity but, as isolated, contained none and consisted of a single polypeptide of M_r 38,000. An antibody raised against the preparation inhibited NADH oxidase activity in membranes, but this must be a heterogeneous antibody preparation. A separate enzyme isolated by this group (43) (M_r = 45,000) contains one iron atom and, although apparently lacking flavin, may be the same as Jaworowski's enzyme (232). The lack of flavin may account for its greatly reduced activity. The relationship between the enzymes of M_r 37,000 and 45,000 is unclear. An immunological cross-reaction of an antibody to the M_r 37,000 enzyme against the M_r 45,000 enzyme has been reported (479), but this assessment was done in a manner which could not counter the impurity of the antibody preparation. Nevertheless, the kinetic analysis of the smaller enzyme gave strong circumstantial evidence for it being functional, suggesting that it might be a derivative of the M_r 45,000 enzyme. This could be a proteolytic modification or perhaps glycosylation; the latter is known to cause underestimates of M_r values in denaturing gels.

In conclusion, a respiratory NADH dehydrogenase from *E. coli* has now been extensively characterized. Some questions do remain, however; is the same dehydrogenase developed in all growth conditions (483) and does the enzyme contain iron? One preparation (232) contains very little, if any, iron, whereas the arc on crossed-immunoelectrophoretic gels attributable to NADH dehydrogenase definitely contains iron. It is possible that only the flavin-containing catalytic subunit of the NADH dehydrogenase has so far been characterized but that, in situ, this subunit is associated with Fe-S-containing subunits.

Transhydrogenase

Transhydrogenase (EC 1.6.1.1) catalyzes the exchange of reducing equivalents between the pyridine nucleotide couples NADH/NAD^+ and NADPH/$NADP^+$. There are two classes of transhydrogenase activity, energy linked and non-energy linked. Both types have been reported in *E. coli* (for a review, see references 42 and 43). It is possible, however, that only the energy-dependent enzyme is really present in *E. coli* and that this appears as a non-energy-linked activity when assayed in uncoupled preparations. Evidence for this conclusion comes from the observation that a single muta-

tion causes the loss of both activities (510). The coexistence of both activities would give rise to a futile cycle and is unlikely to occur to a significant extent.

The purpose of the energy-linked transhydrogenase under normal metabolic conditions is to generate NADPH for anabolic processes and to do so to an extent which generates a relatively negative electrode potential for the NADPH/$NADP^+$ couple to drive the anabolic reactions. The midpoint potentials of the NADH/NAD^+ and NADPH/$NADP^+$ couples are close (Em_7, −320 and −324 mV, respectively). Thus, the equilibrium constant for equation 6 is close to unity (1.26):

$$NADH + NADP^+ \rightleftharpoons NAD^+ + NADPH \quad (6)$$

Input of energy (in the form of a Δp) pushes the equilibrium to the right-hand side so that the electrode potential of the NADPH/$NADP^+$ couple is more negative than that of the NADH/NAD^+ couple. This can be achieved by the inclusion of a proton-translocating loop between the two couples. Thus, the equation can be rewritten:

$$NADH + NADP^+ + nH^+_{(out)} \rightleftharpoons NAD^+ + NADPH + nH^+_{(cystolic)} \quad (7)$$

where n is the (unknown) stoichoimetry of protons translocated per redox reaction.

Although equation 7 probably functions left to right in the majority of conditions, it is implicit that the reverse reaction can generate a Δp. The generation of a Δp (specifically $\Delta\psi$) by NADPH reduction of NAD^+ has been demonstrated by Chetkauskaite and Grinyus (68), who measured the uptake of the lipid-soluble anion phenyldicarbaundecaborate in inverted membrane vesicles during electron transfer from NADPH to NAD^+. The uptake of phenyldicarbaundecaborate was sensitive to agents and procedures that rendered the vesicle membranes proton-permeable. The magnitude of the phenyldicarbaundecaborate accumulation depended on the ratio [NADPH] [NAD^+]/[NADH][$NADP^+$]. The addition of ATP, which will be hydrolyzed by the proton-translocating ATPase giving a Δp, drives the reaction in the direction of NADPH production. Conversely, addition of NADH and $NADP^+$ in the presence of ATP caused a fall in the magnitude of the ATP-induced Δp.

The energy-linked transhydrogenase has been implicated in the generation of NADPH for use in anabolic processes, although growth yields are unaffected by loss of the enzyme through mutation (205, 510). The enzyme is coinduced with $NAD(P)^+$ glutamate dehydrogenase under conditions of nitrogen limitation and when ammonium ions are the sole nitrogen source; it has been suggested that the transhydrogenase is the source of NADPH for ammonia assimilation (300). Transhydrogenase activity is suppressed by leucine and, to a lesser extent, by methionine and alanine (153). NADPH formation during growth on glucose has been studied in wild-type and mutant strains affected in NADPH-generating reactions (glucose-6-phosphate dehydrogenase, isocitrate dehydrogenase, malate dehydrogenate, and energy-linked transhydrogenase [96]). It was found that, under normal conditions, the hexose monophosphate shunt is a minor pathway in *E. coli* and the authors suggest that the main source of the hydride in NADPH is from oxidation of the C-1 and C-6 positions of glucose via an unidentified pathway. In a phosphoglucose isomerase-deficient mutant, the hexose monophosphate pathway is a major source of NADPH and the transhydrogenase may, in this special case, be used to oxidize NADPH.

Succinate Dehydrogenase

Succinate dehydrogenase (EC 1.3.99.1) catalyzes the oxidation of succinate to fumarate with an electron transport chain as the oxidant. The enzyme is a vital part of the tricarboxylic acid cycle and as such is almost ubiquitous; for a review see reference 209. A comparison of *E. coli* succinate dehydrogenase with fumarate reductase (which catalyzes the reverse reaction) can be found above and in Table 2.

Succinate dehydrogenase is induced by aerobic growth on succinate but not on glucose (429); aerobic growth on a range of nonfermentable carbon sources induced appreciable levels of succinate dehydrogenase activity (Kirby and Ingledew, unpublished data). Only traces of the enzyme are found in cells grown with fumarate as terminal electron acceptor (483), but there is succinate oxidase activity in membranes from cells grown anaerobically with glycerol and nitrate (G. Cumming, personal communication). Fumarate reductase is absent in the nitrate-grown cells (483).

The succinate dehydrogenases from a number of organisms have been purified and extensively characterized. Unfortunately, the *E. coli* enzyme is not one of them. A number of attempts to purify the enzyme from *E. coli* have been rewarded with only limited success (270, 412). Reddy and Hendler (412) resolved a complex (M_r = 150,000) that contained succinate dehydrogenase activity and a *b*-type cytochrome. Analysis of *sdh* mutants indicated the involvement of a subunit (M_r = 67,000) in the enzyme (463). An immunological approach, although indirect, proved more rewarding; in the crossed-immunoelectrophoretic reference profile for *E. coli* (ML308-225), succinate dehydrogenase was initially not detected (362, 363), but subsequent work on membranes derived from cells grown in the presence of radiolabeled riboflavin has led to resolution of the subunit composition of the enzyme (86, 87, 251, 361). Riboflavin is a precursor of FAD which, in succinate dehydrogenase and fumerate reductase, is covalently linked to the protein. On solubilization of the membrane and analysis by crossed-immunoelectrophoresis, two of the precipitin arcs contained covalently bound label. One of these was prominent and already known to contain Fe-S centers; the other labeled arc was present in low and variable concentrations. With a modification of the procedure it became possible to stain these arcs for succinate dehydrogenase activity. The smaller arc exhibited some heterogeneity but is thought to be fumarate reductase. Three lines of evidence have led to the conclusion that the major immunoelectrophoretic arc is due to succinate dehydrogenase: (i) its presence is inducible by aerobic growth on succinate, (ii) it contains covalently linked flavin and nonheme iron, and (iii) some *sdh* mutants lack the arc. Owen and Condon (361), by excision and analysis on denaturing gels of the precipitin arcs, have determined that the covalently bound flavin of the succinate dehydrogenase is attached to a polypeptide of M_r 71,000. This and three other polypeptides were resolved throughout the arc, the others being of M_r 31,000, 29,000, and 13,000, respectively. In addition, a polypeptide of M_r 19,000, which these authors suggested could be cytochrome b_{556}, was detected in the cathodal and central parts of the arc. These findings are more complex than those of Jones et al. (251), who raised antibodies to bands exhibiting succinate dehydroginase activity cut from isoelectric focusing gels. As in previous work, two bands were detected, a major one with pI 5.7 and a minor and variable one (pI = 7.2). In the crossed-immunoelectrophoretic analysis, the two species were found to give

an immunochemical cross-reaction, and it was suggested that the minor component was a different assembly of the same enzyme. The major arc contained subunit polypeptides of M_r 73,000 and 26,000. The arc was absent in an *sdh* mutant; no heme-containing component was detected. An explanation for the discrepancy in the small M_r components may lie in the intramembrane association of the succinate dehydrogenase with other components.

The *E. coli* enzyme appears similar to those studied in other organisms. Mammalian succinate dehydrogenase is composed of polypeptides of M_r 70,000 and 27,000 as normally isolated but, for physiological function, additional polypeptides of M_r 13,500 and 7,000 are required (59, 162). Further, the mammalian enzyme can form complexes with *b*-type cytochromes (207) and some bacterial succinate dehydrogenases are consistently isolated in association with a *b*-cytochrome, e.g., from *Bacillus subtilis* (208) and *Micrococcus lysodeikticus* (54). The *E. coli* enzyme, however, raises an antibody that cross-reacts only with the enzyme from other *Enterobacteriaceae* (87); none of these enzymes has been well studied.

Apart from the flavin component, the prosthetic groups of *E. coli* succinate dehydrogenase have not been analyzed in the purified enzyme, although the presence of nonheme iron has been demonstrated in immunoprecipitates. EPR spectroscopy of membranes from cells grown aerobically with succinate has revealed FeS centers which, on the basis of their spectral similarity to those in the mitochondrial enzyme, have been attributed to *E. coli* succinate dehydrogenase (232; see also Table 2).

A DNA fragment (12.8 kilobases) containing the genes for four enzymes of the tricarboxylic acid cycle, including succinate dehydrogenase, has recently been cloned (484). Further resolution (J. R. Guest, personal communication) has shown that there are four structural genes, coding for the flavoprotein subunit (*hsdA*; M_r = 64,300), iron-sulfur protein subunit (*sdhB*; M_r = 26,000), and two hydrophobic subunits (*sdhC*, M_r = 14,200; and *sdhD*, M_r = 12,800). These genes are linked in a single transcriptional unit in the order *sdhCDAB*.

Lactate Dehydrogenase

Introduction. Lactate is a major product of the bacterial fermentation of glucose and other carbohydrates (151). In heterofermentative bacteria, such as *E. coli*, the conversion of pyruvate to L-(+)- or D-(−)-lactate is a major route for the regeneration of NAD^+ and is catalyzed by cytoplasmic lactate dehydrogenases (EC 1.1.1.27 and EC 1.1.1.28, respectively). The enzyme in *E. coli* that forms D-(−)-lactate has been purified and extensively characterized (473, 474).

However, the enzymes that concern us here are the membrane-bound, NAD^+-independent lactate dehydrogenases that convert lactate to pyruvate (with no evidence for a function in the reverse reaction) and allow *E. coli* to use lactate as a carbon source and lactate oxidation to be coupled to energy transduction. D-(−)-lactate dehydrogenase is constitutive and has been extensively studied, whereas an enzyme specific for L-(+)-lactate is induced by growth on either D- or L-lactate and is also membrane bound but has received less attention. The earlier work on these enzymes has been well covered in the reviews by Bragg (42, 43) and Garvie (151) and what follows concentrates on more recent work.

D-Lactate dehydrogenase. (i) Purification and properties. This enzyme has been extracted with detergent, purified, and characterized by Kaback and his co-workers and by Futai, using the ML308-225 strains of *E. coli* (142, 283). Properties of the homogeneous purified preparations obtained by these groups and others are shown in Table 9 and

TABLE 9. Properties of NADH-independent lactate dehydrogenase purified from *E. coli*

Property	D-Lactate dehydrogenases			L-Lactate dehydrogenase (Kimura and Futai [145, 271]; ML308-225 *dld-3*)
	Kohn and Kaback (285); Kaczorowski et al. (255) (ML308-225)	Futai (142) (ML308-225)	Pratt et al. (399) (W3110 *trpA33*)	
Mol wt	74,000 ± 5,000 (SDS gels) 73,500 − 76,000 (equilibrium centrifugation)	72,000 (SDS gels) 71,000 (sucrose gradient)	75,000 (SDS gels)	43,000 (SDS gels)[a]
Maxima in absorption spectrum (nm)	440–480	455–480	450–480	380 and 460
Prosthetic group	FAD (1.2 mol mol of enzyme^{-1})[b]	FAD (1.2 mol 72,000 mol wt^{-1})		~1 FMN/polypeptide
pH optimum	8.5[c]	8–9	9–9.5	8–9
K_m, D-lactate (mM)	0.9–1.4	0.6	0.4	No appreciable oxidation
K_m, L-lactate (mM)	16–30	18		0.12
Inhibitors of dehydrogenases	2-Hydroxy-3-butynoate, oxamate, oxalate	Cyanide,[d] oxamate, 2,3-phosphoglycerate	2-Methylacetate	Pyruvate (product)

[a] Oligomeric in detergent-free solution.
[b] Using molecular weight of 75,000.
[c] 6.6 in membrane vesicles.
[d] At alkaline pH.

are compared with more recent data on the enzyme purified from strain W3110 *trpA33* (399). The latter strain requires tryptophan and can incorporate fluorotryptophan, a potentially useful spectroscopic marker for the study of membrane proteins and their interactions with lipids (see also reference 400). Enzymes from the two strains are virtually identical, but details of purification differ since, for the W strain, DE52 column chromatography in the presence of Triton X-100 could not be used for final separation of the dehydrogenase. Slight differences in heat inactivation (the ML strain enzyme being more stable) and pH optima suggest that there may be some amino acid substitutions.

There is agreement that the enzyme has an M_r of 71,000 to 75,000 (471). The prosthetic group is noncovalently bound FAD. The K_m for D-lactate varies with the presence or absence of detergent, being lowest with the aggregated enzyme and highest in the membrane (471).

(ii) Membrane localization and coupling to transport. Antibody inhibition (449, 451) and immunoadsorption studies (see below) have shown that the protein is associated with the cytoplasmic aspect of the inner membrane. In crossed-immunoelectrophoresis studies of detergent-solubilized inner membranes, lactate dehydrogenase has been identified in the immunoprecipitation pattern, using specific antisera (167, 363, 461). Despite its predominantly membranous location, mutants constitutive for the synthesis of other dehydrogenases contain an increased proportion of nonsedimentable D-lactate dehydrogenase activity, indicative of competition between dehydrogenases for a common binding site (292). Contradictory results (203), however, showed that purified preparations of D-amino acid dehydrogenase and D-lactate dehydrogenase bind independently to right-side-out and inverted vesicles from *E. coli* as well as phosphatidylcholine liposomes without detectable competition. Each enzyme can feed electrons to a common rate-determining redox component that precedes a site of proton translocation.

The oxidation of D-lactate by lactate dehydrogenase is accompanied by H^+ translocation in intact cells (296, 413) and is coupled to active solute transport in membrane vesicles (19, 20). Indeed, although such vesicles have the capacity for rapidly oxidizing a number of substrates, generation of Δp is most effective with D-lactate as electron donor. The reasons for this substrate specificity are not clear (254). Crude (414) or purified (143, 410) preparations of the enzyme are capable of reconstituting lactate-dependent oxygen uptake and active transport in vesicles from *E. coli* mutants (*dld*) that are defective in D-lactate dehydrogenase activity (218, 453). Although membrane vesicles from both wild-type and *dld* mutants show similar increases in D-lactate oxidase rates on binding the purified dehydrogenase, only in the *dld* mutant vesicles is proline transport significantly stimulated by exogenous dehydrogenase (400).

Antiserum raised to the solubilized and purified D-lactate dehydrogenase is an effective inhibitor of dehydrogenase activity and lactate-dependent active transport (449), but does not react with the soluble, pyridine nucleotide-dependent enzyme or the partially purified L-lactate dehydrogenase (see below). D-Lactate dehydrogenase is inaccessible to antibody in right-side-out vesicles from strain MS308-225. The use of reduced PMS as a membrane-permeable electron carrier, together with a nonpermeable analog, indicated that reduction of the respiratory chain from either side could drive active transport (451).

The "Kaback preparation" of the above membrane vesicles (formation of spheroplasts with EDTA-lysozyme, followed by rapid dilution in hypotonic buffer) has generated some controversy, which has important implications for studies of the localization of membrane-bound respiratory chain components (for a brief review, see reference 73). Whereas the claim that such preparations, especially from ML strains, consist almost exclusively of right-side-out and sealed vesicles has received some support (12, 254, 362, 450, 451), other results suggest that Kaback preparations are heterogeneous with respect to sidedness (144, 493). A suggestion that partly reconciles these differences is that certain membrane proteins become translocated from one side of the membrane to the other or "scrambled" during vesicle preparation, creating a mosaic (8, 12, 144). In the case of D-lactate dehydrogenase in normal strains, however, it is not accessible to antibody from the outside, suggesting that none of this enzyme is translocated to the outer surface (7, 146, 450). Using an alternative method of vesicle preparation involving disruption of spheroplasts in a French press, and which was claimed to yield right-side-out closed vesicles, however, Yamato et al. (503) have presented evidence that 40% of the D-lactate dehydrogenase is dislocated from its original location and found on the outside. This estimate is considerably higher than the value of 11% suggested by others (362, 364) as the maximum extent of dislocation of membrane components from the inner to outer membrane surface. Further work is clearly needed, especially in view of the inevitable high liquid shear forces characteristic of the French press.

(iii) Interaction with lipids. Success in purifying D-lactate dehydrogenase and the ability to reconstitute functional activity in vitro have led to several studies of the lipid dependence of enzyme activity. D-Lactate oxidation is strongly lipid dependent (123). Removal from membranes of neutral lipids and phospholipids resulted in the loss of >90% of D-lactate, NADH, and succinate oxidase activities. Each of the activities had a different requirement for phospholipid, which could be demonstrated by brief incubation of the lipid-depleted particles with a dispersion of ubiquinone-10 and the phospholipid. Cardiolipin was the only lipid that could restore D-lactate dehydrogenase activity and gave a 40-fold decrease in the apparent K_m to 0.18 mM.

In an alternative approach, Fung et al. (141) incubated a purified detergent-free form of the enzyme with lipids and demonstrated extensive enhancement of activity and nuclear magnetic resonance-detectable lipid-protein interactions. Unlike earlier work (123), but in agreement with reference 471, no specificity for a particular kind of lipid was indicated.

Further evidence for the dependency of the D-lactate oxidase activity upon lipid composition has been obtained from reconstitution experiments with the purified enzyme and membrane vesicles prepared from an unsaturated fatty acid auxotroph (ML308-225 *dld*-3 *ufa*), derived from the D-lactate dehydrogenase-deficient strain (152). Reconstitution of oxidase activity, but not binding of the enzyme, was more effective when the membrane lipids were *cis* rather than *trans* fatty acids.

More recently, activation of the delipidated, enzyme has been achieved (287), with well-defined phospholipids of the micelle- and bilayer-forming types. Reactivation depended strongly on the formation of micelles, but may indicate the necessity for formation of an apolar matrix for insertion of the protein. The best phospholipid activators were phosphatidylglycerol and phosphatidylserine. Surprisingly, phosphatidylethanolamines, the predominant lipids of *E. coli* membrane, were poor activators.

(iv) Molecular biology. Amplification of the respiratory D-

lactate dehydrogenase has been made possible by the cloning specific DNA sequences. Two plasmids were isolated from an *E. coli* chromosomal library by their ability to complement an *ndh* mutant, defective in NADH dehydrogenase (see section above). The property of one such plasmid (pIY1) could be attributed to its carrying the gene coding for NADH dehydrogenase, whereas the second plasmid (pIY2), derived from *Hin*dIII-digested chromosomal DNA, did not carry this gene but resulted in overproduction of membrane-bound D-lactate dehydrogenase (507). Complementation by pIY2 of the *ndh* mutant probably arose from the ability of the elevated D-lactate oxidase activities to participate in regeneration of NAD^+, defective in the mutant. Thus, in *ndh* mutants, D-lactate probably accumulates as a result of the reduction of pyruvate by the soluble, pyridine nucleotide-linked D-lactate dehydrogenase (473, 474). The amplified respiratory D-lactate oxidase system, reconverting the lactate to pyruvate, provides a cyclic system for reoxidation of NADH independently of the NADH dehydrogenase.

Synthesis of lactate dehydrogenase has now been studied by using the recombinant plasmid containing the *dld* gene. Expression of the cloned gene, achieved either in vivo with transformed minicells or in vitro with a fractionated transcription/translation system, led to a product identified as the membrane-bound D-lactate dehydrogenase (434). Interestingly, the protein was catalytically active and bound to membrane vesicles during or after synthesis, suggesting that, like NADH dehydrogenase (see section above), it is synthesized in a mature form and binds to the membrane without a leader peptide sequence. Addition of FAD, the cofactor, to the in vitro reaction mixture elicited a twofold increase in synthesis of the enzyme. L factor, a protein involved in regulation of protein elongation, inhibits expression of the *dld* gene but stimulates expression of the *ndh* gene, suggesting additional complexities in its mode of regulating transcription.

L-Lactate dehydrogenase. Early studies (27, 279) indicated that L-lactate dehydrogenase was induced in cells grown on DL-lactate. Futai and Kimura (145) have confirmed tha enzyme activity is 100-fold higher in such cells than in cells grown aerobically on glycerol or anaerobically on glucose. In contrast, activities of D-lactate dehydrogenase (above), NADH dehydrogenase, and, to a lesser extent, succinate dehydrogenase were relatively invariant under the growth conditions tested (see also reference 382). The induction of L-lactate dehydrogenase appears to enhance the synthetic role of the tricarboxylic acid cycle, resulting in elevated levels of heme and protoporphyrin (112, 113). A recent report (347) indicates that, under fermentative as opposed to oxidative conditions, L-lactate dehydrogenase is not induced, even in the presence of lactate.

The cholate-solubilized D-lactate dehydrogenase has been purified to homogeneity by using conventional procedures in the presence of Tween 80 (145). The properties of the isolated enzyme are quite distinct from the D-lactate dehydrogenase (Table 9), especially with regard to specificity and flavin content. Antibody raised to the enzyme inhibited dehydrogenase activity and L-lactate-dependent oxygen uptake in inverted membrane vesicles, indicating (i) that the enzyme is a primary dehydrogenase in the *E. coli* respiratory chain and (ii) that the enzyme is localized (in the intact cell) on the inner aspect of the cytoplasmic membrane.

Subsequently, the enzyme has been freed from lipids and reactivated with various phospholipids (271), concomitant with an increase in the α-helical content, as measured by circular dichroism.

sn-Glycerol-3-Phosphate (L-Glycerol-3-Phosphate) Dehydrogenase

E. coli can grow with glycerol or L-glycerol-3-phosphate as sole source of carbon and energy with oxygen, nitrate, or fumarate as electron acceptor. Utilization of glycerol involves a membrane component catalyzing facilitated diffusion of the substrate, an ATP-dependent kinase, and two membrane-associated glycerol-3-phosphate dehydrogenases. Glycerol-3-phosphate, on the other hand, is taken up by a specific transport system consisting of a periplasmic and a membrane-bound component. The operons coding for the transport systems, the kinase, and dehydrogenases constitute a regulon (*glp*) under the control of a single repressor and induced by glycerol-3-phosphate. For a review and references, see references 295, 301, and 332.

Two classes of membrane-associated dehydrogenases have been identified (272), both of which transfer reducing equivalents to an electron transport chain. These are designated the "aerobic" and the "anaerobic" enzymes. Mutants possessing only the aerobic dehydrogenase can grow on glycerol or glycerol-3-phosphate with nitrate or oxygen (but not fumarate), whereas cells possessing only the anaerobic enzyme can grow with nitrate or fumarate (but not oxygen). Both enzymes are distinct from the soluble biosynthetic glycerol-3-phosphate dehydrogenases (EC 1.1.1.8) which catalyze the NAD(P)H-dependent reduction of dihydroxyacetone phosphate to glycerol phosphate, a precursor necessary for synthesis of all *E. coli* phospholipids (118, 278).

The aerobically induced enzyme. Aerobic growth in the presence of glycerol results in induction of a dehydrogenase (encoded by the *glpD* gene) which participates in coupled respiratory electron transport to oxygen as terminal acceptor. The enzyme is membrane bound (292, 461) and can comprise up to 10% of the inner membrane protein in constitutive strains (495). The active site has been located at the cytoplasmic (inner) face of the membrane (493), since (i) exogenous glycerol-3-phosphate fails to energize glutamine uptake in a mutant unable to transport the ester and (ii) the dehydrogenase activity is latent in intact cells or spheroplasts when the nonpenetrant ferricyanide was used as electron acceptor.

A partial purification of the cholate-extracted enzyme was described by Weiner and Heppel (495), who reported an apparent M_r of 80,000, comprising two subunits of M_r 35,000. The protein had noncovalently bound FAD as coenzyme. Replacement of detergent (Brij 58) in the preparation with perchlorate yielded a partially inactivated enzyme, which was still active in reconstituting glycerol-3-phosphate-dependent transport of L-proline in vesicles from a strain lacking dehydrogenase activity (439). Activity of the detergent-depleted enzyme could be restored by addition of various phospholipids, as reported for purified D-lactate dehydrogenase (see above). In membranes from unsaturated fatty acid autotrophs, glycerol-3-phosphate dehydrogenase activity is unaffected by the membrane fatty acid composition (324).

When dehydrogenase activity is assayed by PMS-coupled reduction of 3-(4,5-dimethylthiazolyl-2)-2,5-diphenzyltetrazolium bromide, the detergent-depleted enzyme shows a marked loss of activity, which can be restored with amphipaths (421). The stimulation by detergents is not accompanied by any change in the structure of the enzyme (as detected in cross-linking studies) or alteration in the affinity of the enzyme for substrate. Cupric ions specifically inhibited the PMS-coupled dye reduction and this was exploited, in

conjunction with circular dichroism and tryptophan fluorescence of conformational changes, to demonstrate that the effect of detergents is probably the exposure of a binding site for PMS. Previously (143), a partially purified preparation had been used to reconstitute glycerol-3-phosphate-dependent oxidation and transport in membrane vesicles from cells uninduced for this enzyme. A comparison of the reconstitution obtained and its inhibition by ferricyanide in these vesicles with vesicles from induced cells indicated that the dehydrogenase in the latter was dislocated, during vesicle preparation, to the outer face.

The anaerobically induced enzyme. Under anaerobic growth conditions with fumarate as terminal acceptor, a different dehydrogenase is induced, coded for by the *glpA* gene (273). The level of the enzyme is similar in cells grown either aerobically or anaerobically with nitrate. The enzyme passes reducing equivalents to an electron transport chain that uses fumarate as terminal acceptor. It is characterized by its solubility or at least loose attachment to the membrane, its slow sedimentation in sucrose, and its stimulation in vitro by added flavins. Kistler and Lin (274) partially purified the dehydrogenase (M_r = 80,000 ± 10,000) from a strain with a deletion in the structural gene (*glpD*) for aerobic glycerol-3-phosphate dehydrogenase and in the specific repressor (*glpR*). Subsequently, Schryvers and Weiner (440) have achieved a purification (Table 10) from a strain harboring a recombinant COlE1:*E. coli* plasmid carrying the *glpA* gene to amplify enzyme levels. Detergent solubilization was unnecessary.

When *E. coli* strain 135 (lacking both the aerobic glycerol-3-phosphate dehydrogenase and succinate dehydrogenase) is grown aerobically with glycerol as carbon source in the presence of fumarate, the anaerobic glycerol-3-phosphate dehydrogenase and fumarate reductase are induced simultaneously. Vesicles from these cells are capable of ATP synthesis and active transport of lactose analogs (330, 331), amino acid transport (456), and energy-dependent quenching of atebrin fluorescence (199), linked to the dehydrogenation of glycerol-3-phosphate at the expense of fumarate (329). The transhydrogenation of glycerol-3-phosphate is associated with proton extrusion from intact cells with a stoichiometry of $2H^+$/dihydroxyacetone phosphate formed, whereas everted membrane vesicles take up protons in the presence of added glycerol-3-phosphate and fumarate (333) (but see also "Fumarate Reductase and Its Associated Respiratory Chain").

Crossed-immunoelectrophoresis of membrane vesicles from cells grown anaerobically with glycerol and fumarate has revealed a glycerol-3-phosphate dehydrogenase, attributed to the anaerobic enzyme (483). Only one precipitation line was associated with the activity, and immunoadsorption studies indicated that the antigen, like that of ATPase, was located at the cytoplasmic site of the vesicle membrane.

D-Amino Acid Dehydrogenases

D-Amino acids, in particular D-alanine and D-glutamate, are important constituents of the cell wall peptidoglycan. Formation of D-amino acids from L-isomers occurs either from equilibrium of the configuration at the α-carbon (racemase action) or by transamination of the appropriate imino acid. Degradation of D-amino acids is catalyzed by membrane-bound or membrane-associated D-amino acid dehydrogenases; oxidation yields the corresponding imino acids which are hydrolyzed to the keto acid and NH_3 (Fig. 11). There is evidence that certain L-amino acids, notably alanine and serine, are degraded indirectly by prior conversion to the D-enantiomers by a membrane-bound racemase (256, 257, 409). In addition, D-amino acid dehydrogenases allow *E. coli* to use D-alanine as sole source of carbon and nitrogen for growth; an alaninase or D-alanine dehydrogenase is responsible for deaminating D-alanine to pyruvate.

The enzyme responsible for D-alanine oxidation in *E. coli* strain B is inducible by L-alanine or DL-alanine but not by D-alanine (410). A partial explanation of this surprising finding

TABLE 10. Properties of L-glycerol-3-phosphate dehydrogenase purified from *E. coli*

Property	Aerobic (439)	Anaerobic (440)
Solubilized by:	Deoxycholate	(Extrinsic membrane protein)
Subunits (M_r; stoichiometry)	58,000, 58,000; 1:1	62,000,[a] 43,000; 1:1
Native mol wt	130,000[b]	93,500–106,000
Cofactor	0.5 mol of FAD 58,000-dalton protein^{-1}	1 mol of FAD mol of dimer^{-1} 2 mol of nonheme Fe mol of dimer^{-1}
K_m (mM)	0.8 0.6	0.339 (with FMN) 0.100 (absence)
V_{max}		34.4 U mg^{-1} (with FMN) 7.18 U mg^{-1} (absence)
Inhibitors	Dihydroxyacetone-3-P (product) Phosphoenol pyruvate, phosphoglycolate and other structural analogs, purine nucleotides, iron chelators, and sulfhydryl reagents	
Subcellular location	Membrane bound (cytoplasmic aspect)	Membrane associated (cytoplasmic aspect)

[a] Dissocation prevented by ethylene glycol.
[b] In presence of detergent.

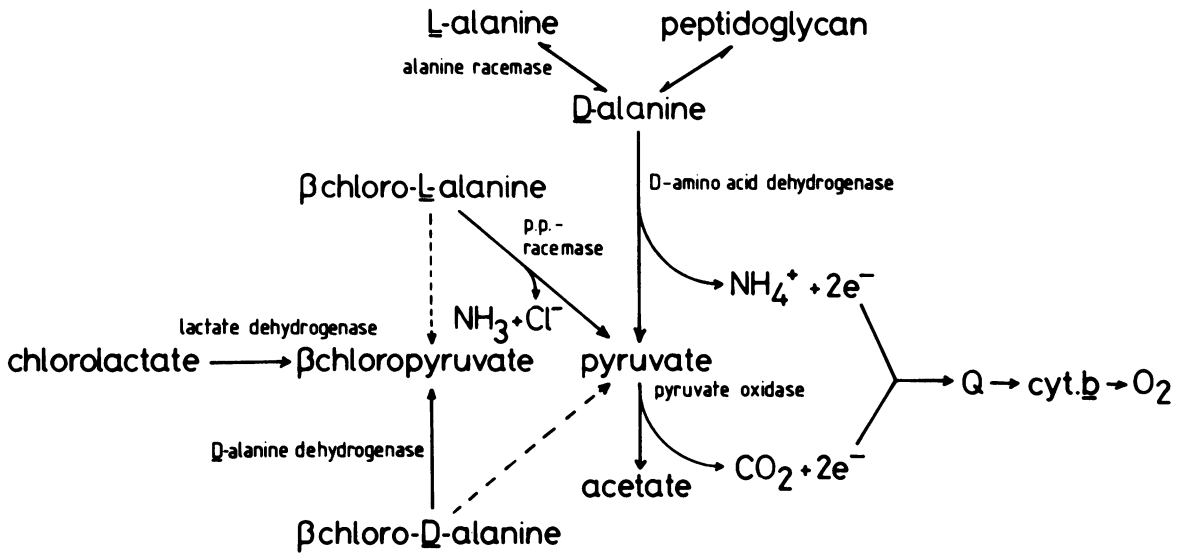

FIG. 11. Metabolic transformation of alanine and its analogs and proposed coupling of oxidation to the respiratory chain. For details, see text (from references 203, 256–258, 357, 358, 492). p.p.-racemase is a pyridoxal phosphate-dependent enzyme.

is that the D-alanine dehydrogenase can oxidize, albeit less rapidly, the L-enantiomer (409). A membrane-bound racemase is intimately associated with the D-alanine dehydrogenase and appears to be the rate-limiting enzyme in the oxidation of L-alanine. In *E. coli* K-12, however, both D- and L-alanine are inducers of the racemase, whereas only the D-isomer induces synthesis of the dehydrogenase (133).

The D-amino acid dehydrogenase is a primary dehydrogenase in the sense that electrons arising from the oxidation reaction are transferred directly to the proton-translocating respiratory chain, so that D-amino acid oxidation can energize active transport of solute (Fig. 11).

Reversible (amino oxyacetate) and irreversible (β-chloroalanine) inhibitors of alanine racemase have been used to show that racemase activity is essential for transport driven by L-alanine but not by D-alanine (256). β-Chloro-L-alanine, unlike the D form, fails to uncouple transport, perhaps due to racemization followed by dehydrogenation to give pyruvate (Fig. 11), whose oxidation by membrane-bound pyruvate oxidase is also coupled to active transport of solutes (256, 257). The inhibitory chloropyruvate is also produced by lactate dehydrogenase-catalyzed oxidation of chloroacetate (257). The precise mode of action of chloropyruvate is uncertain. It does not inhibit D-alanine dehydrogenase, D-lactate dehydrogenase, or electron transfer to cytochromes (258), but does inactivate alanine racemase and pyruvate oxidase.

The D-amino acid dehydrogenase has been solubilized and purified in the presence of Triton X-100 to ≈65% homogeneity (357). The requirement for nonionic detergents for extensive solubilization distinguishes the *E. coli* dehydrogenase from that of *Pseudomonas aeruginosa* (239, 240). The enzyme comprises two subunits of M_r 55,000 and 45,000 and contains FAD and nonheme iron in the ratio 1:2 to 1:3 (357). Preliminary EPR data confirm the presence of an Fe-S center. The enzyme oxidizes several D-amino acids with kinetic constants similar to the membrane-bound enzyme and uses dichlorophenolindophenol or quinone analogs, but not oxygen, as electron acceptors. Quinones also mediate electron transfer to dichlorophenolindophenol or other acceptors, such as cytochrome *c* or ferricyanide and, in vivo, may couple amino acid oxidation to cytochrome reduction (see also reference 241). The substrate specificity of the purified enzyme from *E. coli* B (D-alanine, D-phenylalanine, D-methionine, and D-α-aminobutyrate being the best substrates) is substantially different from that of the *E. coli* K-12 enzyme (133, 240). Mutants of the latter strain (*alnA* or *dad*, mapping at 1.5 min) are defective in D-alanine dehydrogenase (134) and lack a protein of M_r 55,000 to 60,000, which is perhaps the larger of the two subunits (357). A second locus (*dadA* at 26 min [134, 496] may code for the smaller subunit. Beelen et al. (26) have mapped a third locus, *alnR*, at about 99 min, believed to be involved in positive control of *dad* expression.

Recently, reconstitution of D-alanine-dependent active transport has been achieved (358) by incubating the purified dehydrogenase with membrane vesicles. Right-side-out vesicles and inside-out vesicles bind the enzyme to that surface exposed to the medium and, since the normal location of the enzyme is on the inner aspect, right-side-out vesicles bind enzyme to the "wrong" face. Coupled to D-alanine oxidase activity, reconstituted vesicles of both types generate a Δp of similar magnitude. It was suggested that respiration-driven proton translocation occurs distal to the site where electrons enter the chain from the dehydrogenases and that the D-amino acid dehydrogenase cannot, therefore, form part of a proton-translocating loop. However, a loop-type mechanism incorporating these observations can be devised.

The dehydrogenases for D-alanine and D-lactate can be reconstituted simultaneously with right-side-out or inverted membrane vesicles from *E. coli* or to phosphatidylcholine liposomes without detectable competition (203). Although binding is nonspecific, there appears to be a common site for proton translocation in the membrane between the two flavin-linked dehydrogenases and cytochrome *b*; this site must be accessible to electron transfer from primary dehydrogenases on either surface of the membrane.

Recently, it has been confirmed that the solubilized and partially purified D-amino acid dehydrogenase binds to membranes from either induced or noninduced cells, but in an

Mg^{2+}-sensitive fashion (240). The alanine racemase (EC 5.1.1.1) has been solubilized with Triton X-100 and purified about 9,000-fold (492). It is a dimer of M_r 100,000 containing one pyridoxal phosphate per subunit.

Hydrogenases

Hydrogenases (EC class 1.12.-.-) catalyze the reversible oxidation of dihydrogen to protons and electrons. Two major functions are effected by hydrogenase(s) in *E. coli*. First, H_2 production enables the organism to dispose of excess reductant formed in fermentation. Thus, pyruvate is converted to formate by pyruvate:formatelyase with the concomitant production of acetyl coenzyme A. The formate is subsequently converted to H_2 and CO_2 by the formate-hydrogenlyase complex (176). This multienzyme system consists of a formate dehydrogenase and hydrogenase linked by unidentified intermediate electron carriers (for references, see reference 6). This pathway for the disposal of reducing equivalents as H_2 is controlled by repression of the formate hydrogenlyase by nitrate and oxygen, which can serve as terminal electron acceptors in ATP-generating pathways.

Second, H_2 may be used as a reductant. Macy et al. (316) found that *E. coli* could grow anaerobically with fumarate or L-malate when H_2 or formate was present as electron donor. Succinate was the major product of malate "fermentation," and a mutant lacking fumarate reductase could not grow on malate or H_2. These findings, and the fact tha only traces of acetate were produced, suggested that ATP was synthesized during cytochrome-mediated electron flow from hydrogen to fumarate reductase (28).Nitrate or trimethylamine can also act as oxidants for anaerobic growth on H_2 (501).

Measurement of the quenching of fluorescence of the acridine dye atebrin (indicative of ΔpH) in inverted membrane vesicles has shown that H_2-dependent reduction of fumarate translocates protons inwards (243); this would be an outward translocation in intact cells. Further experiments with spheroplasts (i.e., with the same membrane polarity as intact cells) gave the predicted outward proton translocation and showed H_2-dependent $H^+/2e^-$ stoichiometries of 1.85 and 3.3, with fumarate and nitrate as respective electron acceptors. Proton translocation was sensitive to an uncoupler and HOQNO. In contrast, proton movement driven by H_2-dependent reduction of menadione and ubiquinone-1 was uncoupler sensitive, but HOQNO insensitive, with an $H^+/2e^-$ stoichiometry of approximately 2.

The directionality of H^+ release from H_2 was examined by loading spheroplasts with oxidized benzyl viologen (BV^{2+}), which cannot readily cross the membrane and which acts as an electron (but not proton) acceptor, and pulsing with H_2 (244). Parallel spectrophotometric and pH measurements showed the rate of reduction of BV^{2+} to BV^+ to be similar to that of H^+ ejection, and the ratio $\Delta e^-/H_2$ was consistent with the stoichiometric release of protons:

$$H_2 \rightarrow 2H^+ + 2e^- \quad (8)$$

That H_2-dependent BV^{2+} reduction is independent of cytochromes (242), together with other considerations (5, 244), suggests that hydrogenase reduces BV^{2+} directly, as it does menadione (an analog of the endogenous menaquinone) and menaquinone itself. Proposed H_2-dependent pathways for fumarate and nitrate reduction are given by Jones (244), the fumarate pathway being similar to the linear pathway proposed by Bernhard and Gottschalk (29) in postulating an HOQNO-sensitive site on the fumarate side of menaquinone.

Direct covalent modification of the enzyme with non-membrane-permeant reagents ([^{125}I]diiodosulfanilic acid and lactoperoxidase-catalyzed incorporation of ^{125}I) has been compared with spheroplasts and predominantly inside-out membrane vesicles (167) prepared from cells grown on glucose plus nitrate. These studies show the enzyme to span the cytoplasmic membrane. Confirmation of this topography was obtained in immunoadsorption studies. However, similar experiments with intact and solubilized membrane vesicles from cells grown anaerobically on glycerol plus fumarate have shown that hydrogenase is exposed at the inner aspect of the membrane only and have not confirmed a transmembranous location (483). A transmembranous organization is not essential if the catalytic site is periplasmic, but if the active site is cytoplasmic, a transmembrane proton-translocating complex is required.

The membrane-bound hydrogenase of aerobically grown *E. coli* has been solubilized with deoxycholate and pancreatin and purified by conventional chromatographic procedures (5). The enzyme is a dimer of identical subunits with M_r 113,000 (2 × 56,500). Like all hydrogenases (504), it is an FeS protein, in this case containing 12 Fe and 12 acid-labile sulfur atoms per molecule. Iron-deficient cells lack hydrogenase and formate hydrogenlyase activities (140). As prepared in the oxidized form, a narrow EPR signal at about g = 2.02, characteristic of HiPIP-type FeS centers, has been observed (56), and its midpoint potential has been measured as +25 mV. This surprisingly high value, in view of the potential of the H^+/H_2 couple (−420 mV at pH 7), has led to the suggestion that the cluster(s) responsible for the g = 2.02 signal is not directly involved in electron transfer reactions with hydrogen but may have a regulatory role or be involved in protecting the active site from oxygen. Alternatively, the HiPIP center may be involved in redox reactions with the quinone pool. Spectra of the reduced form were not reported.

There is evidence for the existence of multiple forms or states of hydrogenase. Thus, the solubilized enzyme on polyacrylamide gels gave initially a single stainable band of activity on incubation with methyl viologen, but after prolonged incubation additional staining bands appeared (5). Further purification by chromatography on octyl-Sepharose CL-43 gave only a single band, presumably as a result of the removal of small amounts of other hydrogenase types, hydrogenase binding to other proteins, or the presence in the crude preparation of modifiers of enzyme activity or all three. Earlier, up to six types of hydrogenase were found on polyacrylamide gels (501), the relative amounts of each form depending on the growth conditions. The R_f of 0.27 (10% [wt/vol] acrylamide) of one such form corresponded to the value in reference 5. Ackrell et al. (4) also reported a multiplicity of bands of hydrogenase activity after gel electrophoresis of aerobically and "semiaerobically" grown cells, whereas only one form of hydrogenase was precipitated with specific antibody by Graham et al. (173).

The enzyme from cells grown anaerobically with fumarate and H_2 has been partially purified and characterized after solubilization with deoxycholate, ammonium sulfate fractionation, and Sephadex G-200 chromatography (29). The enzyme had an M_r of 19,000 and was highly unstable, even when stored under H_2. In vivo, the location of the enzyme was deduced to be at the inner aspect of the cytoplasmic membrane, by virtue of its inaccessibility to viologen dyes.

An alternative approach to studying the enzyme of anaerobically grown cells has been to prepare antibodies specific for hydrogenase from activity-stained precipitation arcs located after analysis of crude fractions by crossed-immuno-

electrophoresis, using antisera raised to detergent-solubilized membranes. SDS gel analysis (cylindrical gels) of immunoprecipitates recovered from ^{35}S-labeled, solubilized membranes, using hydrogenase-specific antibodies (173), gave a single radioactive band of M_r 58,000. This is in close agreement with the single polypeptide (M_r = 56,500) found for hydrogenase from aerobically grown cells (5) and with a later value (for slab gels) of 63,000 (167). However, recent work has shown that two hydrogenases exist in *E. coli*, the oxidative and the H_2-evolving enzymes (D. H. Boxer, personal communication).

In the above aerobically grown cells (5), formate hydrogenlyase activity was absent, probably as a result of the lack of an appropriate formate dehydrogenase. Cytochrome c_{552} was also absent in aerobically grown cells; in fact, no physiological endogenous carrier for electron transfer to hydrogenase from dithionite or exogenous flavin nucleotides was found, suggesting that hydrogenase is without function in the absence of the formate hydrogenlyase pathway. The purified hydrogenase, however, catalyzed both H_2 evolution and H_2 uptake with a variety of artificial electron carriers.

Further evidence for the function of hydrogenase in anaerobic growth comes from the isolation (using a selection method based on reduction of methyl viologen) and characterization of an *E. coli* mutant with lowered activity of menbrane-bound hydrogenase (164). This strain, Hb1, grew aerobically, but much more slowly under anaerobic conditions unless ferricyanide or preferably nitrate was added as the alternative electron acceptor.

Mutants deficient in hydrogenase activity have been identified by Graham et al. (173), using a dye overlay technique. These mutants lacked hydrogen-dependent benzyl viologen reductase activity, thus resembling *hyd* mutants (368). Phage-mediated transduction experiments showed that *hyd* was closer to *cysC* than once thought. That hydrogenase antigen was absent from both mutants was demonstrated by crossed-immunoelectrophoresis of Triton X-100-solubilized membranes against anti-"membrane vesicle" serum, which failed to show the precipitin arc corresponding to hydrogenase. Defective hydrogenase protein was not found in the cytoplasm (173).

OTHER OXIDASE AND DEHYDROGENASE ACTIVITIES

Pyruvate Oxidase

The pyruvate-oxidizing (dehydrogenase) activity of membrane vesicles (see above) observed by Kaczorowski et al. (256) is due (446) to a thymine pyrophosphate- and FAD-requiring pyruvate oxidase (EC 1.2.3.3), a tetrameric protein with identical subunits of M_r 60,000 (350, 407). Unlike the other flavoprotein dehydrogenases from *E. coli*, it can be released from the membrane by sonication and purified to yield a lipid- and detergent-free preparation. It is a peripheral membrane protein whose activity is dramatically stimulated by a variety of lipids, phospholipids, and detergents (30, 431). The lipid-protein interactions, primary hydrophobic (30), have been the subject of intensive studies (for a review, see reference 320). Lipids modulate the turnover number of the enzyme as well as the strength and cooperativity of substrate and cofactor binding (349). Similarly and significantly, the catalytic ligands have a strong influence on the affinity of the protein for lipids (97, 431, 438). Recent biophysical studies (351) have revealed localized conformational changes in the protein, due to either reduction of the flavin or the binding of lipid activators. The influence of substrate and cofactor on lipid affinity is well illustrated by the sedimentation behavior of the enzyme with dipalmitoylphosphatidylcholine vesicles. In the absence of catalytic ligands, the protein and lipid vesicles sediment separately but migrate as a single species in the presence of ligands (438).

Recent studies have highlighted the importance of FAD in lipid activation and stabilization of the enzyme structure. Acid removal of the flavin group results in dissociation of the protein into apoenzyme monomers (411). Kinetic studies of the reconstitution process show a fast reassociation of FAD with the monomers followed by a rate-limiting (for activation) folding of the polypeptide monomer to reform the FAD binding site, and formation of native tetramers by assembly of dimers. Reconstitution studies with synthetic analogs of FAD (321) have shed light on the nature of the FAD binding site and shown that the flavin is substantially buried within the protein.

The activity in spheroplasts is insensitive to pyruvate oxidase antibody. This together with the use of impermeant, inhibitory analogs of thymine pyrophosphate have established that the enzyme is located at the inner surface of the cytoplasmic membrane (446). However, the studies outlined above on lipid interactions suggest that, in vivo, binding to the membrane may be controlled by concentrations of substrate and cofactor.

This enzyme is distinct from the pyruvate dehydrogenase multienzyme complex (which provides acetyl-coenzyme A) in acting as a primary dehydrogenase, generating substrate-derived electrons to the membrane-bound respiratory chain, and generating a Δp. Solubilized pyruvate oxidase will bind to membrane vesicles, resulting in extensive stimulation of respiration but only a modest increase in solute uptake, suggesting a low coupling efficiency. The pathway of electron flow from pyruvate to oxygen is not known with certainty, but it is most likely that reoxidation of the flavin coenzyme is catalyzed by an oxidant in the membrane, possibly ubiquinone (98), and that electron transfer proceeds via the membrane-bound cytochromes (284).

Mutants in the structural gene for pyruvate oxidase (*poxB*) have recently been isolated and characterized (64). Isolation was facilitated by the very slow aerobic growth on acetate of previously isolated mutants (*poxA*) carrying a deletion of the pyruvate dehydrogenase locus (Δ*aceEF* [63]). Strains that also contained a lesion in the regulatory gene *poxA* were completely unable to grow under these conditions, presumably due to the lack of pyruvate oxidase-dependent production of acetate, the carbon source. The mutants contain normal levels of pyruvate oxidase antigen but have no, or reduced, pyruvate oxidase activities. The *poxB* locus maps at 18.7 min, a location far removed from that of the regulatory gene, *poxA*.

Malate Oxidase

The malate oxidase (dehydrogenase) from *E. coli* (343) shares many properties with pyruvate oxidase (see above). Both are peripheral membrane proteins, which can be obtained in a lipid-free, soluble state without the use of detergents and which, in situ, probably transfer electrons from substrates via FAD to the membrane-bound respiratory chain. Both enzymes are present at low levels in normal cells but have elevated activities in mutants lacking the activity of the corresponding tricarboxylic acid cycle enzyme (i.e., pyruvate dehydrogenase and the NADH-dependent malate dehydrogenase, respectively). However, the ability of the FAD-dependent malate oxidase to generate proton gradients

and drive active transport has not been reported. The partially purified enzyme from an *E. coli* strain, highly derepressed for malate oxidase, transfers electrons to various artificial electron accepts and to menaquinone (343). It is significantly activated by nonionic detergents, some lipids, cardiolipin, and azolectin (a lipid mixture); the lipids dramatically alter the K_m and V_{max} for FAD, but not the K_m for malate or the electron acceptor. FAD thus appears to act as both substrate and regulatory ligand. The enzyme is inhibited by AMP, ADP, ATP, and NAD, the inhibition being competitive against FAD. The inhibition of malate oxidation by the antimicrobial agent phenoxyethanol (154) is probably that of the tricarboxylic acid cycle malate dehyrogenase.

Dihydroorotate Dehydrogenases

Dihydroorotate dehydrogenases catalyze both the synthesis and the degradation of pyrimidines by the following reaction:

$$\text{L-5,6-dihydroorotate} + X \rightleftharpoons \text{orotate} + XH_2 \quad (9)$$

In *E. coli*, the biosynthetic enzyme (EC 1.3.3.1) is membrane bound, is repressible by pyrimidines and products (476, 504), and passes reducing equivalents to the membrane-bound electron transport chains either aerobically (268) or anaerobically (344). This enzyme is distinct from the soluble FeS-containing enzyme involved in orotic acid fermentation found in, for example, *Clostridium oroticum* (504).

The purified membrane-bound *E. coli* enzyme has an M_r of 67,000 (261). The effect of trypsin on the enzyme in extracts and in cells from which the outer envelope layer was removed suggests that the enzyme is located on the inner side of the cytoplasmic membrane. Owen and Kaback (362) have drawn the same conclusion by using crossed-immunoelectrophoresis.

The anaerobic oxidation of dihydroorotate has been studied in various mutants and shown to be linked via menaquinone (344) to the fumarate reductase and independent of the cytochromes. Ferricyanide can act as artificial electron acceptor for the dehydrogenase, which can be effectively solubilized with 2 M guanidine · HCl (15).

NAD^+-Dependent Glycerol Dehydrogenase

Glycerol and glycerol-3-phosphate utilization in *E. coli* is dependent on the presence of an exogenous electron acceptor (oxygen, nitrate, or fumarate; see above); cells cannot grow anaerobically on glycerol alone. In contrast, certain strains of *Klebsiella pneumoniae* can grow anaerobically on glycerol in the absence of an external oxidant by using two parallel pathways (the *dha* system; e.g., see reference 425). In the first, an NAD^+-linked dehydrogenase and ATP-dependent kinase convert glycerol to dihydroxyacetone phosphate. In the second, a coenzyme B_{12}-dependent glycerol dehydratase and an NADH-linked β-hydroxypropionaldehyde reductase generate 1,3-propanediol and regenerate NAD^+. More glycerol is thus converted to dihydroxyacetone phosphate, a key glycolytic intermediate. The inducer of the *dha* system is thought to be dihydroxyacetone (for further details, see reference 472).

Knowing that some *E. coli* strains synthesize low levels of an NAD^+-linked glycerol dehydrogenase of unknown physiological function, Tang and others (472) have derived from a strain lacking both glycerol kinase and aerobic glycerol-3-phosphate dehydrogenase a mutant with elevated levels of the NAD^+-linked glycerol dehydrogenase. The strain grows equally well aerobically with glycerol or dihydroxyacetone as carbon and energy source but does not grow anaerobically unless nitrate is also present. In contrast to wild-type cells utilizing the *glp* system, fumarate is not an effective terminal electron acceptor.

Proline Dehydrogenase

E. coli oxidizes L-proline to glutamate via the intermediate Δ′-pyrroline-5-carboxylate (131, 437), using an inducible enzyme (132) which was in earlier work referred to as proline oxidase. The enzyme has been solubilized without detergents and purified to near homogeneity (437). A single polypeptide with an M_r of 124,000 was detected in denaturing SDS gel electrophoresis, but the enzyme may exist as a dimer as isolated. The preparation contained about 0.24 equivalent of FAD per polypeptide chain. Activity of the enzyme in vitro requires the mediator PMS and an acceptor such as *p*-iodonitrotetrazolium, whereas the membranous enzyme, in the presence of NAD, catalyzes the complete conversion of L-proline to glutamate; the purified enzyme forms only the intermediate Δ′-pyrroline-5-carboxylate, presumably due to lack of the appropriate dehydrogenase. In view of the requirement for an artificial electron donor and the lack of a direct electron-accepting role for oxygen, it is probable that the enzyme is better described as a dehydrogenase (437). At present, there appears to be no further information on the coupling of this dehydrogenase to the respiratory chain.

6-Phosphogluconate Dehydrogenase

Immunochemical studies (363, 483) have indicated that at least some of the *E. coli* 6-phosphogluconate dehydrogenase (EC 1.1.1.43) is membrane associated in cells grown either aerobically or anaerobically (with nitrate or fumarate). The zymogen-staining arcs for 6-phosphogluconate dehydrogenase in the study on solubilized aerobic membranes (arc 7 in reference 363) are close enough to the arc from the glycerol-fumarate membranes (arc 17 in reference 483) to suggest that there is only one enzyme and that it is present under different growth conditions. The *E. coli* enzyme is highly anionic and cross-reacts with antibodies to *S. typhimurium* membranes.

6-Phosphogluconate dehydrogenase has been isolated and purified from *E. coli* as a soluble enzyme (109), and the effect of various metabolites on its reaction velocities has been studied. The enzyme is specific for $NADP^+$ as cofactor (oxidant) and this is not a primary respiratory chain dehydrogenase.

REPLICATION OF RESPIRATORY CHAIN COMPONENTS IN THE CELL CYCLE

The cytoplasmic membrane of *E. coli* provides an excellent example of biological organization in space and time. The hierarchy of spatial organization (304) extends from, for example, the transmembrane distribution of small ions that constitute electrochemical gradients to the complex electron transfer proteins, e.g., hydrogenase and nitrate reductase, that span the entire membrane. These macromolecules are organized in the hydrophobic membrane such that they catalyze vectorial reactions and are in appropriate proximity to functionally related components.

This spatial hierarchy is accompanied by a temporal organization which, in bioenergetic systems generally, is particularly spectacular in its scope. Among the fastest events are the rotational and diffusional mobilities of cytochromes *o* and a_1 in *E. coli* membranes (147, 149), with relaxation times (the time taken for the effect of a perturbation to have decreased to e^{-1} of its initial value) of 100 to 300 μs. Still in the "metabolic time domain" are the reactions of

electron transfer, which extend, for example, from those catalyzed by terminal oxidases ($t_{1/2} < 3.3$ ms) to the relatively sluggish oxidation by nitrate of *b*-type cytochromes ($t_{1/2} \approx$ 300 ms) (196). Slower reactions of the metabolic time domain are exemplified by the reaction sequences and cycles of intermediary metabolism, in which diffusion, interaction, and enzyme-catalyzed transformation of small molecules play rate-determining roles. Characteristic of such systems are the oscillatory states resulting from nonlinear kinetics of the constituent reactions and poising of the system far from equilibrium. The best-understood biochemical oscillator is that of glycolysis in yeasts, but oscillations on a similar time scale have also been observed in bacterial energetics. Thus, in *Klebsiella aerogenes* undamped oscillations (period, 2 to 3 min) were observed in oxygen tension and pyridine nucleotide fluorescence after an anaerobic shock (206), and oscillations in the fluorescence of flavins and pyridine nucleotides (period, 0.6 to 2 min) are induced when the air supply to *E. coli* cultures is disturbed in the late exponential phase of growth (C. L. Bashford, R. Misri, and R. K. Poole, unpublished data). The hierarchy proceeds through the epigenetic time domain, in which the biosynthesis and processing of macromolecules are found, to the cell division cycle. The cell cycle is characterized by recurrent and regular replication of DNA and the approximate doubling in amount of each cellular constituent before segregation at division. This is a particularly neglected area of study with respect to energetic systems (for a survey, see reference 304).

Any measurements made on membranes or other material derived from exponentially growing (i.e., asynchronous) cultures are open to the criticism that the data are time averaged over the cell cycle so that the properties described may not reflect those of any one cell. However, relatively few studies have been made of respiratory development during the cell cycle of bacteria (for reviews, see references 348 and 375). Synchronous cultures of *E. coli*, prepared by continuous-flow selection of slowly sedimenting cells, exhibit complex oscillatory and stepwise patterns of increasing whole-cell oxygen uptake during the cycle (124, 373). In one study, and in contrast to comparable experiments with certain eucaryotic microorganisms (374, 385), respiratory oscillations were shown not to be the consequence of classical respiratory (acceptor) control mechanisms (373). However, in contrast to these complex patterns, both earlier (318) and the most recent measurements made by continuously monitoring oxygen tension in an electrode system open to the atmosphere (336) reveal a simple, continuous increase in cellular respiration rates. To what extent these disparate findings reflect the method of synchronization remains to be established. A continuous increase in respiration rates during the cell cycle is consistent with recent physiological data whch suggest that electron transfer is rate limiting for growth of *E. coli* and other bacteria (14, 378, 467) and the finding that uncouplers frequently do not stimulate respiration rates of cells from rapidly growing cultures (52, 373).

Cell cycle analysis by zonal fractionation of cells from exponentially growing cultures has revealed that this gradual increase in respiration is accompanied by continuous, probably exponential increases in the levels of components of the aerobic electron transport chain (see, however, reference 352). These components include cytochrome *o* (identified and quantified in photodissociation spectra; 441), all other cytochromes resolvable by fourth-order finite difference analysis (442), certain FeS proteins (387), and the activity of succinate dehydrogenase (R. Misri and R. K. Poole, unpublished data). These findings are consistent with, but not necessarily required by, recent reports (e.g., reference 308) that proteins resolvable by two-dimensional gel electrophoresis accumulate continuously during the cell cycle.

When the three-dimensional orientations within the membrane of (i) low-spin cytochrome heme (380) and (ii) a ferredoxin-type FeS cluster (387) were determined in oriented "multilayers" of isolated membranes, no evidence was obtained for a cell cycle-specific rearrangement of these components.

Virtually nothing is known about the contributions of synthesis and turnover to the observed continuous accumulation of membrane proteins. A membrane-bound, ATP-stimulated endoprotease, which could function in such a turnover, has been reported recently (489).

CONCLUDING REMARKS

We have attempted to survey the exceedingly complex and diverse respiratory chains of *E. coli*, concentrating on more recent work. Such a review cannot be exhaustive and we apologize for the omission of work whose publication or significance we have overlooked.

Studies of the respiration of *E. coli* are not recent in origin. The current upsurge in interest extends to some extent to the respiratory systems of all bacteria, but is particularly spectacular in *E. coli* because of the special advantages that this organism offers to the experimentalist. These hardly need reiteration in detail here, but chief among them are the ability to manipulate, by appropriate choice of growth conditions, the pathways of electron transport and the components responsible for electron transfer, and the availability, and potential for isolation, of mutants defective in specific respiratory components.

These approaches have already allowed an overall view such as that in Fig. 3 to be conceived. It is clear that a simplistic linear flow of electron transport to O_2 is not a realistic model and that instead it is more appropriate to regard the respiratory system overall as comprising modules or segments, many of which can coexist. Low-potential modules interact with high-potential modules via quinones and although there is some restriction and preference for combinations of low and high segments, a certain promiscuity of electron flow is evident.

The methods of molecular biology have made spectacular contributions to our understanding of the structure and biosynthesis of many of the protein components of the respiratory chains. Fumarate and succinate dehydrogenous provide notable examples. Amplification of protein levels, already begun, for example with NADH dehydrogenase, will hopefully be extended to those chromophoric proteins whose mutual spectral overlap and low signal-to-noise characteristics in situ have frustrated analysis. Indeed, the interpretation of optical spectra is still fraught with difficulty and uncertainty. The identification of a stable oxygenated form of cytochrome *d* and the possibility that cytochrome a_1 may in reality be a *b*-type heme protein, perhaps with hydroperoxidase function, illustrate how long-established views may be erroneous.

We believe that such studies on the *E. coli* respiratory chains can yield answers of general relevance to respiration and oxidative phosphorylation.

ACKNOWLEDGMENTS

We thank our many colleagues and co-workers, especially D. H. Boxer for critical reading of parts of the typescript and P. D. Bragg, R. B. Gennis, and J. R. Guest for sending unpublished manuscripts and data.

Our own work described in this review was financed by the Royal Society and the Nuffield Foundation (to W.J.I. and R.K.P.), the Science and Engineering Research Council, United Kingdom (to W.J.I. and R.K.P.), and the University of London Central Research Fund (to R.K.P.).

LITERATURE CITED

1. **Abou-Jaoudé, A., M. Chippaux, and M.-C. Pascal.** 1979. Formate-nitrite reduction in *Escherichia coli* K12. 1. Physiological study of the system. Eur. J. Biochem. **95**:309–314.
2. **Abou-Jaoudé, A., M.-C. Pascal, F. Casse, and M. Chippaux.** 1978. Isolation and phenotypes of mutants from *Escherichia coli* K12 defective in nitrite-reductase activity. FEMS Microbiol. Lett. **3**:235–239.
3. **Abou-Jaoudé, A., M.-C. Pascal, and M. Chippaux.** 1979. Formate-nitrite reductase in *Escherichia coli* K12. 2. Identification of components involved in the electron transfer. Eur. J. Biochem. **95**:315–321.
4. **Ackrell, B. A. C., R. N. Asato, and H. F. Mower.** 1966. Multiple forms of bacterial hydrogenases. J. Bacteriol. **92**:828–838
5. **Adams, M. W. W., and D. O. Hall.** 1978. Purification of the membrane-bound hydrogenase of *Escherichia coli*. Biochem. J. **183**:11–22.
6. **Adams, M. W. W., L. E. Mortenson, and J. S. Chen.** 1981. Hydrogenase. Biochim. Biophys. Acta **594**:105–176.
7. **Adler, L. W., T. Ichikawa, S. M. Hasan, T. Tsuchiya, and B. P. Rosen.** 1977. Orientation of the protonmotive force in membrane vesicles of *Escherichia coli*. J. Supramol. Struct. **1**:15–27.
8. **Adler, L. W., and B. P. Rosen.** 1977. Functional mosaicism of membrane proteins in vesicles of *Escherichia coli*. J. Bacteriol. **129**:959–966.
9. **Alben, J. O., P. P. Moh, F. G. Fiamingo, and R. A. Altschuld.** 1981. Cytochrome oxidase (a_3) heme and copper observed by low-temperature Fourier transform infrared spectroscopy of the CO complex. Proc. Natl. Acad. Sci. U.S.A. **78**:234–237.
10. **Alexander, K., and I. G. Young.** 1978. Three hydroxylations incorporating molecular oxygen in the aerobic biosynthesis of ubiquinone in *Escherichia coli*. Biochemistry **17**:4745–4750.
11. **Alexander, K., and I. G. Young.** 1978. Alternative hydroxylases for the aerobic and anaerobic biosynthesis of ubiquinone in *Escherichia coli*. Biochemistry **17**:4750–4755.
12. **Altendorf, K. H., and L. A. Staehelin.** 1974. Orientation of membrane vesicles from *Escherichia coli* as detected by freeze-cleave electron microscopy. J. Bacteriol. **117**:888–899.
13. **Amy, N. K.** 1981. Identification of the molybdenum cofactors in chlorate-resistant mutants of *Escherichia coli*. J. Bacteriol. **148**:274–282.
14. **Andersen, K. B., and K. Von Meyenburg.** 1980. Are growth rates of *Escherichia coli* in batch cultures limited by respiration? J. Bacteriol. **144**:114–123.
15. **Andrews, S., G. B. Cox, and F. Gibson.** 1977. The anaerobic oxidation of dihydroorotate by *Escherichia coli* K12. Biochim. Biophys. Acta **462**:153–160.
16. **Ashcroft, J. R., and B. A. Haddock.** 1975. Synthesis of alternative membrane-bound redox carriers during aerobic growth of *Escherichia coli* in the presence of potassium cyanide. Biochem. J. **148**:349–352.
17. **Azoulay, E., C. Rivière, G. Giordano, J. Pommier, M. Denis, and G. Ducet.** 1977. Participation of cytochrome *b* to the *in vitro* reconstitution of the membrane-bound formate-nitrate reductase of *Escherichia coli* K12 and the possible role of sulfhydryl groups and temperature in the reconstitution process. FEBS Lett. **79**:321–326.
18. **Bachmann, B. J.** 1983. Linkage map of *Escherichia coli* K-12, edition 7. Microbiol. Rev. **47**:170–230.
19. **Barnes, E. M., and H. R. Kaback.** 1970. Beta galactoside transport in bacterial membrane preparations. Energy coupling via membrane bound D-lactic dehydrogenase. Proc. Natl. Acad. Sci. U.S.A. **66**:1190–1198.
20. **Barnes, E. M., and H. R. Kaback.** 1971. Mechanisms of active transport in isolated membrane vesicles. Part 1. The site of energy coupling between D-lactic dehydrogenase and beta galactoside transport in *Escherichia coli* membrane vesicles. J. Biol. Chem. **246**:5518–5522.
21. **Barr, G. C., and S. E. Palm-Nicholls.** 1981. Cloning the *chlC* gene for nitrate reductase of *Escherichia coli*. FEMS Microbiol. Lett. **11**:213–216.
22. **Barrett, J.** 1956. The prosthetic group of cytochrome a_2. Biochem. J. **64**:626–639.
23. **Barrett, J., and P. R. Sinclair.** 1967. The cytochrome *c* (552) of aerobically grown *Escherichia coli* str. McElroy and its function. Biochim. Biophys. Acta **143**:279–281.
24. **Bartana, J., B. J. Howlett, and D. E. Koshland.** 1977. Flagellar formation in *Escherichia coli* electron transport mutants. J. Bacteriol. **130**:787–792.
25. **Barton, L. L., J. LeGall, and H. D. Peck.** 970. Phosphorylation coupled to oxidation of hydrogen with fumarate in extracts of the sulfate reducing bacterium, *Desulfovibrio gigas*. Biochem. Biophys. Res. Commun. **41**:1036–1042.
26. **Beelen, R. H. J., A. M. Feldmann, and H. J. W. Wijsman.** 1973. A regulatory gene and a structural gene for alaninase in *Escherichia coli*. Mol. Gen. Genet. **121**:369–374.
27. **Bennett, R., D. R. Taylor, and A. Hurst.** 1966. D- and L-lactate dehydrogenases in *Escherichia coli*. Biochim. Biophys. Acta **118**:512–521.
28. **Bernhard, T., and G. Gottschalk.** 1978. Cell yields of *Escherichia coli* during anaerobic growth on fumarate and molecular hydrogen. Arch. Microbiol. **116**:235–238.
29. **Bernhard, T., and G. Gottschalk.** 1978. The hydrogenase of *Escherichia coli*. Purification, some properties and the function of the enzyme, p. 199–208. *In* H. G. Schlegel and K. Schneider (ed.), Hydrogenases: their catalytic activity, structure and function. E. Goltze, Göttingen.
30. **Blake, R., L. P. Hager, and R. B. Gennis.** 1978. Activation of pyruvate oxidase by monomeric and micellar amphiphiles. J. Biol. Chem. **258**:1963–1971.
31. **Blum, H., and R. K. Poole.** 1982. The molybdenum and iron-sulphur centres of *Escherichia coli* nitrate reductase are non-randomly oriented in the membrane. Biochem. Biophys. Res. Commun. **107**:903–909.
32. **Blum, H., R. K. Poole, and T. Ohnishi.** 1980. The orientation of iron-surphur clusters in membrane multilayers prepared from aerobically-grown *Escherichia coli* K12 and a cytochrome-deficient mutant. Biochem. J. **190**:385–393.
33. **Bonnefoy-orth, V., M. Lepelletier, M.-C. Pascal, and M. Chappaux.** 1981. Nitrate reductase and cytochrome $b_{\text{nitrate reductase}}$ structural genes as parts of the nitrate reductase operon. Mol. Gen. Genet. **181**:535–540.
34. **Boogerd, F. C., H. W. Van Verseveld, and A. H. Stouthamer.** 1983. Dissimilatory nitrate uptake in *Paracoccus denitrificans* via a $\Delta\mu_{H^+}$ dependent system and a nitrate-nitrite antiport system. Biochim. Biophys. Acta **723**:415–427.
35. **Boonstra, J., J. A. Downie, and W. N. Konings.** 1978. Energy supply for active transport in anaerobically grown *Escherichia coli*. J. Bacteriol. **136**:844–853.
36. **Boonstra, J., M. T. Huttunen, and W. N. Konings.** 1975. Anaerobic transport in *Escherichia coli* membrane vesicles. J. Biol. Chem. **250**:6792–6798.
37. **Boonstra, J., and W. N. Konings.** 1977. Generation of an electrochemical proton gradient by nitrate respiration in membrane vesicles from anaerobically grown *Escherichia coli*. Eur. J. Biochem. **78**:361–368.
38. **Boonstra, J., H. J. Sips, and W. N. Konings.** 1976. Active transport by membrane vesicles from anaerobically grown *Escherichia coli* energized by electron transfer to ferricyanide and chlorate. Eur. J. Biochem. **69**:35–44.
39. **Boxer, D. H., and R. A. Clegg.** 1975. A transmembrane location for the proton-translocating reduced ubiquinone → nitrate reductase of the respiratory chain of *Escherichia coli*. FEBS Lett. **60**:54–57.
40. **Boxer, D. H., A. Malcolm, and A. Graham.** 1982. *Escherichia coli* formate to nitrate respiratory pathway: structural analysis. Biochem. Soc. Trans. **10**:480–481.
41. **Bragg, P. D.** 1971. Effect of near-ultraviolet light on the respiratory chain of *Escherichia coli*. Can. J. Biochem. **49**:492–

495.
42. **Bragg, P. D.** 1979. Electron transport and energy-transducing systems of *Escherichia coli*, p. 341–449. *In* R. A. Capaldi (ed.), Membrane proteins in energy transduction. Marcel Dekker AG, Basel.
43. **Bragg, P. D.** 1980. The respiratory system of *Escherichia coli*, p. 115–136. *In* C. J. Knowles (ed.), Diversity of bacterial respiratory systems, vol. 1. CRC Press Inc., Boca Raton, Fla.
44. **Bragg, P. D., and C. Hou.** 1967. Reduced nicotinamide adenine dinucleotide oxidation in *Escherichia coli* particles. II. NADH dehydrogenases. Arch. Biochem. Biophys. **119**:202–208.
45. **Bragg, P. D., and W. J. Polglase.** 1963. Electron-transport components of streptomycin-dependent *Escherichia coli*. J. Bacteriol. **86**:544–547.
46. **Bragg, P. D., and D. J. Rainnie.** 1974. The effect of silver ions on the respiratory chain of *Escherichia coli*. Can. J. Microbiol. **20**:883–889.
47. **Bray, R. C., S. P. Vincent, D. J. Lowe, R. A. Clegg, and P. B. Garland.** 1976. Electron-paramagnetic-resonance studies on the molybdenum of nitrate reductase from *Escherichia coli* K12. Biochem. J. **155**:201–203.
48. **Brice, J. M., J. F. Law, D. J. Meyer, and C. W. Jones.** 1974. Energy conservation in *Escherichia coli* and *Klebsiella pneumoniae*. Biochem. Soc. Trans. **2**:523–526.
49. **Brock, T. D.** 1971. Microbial growth rates in nature. Bacteriol. Rev. **35**:39–58.
50. **Brookman, J. J., J. A. Downie, F. Gibson, G. B. Cox, and H. Rosenberg.** 1979. Proton translocation in cytochrome-deficient mutants of *Escherichia coli*. J. Bacteriol. **137**:705–710.
51. **Bullock, P. A., and Y. P. Meyer.** 1978. Circular dichroism and resonance Raman studies of cytochrome b_{562} from *Escherichia coli*. Biochemistry **17**:3084–3091.
52. **Burstein, C., L. Tiankova, and A. Kepes.** 1979. Respiratory control in *Escherichia coli* K12. Eur. J. Biochem. **94**:387–392.
53. **Butler, W. L.** 1979. 4-th Derivative spectra. Methods Enzymol. **56**:501–515.
54. **Cammack, R., B. Crowe, and P. Owen.** 1982. Characterization of succinate dehydrogenase from *Micrococcus lysodeikticus*. Biochem. Soc. Trans. **10**:261–262.
55. **Cammack, R., R. H. Jackson, A. Cornish-Bowden, and J. A. Cole.** 1982. Electron-spin-resonance studies of the NADH-dependent nitrite reductase from *Escherichia coli* K12. Biochem. J. **207**:333–339.
56. **Cammack, R., W. V. Lalla-Maharajh, and K. Schneider.** 1982. EPR studies of some oxygen-stable hydrogenases, p. 411–415. *In* C. Ho (ed.), Electron transport and oxygen utilization. Elsevier/North-Holland Inc., Amsterdam.
57. **Capaldi, R. A., J. Sweetland, and A. Merli.** 1977. Polypeptides in the succinate-coenzyme Q reductase segment of the respiratory chain. Biochemistry **16**:5707–5710.
58. **Castor, L. N., and B. Chance.** 1955. Photochemical action spectra of carbon-monoxide-inhibited respiration. J. Biol. Chem. **217**:453–465.
59. **Castor, L. N., and B. Chance.** 1959. Photochemical determinations of the oxidases of bacteria. J. Biol. Chem. **234**:1587–1592.
60. **Chance, B.** 1978. Cytochrome kinetics at low temperatures: trapping and ligand exchange. Methods Enzymol. **54**:102–111.
61. **Chance, B., C. Saronio, and J. S. Leigh.** 1975. Functional intermediates in the reaction of membrane-bound cytochrome oxidase with oxygen. J. Biol. Chem. **250**:9226–9237.
62. **Chance, B., C. Saronio, and J. S. Leigh.** 1979. Compound C_2, a product of the reaction of oxygen and the mixed-valence state of cytochrome oxidase. Optical evidence for a type I copper. Biochem. J. **177**:931–941.
63. **Chang, Y. Y., and J. E. Cronan.** 1982. Mapping nonselectable genes of *Escherichia coli* by using transposon Tn*10*: location of a gene affecting pyruvate oxidase. J. Bacteriol. **151**:1279–1289.
64. **Chang, Y.-Y. and J. E. Cronan.** 1983. Genetic and biochemical analyses of *Escherichia coli* strains having a mutation in the structural gene (*poxB*) for pyruvate oxidase. J. Bacteriol. **154**:756–762.
65. **Chaudhry, G. R., I. M. Chaiken, and C. H. MacGregor.** 1983. An activity from *Escherichia coli* membranes responsible for the modification of nitrate reductase to its precursor form. J. Biol. Chem. **258**:5828–5833.
66. **Chaudhry, G. R., and C. H. MacGregor.** 1983. *Escherichia coli* nitrate reductase subunit A: its role as the catalytic site and evidence for its modification. J. Bacteriol. **154**:387–394.
67. **Chaudhry, G. R., and C. H. MacGregor.** 1983. Cytochrome b from *Escherichia coli* nitrate reductase: its properties and association with the enzyme complex. J. Biol. Chem. **258**:5819–5827.
68. **Chetkauskaite, A. V., and L. L. Grinyus.** 1979. Transhydrogenase as an additional site of energy accumulation in the *Escherichia coli* respiratory chain. Biokhimiya **44**:869–876. (In English.)
69. **Chippaux, M., V. Bonnefoy-Orth, J. Ratouchniak, and M.-C. Pascal.** 1981. Operon fusions in the nitrate reductase operon and study of the control gene *nirR* in *Escherichia coli*. Mol. Gen. Genet. **182**:477–479.
70. **Clark, D., and J. E. Cronan.** 1980. *Escherichia coli* mutants with altered control of alcohol dehydrogenase and nitrate reductase. J. Bacteriol. **141**:177–183.
71. **Clarke, R. T. J., and T. Bauchop** (ed.). 1977. Microbial ecology of the gut. Academic Press, London.
72. **Clegg, R. A.** 1976. Purification and some properties of nitrate reductase (EC 1.7.99.4) from *Escherichia coli* K12. Biochem. J. **153**:533–541.
73. **Coakley, W. T., A. J. Bater, and D. Lloyd.** 1977. Disruption of microorganisms. Adv. Microb. Physiol. **16**:279–341.
74. **Cohen, G. N., and H. W. Rickenberg.** 1956. Concentration specifique reversible des amino acids chez *Escherichia coli*. Ann. Inst. Pasteur Paris **91**:693–720.
75. **Cole, J. A.** 1968. Cytochrome c_{552} and nitrite reduction in *Escherichia coli*. Biochim. Biophys. Acta **162**:356–368.
76. **Cole, J. A.** 1982. Independent pathways for the anaerobic reduction of nitrite to ammonia by *Escherichia coli*. Biochem. Soc. Trans. **10**:476–478.
77. **Cole, J. A., K. J. Coleman, B. E. Compton, B. M. Kavanagh, and C. W. Keevil.** 1974. Nitrite and ammonia assimilation by anaerobic continuous cultures of *Escherichia coli*. J. Gen. Microbiol. **85**:11–22.
78. **Cole, J. A., B. M. Newman, and P. White.** 1980. Biochemical and genetic characterization of *nirB* mutants of *Escherichia coli* K12 pleiotropically defective in nitrite and sulphite reduction. J. Gen. Microbiol. **120**:475–483.
79. **Cole, S. T.** 1982. Nucleotide sequence coding for the flavoprotein subunit of the fumarate reductase of *Escherichia coli*. Eur. J. Biochem. **122**:479–484.
80. **Cole, S. T., T. Grundström, B. Jaurin, J. J. Robinson, and J. H. Weiner.** 1982. Location and nucleotide sequence of *frdB*, the gene coding for the iron-sulphur protein subunit of the fumarate reductase of *Escherichia coli*. Eur. J. Biochem. **126**:211–216.
81. **Cole, S. T., and J. R. Guest.** 1979. Amplification and aerobic synthesis of fumarate reductase in ampicillin-resistant mutants of *Escherichia coli* K12. FEMS Microbiol. Lett. **5**:65–67.
82. **Cole, S. T., and J. R. Guest.** 1979. Production of a soluble form of fumarate reductase by multiple gene duplication in *Escherichia coli* K12. Eur. J. Biochem. **102**:65–71.
83. **Cole, S. T., and J. R. Guest.** 1980. Amplification of fumarate reductase synthesis with lambda-*frdA* transducing phages and orientation of *frdA* gene expression. Mol. Gen. Genet. **179**:377–385.
84. **Cole, S. T., and J. R. Guest.** 1982. Molecular genetic aspects of the succinate:fumarate oxidoreductases of *Escherichia coli*. Biochem. Soc. Trans. **10**:473–475.
85. **Coleman, K. J., A Cornish-Bowden, and J. A. Cole.** 1978. Purification and properties of nitrite reductase from *Escherichia coli* K12. Biochem. J. **175**:483–493.
86. **Condon, C., and P. Owen.** 1982. The succinate dehydrogenase of *Escherichia coli*: resolution as a major membrane-bound immunogen possessing covalently bound flavin. FEMS Microbiol. Lett. **14**:217–221.
87. **Condon, C., and P. Owen.** 1982. Succinate dehydrogenase: a major cross-reacting antigen in the Enterobacteriaceae. FEMS

Microbiol. Lett. **15**:109–113.
88. **Coughlan, M.** (ed.). 1980. Molybdenum and molybdenum-containing enzymes. Pergamon Press, Oxford.
89. **Cowan, S. T., and K. J. Steel.** 1965. Manual for the identification of medical bacteria. University Press, Cambridge.
90. **Cox, G. B., N. A. Newton, F. Gibson, A. M. Snoswell, and J. A. Hamilton.** 1970. The function of ubiquinone in *Escherichia coli*. Biochem. J. **117**:551–562.
91. **Cox, G. B., I. G. Young, L. M. McCann, and F. Gibson.** 1969. Biosynthesis of ubiquinone in *Escherichia coli* K12: location of genes affecting the metabolism of 3-octaprenyl-4-hydroxybenzoic acid and 2-octaprenylphenol. J. Bacteriol. **99**:450–458.
92. **Cox, J. C., E. S. Edwards, and J. A. De Moss.** 1981. Resolution of distinct selenium-containing formate dehydrogenase from *Escherichia coli*. J. Bacteriol. **145**:1317–1324.
93. **Cox, J. C., and R. Knight.** 1981. Trimethylamine N-oxide (TMAO) reductase activity in chlorate-resistant or respiration-deficient mutations of *Escherichia coli*. FEMS Microbiol. Lett. **12**:249–252.
94. **Creaghan, I., and J. R. Guest.** 1972. Amber mutants of the α-ketoglutarate dehydrogenase gene of *Escherichia coli* K12. J. Gen. Microbiol. **71**:207–220.
95. **Crispin, J. A. S., M. Dubourdieu, and M. Chippaux.** 1979. Localization and characterization of cytochromes from membrane vesicles of *Escherichia coli* K12 grown in anaerobiosis with nitrate. Biochim. Biophys. Acta **547**:198–210.
96. **Csonka, L. N., and D. G. Fraenkel.** 1977. Pathways of NADPH formation in *Escherichia coli*. J. Biol. Chem. **252**:3382–3391.
97. **Cunningham, C. C., and L. P. Hager.** 1971. Crystalline pyruvate oxidase from *Escherichia coli*. III. Activation by phospholipids. J. Biol. Chem. **246**:1583–1589.
98. **Cunningham, C. C., and L. P. Hager.** 1975. Reactivation of the lipid-depleted pyruvate oxidase system from *Escherichia coli* with cell envelope neutral lipids. J. Biol. Chem. **250**:7139–7146.
99. **Czerwinski, E. W., and F. S. Mathews.** 1974. Location of the iron atom and the non-crystallographic symmetry elements in cytochrome b_{562}. J. Mol. Biol. **86**:49–57.
100. **Czerwinski, E. W., F. S. Mathews, P. Hollenberg, K. Drickamer, and L. P. Hager.** 1972. Crystallographic study of cytochrome b_{562} from *Escherichia coli*. J. Mol. Biol. **71**:819–821.
101. **Dancey, G. F., A. E. Levine, and B. M. Shapiro.** 1976. The NADH dehydrogenase of the respiratory chain of *Escherichia coli*. J. Biol. Chem. **251**:5911–5920.
102. **Dancey, G. F., and B. M. Shapiro.** 1976. The NADH dehydrogenase of the respiratory chain of *Escherichia coli*. J. Biol. Chem. **251**:5921–5928.
103. **Daoud, M. S., and B. A. Haddock.** 1976. Electron transport in mutants of *Escherichia coli* defective in their ability to synthesize adenosine 3′:5′-cyclic monophosphate and the catabolite-gene activator protein. Biochem. Soc. Trans. **4**:711–714.
104. **Davenport, H. W.** 1971. Physiology of the digestive tract. Year Book Medical Publishers Inc., Chicago.
105. **Deeb, S. S., and L. P. Hager.** 1964. Crystalline cytochrome b_1 from *Escherichia coli*. J. Biol. Chem. **239**:1024–1031.
106. **De Moss, J. A.** 1977. Limited proteolysis of nitrate reductase purified from membranes of *Escherichia coli*. J. Biol. Chem. **252**:1696–1701.
107. **De Moss, J. A., T. Y. Fan, and R. H. Scott.** 1981. Characterization of subunit structural alterations which occur during purification of nitrate reductase from *Escherichia coli*. Arch. Biochem. Biophys. **206**:54–64.
108. **Dervartanian, D. V., L. K. Iburg, and T. V. Morgan.** 1973. EPR studies on phosphorylating particles from *Azotobacter vinelandii*. Biochim. Biophys. Acta **305**:173–178.
109. **De Silva, A. O., and D. G. Fraenkel.** 1979. The 6-phosphogluconate dehydrogenase reaction in *Escherichia coli*. J. Biol. Chem. **254**:10237–10242.
110. **Devor, K. A., H. U. Schairer, D. Renz, and P. Overath.** 1974. Active transport of β-galactosides by a mutant of *Escherichia coli* defective in haem synthesis. Eur. J. Biochem. **45**:451–456.
111. **Dickie, P., and J. H. Weiner.** 1979. Purification and characterization of membrane-bound fumarate reductase from anaerobically-grown *Escherichia coli*. Can. J. Biochem. **57**:813–821.
112. **Doss, M., and W. K. Philipp-Dormston.** 1973. Regulatory link between lactate dehydrogenase and biosynthesis of porphyrin and heme in microorganisms. Enzyme **16**:1–6.
113. **Doss, W., and W. K. Philipp-Dormston.** 1974. The effect of DL-lactate on regulation of porphyrin and haem biosynthesis in *Escherichia coli* and *Achromobacter*. FEBS Lett. **40**:173–175.
114. **Douglas, M. W., F. B. Ward, and J. A. Cole.** 1974. The formate hydrogenlyase activity of cytochrome c_{552}-deficient mutants of *Escherichia coli* K12. J. Gen. Microbiol. **80**:557–560.
115. **Downie, J. A., and G. B. Cox.** 1978. Sequence of *b* cytochromes relative to ubiquinone in the electron transport chain of *Escherichia coli*. J. Bacteriol. **133**:477–484.
116. **Downie, J. A., F. Gibson, and G. B. Cox.** 1979. Membrane adenosine triphosphatases of prokaryotic cells. Annu. Rev. Biochem. **48**:103–131.
117. **Eberspächer, B., and V. Braun.** 1980. The involvement of cytochromes in the uptake of ferrichrome by *Escherichia coli* K12. FEMS Microbiol. Lett. **7**:61–64.
118. **Edgar, J. R., and R. M. Bell.** 1979. Biosynthesis in *Escherichia coli* of sn glycerol-3-phosphate, a precursor of phospholipid palmitoyl coenzyme A. Inhibition of the biosynthetic sn glycerol 3-phosphate dehydrogenase EC 1.1.1.8. J. Biol. Chem. **254**:1016–1021.
119. **Edlund, T., T. Grundström, and S. Normark.** 1979. Isolation and characterization of DNA repetitions carrying the chromosomal β-lactamase gene of *Escherichia coli* K12. Mol. Gen. Genet. **173**:115–125.
120. **Edwards, C., S. Beer, A. Siviram, and B. Chance.** 1981. Photochemical action spectra of bacterial *a*- and *o*-type oxidases using a dye laser. FEBS Lett. **128**:205–207.
121. **Edwards, E. S., S. S. Rondean, and J. A. De Moss.** 1983. *chlC* (*nar*) operon of *Escherichia coli* includes structural genes for α and β subunits of nitrate reductase. J. Bacteriol. **153**:1513–1520.
122. **Enoch, H. G., and R. L. Lester.** 1975. The purification and properties of formate dehydrogenase and nitrate reductase in *Escherichia coli*. J. Biol. Chem. **250**:6693–6705.
123. **Esfahani, M., B. B. Rudkin, C. J. Cutler, and P. E. Waldron.** 1977. Lipid protein interactions in membranes: interaction of phospholipids with respiratory enzymes of *Escherichia coli* membrane. J. Biol. Chem. **252**:3194–3198.
124. **Evans, J. B.** 1975. Preparation of synchronous cultures of *Escherichia coli* by continuous-flow size selection. J. Gen. Microbiol. **91**:188–190.
125. **Farmer, I. S., and C. W. Jones.** 1976. The energetics of *Escherichia coli* during aerobic growth in continuous culture. Eur. J. Biochem. **67**:115–122.
126. **Fimmel, A. L., and B. A. Haddock.** 1979. Use of *chlC-lac* fusions to determine regulation of gene *chlC* in *Escherichia coli* K-12. J. Bacteriol. **138**:726–730.
127. **Fimmel, A. L., and B. A. Haddock.** 1981. Characterisation of the *Escherichia coli chlC* regulatory region in a cloned *chlC-lac* gene fusion. FEMS Microbiol. Lett. **12**:125–129.
128. **Forget, P.** 1974. The bacterial nitrate reductases. Solubilization, purification and properties of the enzyme A of *Escherichia coli* K12. Eur. J. Biochem. **42**:325–332.
129. **Forget, P., and M. Dubourdieu.** 1982. Evidence for the presence of a small subunit as the principal component of the nitrate reductase of *Escherichia coli* K12. Biochem. Biophys. Res. Commun. **105**:450–456.
130. **Forget, P. A., and R. Rimassa.** 1977. Evidence for the presence of carbohydrate units in the nitrate reductase A of *Escherichia coli* K12. FEBS Lett. **77**:182–186.
131. **Frank, L., and B. Ranhand.** 1964. Proline metabolism in *Escherichia coli*. III. The proline catabolic pathway. Arch. Biochem. Biophys. **107**:325–331.
132. **Frank, L., and P. Rybicki.** 1961. Studies of proline metabolism in *Escherichia coli*. 1. The degradation of proline during growth of a proline-requiring auxotroph. Arch. Biochem. Biophys. **95**:441–449.
133. **Franklin, F. C. H., and W. A. Venables.** 1976. Biochemical, genetic and regulatory studies of alanine catabolism in *Esche-*

richia coli K12. Mol. Gen. Genet. **149**:229–237.
134. **Franklin, F. C. H., W. A. Venables, and H. J. W. Wijsman.** 1981. Genetic studies of D alanine dehydrogenaseless mutants of *Escherichia coli* K12. Genet. Res. **38**:197–208.
135. **Fujita, T.** 1966. Studies on soluble cytochromes in Enterobacteriaceae: cytochrome b_{562} and c_{550}. J. Biochem. (Tokyo) *60*:329–334.
136. **Fujita, T., E. Itagaki, and R. Sato.** 1963. Purification and properties of cytochrome b_1 from *Escherichia coli*. J. Biochem. (Tokyo) **53**:282–290.
137. **Fujita, T., and R. Sato.** 1966. Studies on soluble cytochromes in Enterobacteriaceae. III. Localization of cytochrome c_{552} in the surface layer of cells. J. Biochem. (Tokyo) **60**:568–577.
138. **Fujita, T., and R. Sato.** 1966. Studies on soluble cytochromes in Enterobacteriaceae. IV. Possible involvement of cytochrome c_{552} in anaerobic nitrite metabolism. J. Biochem. (Tokyo) **60**:691–700.
139. **Fujita, T., and R. Sato.** 1967. Studies on soluble cytochromes in Enterobacteriaceae. V. Nitrite-dependent gas evolution in cells containing cytochrome c_{552}. J. Biochem. (Tokyo) **60**:230–238.
140. **Fukuyama, T., and E. J. Ordal.** 1965. Induced biosynthesis of formic hydrogenlyase in iron-deficient cells of *Escherichia coli*. J. Bacteriol. **90**:673–680.
141. **Fung, L. W. M., E. A. Pratt, and C. Ho.** 1979. Biochemical and biophysical studies on the interaction of a membrane bound enzyme D lactate dehydrogenase from *Escherichia coli* with phospholipids. Biochemistry **18**:317–324.
142. **Futai, M.** 1973. Membrane D-lactate dehydrogenase from *Escherichia coli*. Purification and properties. Biochemistry **12**:2468–2474.
143. **Futai, M.** 1974. Reconstitution of transport dependent on D-lactate or glycerol-3-phosphate in membrane vesicles of *Escherichia coli* deficient in the corresponding dehydrogenase. Biochemistry **13**:2327–2333.
144. **Futai, M.** 1974. Orientation of membrane vesicles from *Escherichia coli* prepared by different procedures. J. Membr. Biol. **15**:15–28.
145. **Futai, M., and H. Kimura.** 1977. Inducible membrane bound D-lactate dehydrogenase from *Escherichia coli*. Purification and properties. J. Biol. Chem. **252**:5820–5827.
146. **Futai, M., and Y. Tanaka.** 1975. Localization of D-lactate dehydrogenase in membrane vesicles prepared by using a French press or ethylenediaminetetraacetate-lysozyme from *Escherichia coli*. J. Bacteriol. **124**:470–475.
147. **Garland, P. B., M. T. Davison, and C. H. Moore.** 1978. Rotational mobility of membrane-bound cytochrome *o* of *Escherichia coli* and cytochrome a_1 of *Thiobacillus ferro-oxidans*. Biochem. Soc. Trans. **7**:1112–1114.
148. **Garland, P. B., J. A. Downie, and B. A. Haddock.** 1975. Proton translocation and the respiratory nitrate reductase of *Escherichia coli*. Biochem. J. **152**:547–559.
149. **Garland, P. B., K. Johnson, and G. A. Reid.** 1982. The diffusional mobility of proteins in the cytoplasmic membrane of *Escherichia coli*. Biochem. Soc. Trans. **10**:484–485.
150. **Garland, P. B., and R. W. Jones.** 1977. The mechanism of proton translocation by the respiratory nitrate-reductase complex of *Escherichia coli* is chemiosmotic not conformational, p. 117–126. *In* K. Van Dam and B. F. Van Gelder (ed.), Structure and function of energy-transducing membranes. Elsevier/North-Holland Biomedical Press, Amsterdam.
151. **Garvie, E. I.** 1980. Bacterial lactate dehydrogenases. Microbiol. Rev. **44**:106–139.
152. **George-Nascimento, C., S. J. Wakk, S. A. Short, and H. R. Kaback.** 1976. Effects of lipids on the reconstitution of D-lactate oxidase in *Escherichia coli* membrane vesicles. J. Biol. Chem. **251**:6662–6666.
153. **Gerolimatos, B., and R. L. Hanson.** 1978. Repression of *Escherichia coli* pyridine nucleotide transhydrogenase by leucine. J. Bacteriol. **134**:394–400.
154. **Gilbert, P., E. G. Beveridge, and P. B. Crone.** 1977. Inhibition of some respiration and dehydrogenase enzyme systems in *Escherichia coli* NCTC 5933 by phenoxyethanol. Microbios **20**:29–37.
155. **Giordano, G., A. L. Fimmel, L. M. Powell, B. A. Haddock, and G. C. Barr.** 1981. Cloning and expression of the *chlA* gene of *Escherichia coli* K12. FEMS Microbiol. Lett. **12**:61–64.
156. **Giordano, G., A. Graham, D. H. Boxer, B. A. Haddock, and E. Azoulay.** 1978. Characterization of the membrane-bound nitrate reductase activity of aerobically-grown chlorate-sensitive mutants of *Escherichia coli* K12. FEBS Lett. **95**:290–294.
157. **Giordano, G., L. Grillet, J. Pommier, C. Terriere, B. A. Haddock, and E. Azoulay.** 1980. Precursor forms of the subunits of nitrate reductase in *chlA* and *chlB* mutants of *Escherichia coli* K12. Eur. J. Biochem. **105**:297–306.
158. **Giordano, G., L. Grillet, R. Rosset, J. H. Dou, E. Azoulay, and B. A. Haddock.** 1978. Characterization of an *Escherichia coli* K12 mutant that is sensitive to chlorate when grown aerobically. Biochem. J. **176**:553–561.
159. **Giordano, G., B. A. Haddock, and D. H. Boxer.** 1980. Molybdenum-limited growth achieved either phenotypically or genotypically and its effect on the synthesis of formate dehydrogenase and nitrate reductase by *Escherichia coli* K12. FEMS Microbiol. Lett. **8**:229–235.
160. **Giordano, G., C.-L. Medani, M. A. Mandrand-Berthelot, and D. H. Boxer.** 1983. Formate dehydrogenases from *Escherichia coli*. FEMS Microbiol. Lett. **17**:171–177.
161. **Giordano, G., C. Rivière, and E. Azoulay.** 1977. Oxidative phosphorylation in intact *chl-r* mutants of *Escherichia coli* K12. Biochimie **59**:403–409.
162. **Girdlestone, J., R. Bisson, and R. A. Capaldi.** 1981. Interaction of succinate-ubiquinone reductase (complex II) with (arylazido) phospholipids. Biochemistry **20**:152–156.
163. **Glaser, J. H., and J. A. De Moss.** 1971. Phenotypic restoration by molybdate of nitrate reductase activity in *chlD* mutants of *Escherichia coli*. J. Bacteriol. **108**:854–860.
164. **Glick, B. R., P. Y. Wang, H. Schneider, and W. G. Martin.** 1980. Identification and partial characterisation of an *Escherichia coli* mutant with altered hydrogenase activity. Can. J. Biochem. **58**:361–367.
165. **Goldberg, I., K. Lonberg-Holm, E. A. Bagley, and B. Stieglitz.** 1983. Improved conversion of fumarate to succinate by *Escherichia coli* strains amplified for fumarate reductase. Appl. Environ. Microbiol. **45**:1838–1847.
166. **Gonzales-Prevatt, V., and D. A. Webster.** 1979. Reduction of cytochrome *o*, p. 375–393. *In* W. J. Caughey (ed.), Biochemical and clinical aspects of oxygen. Academic Press, Inc., New York.
167. **Graham, A.** 1981. The organization of hydrogenase in the cytoplasmic membrane of *Escherichia coli*. Biochem. J. **197**:283–291.
168. **Graham, A., and D. H. Boxer.** 1978. Immunochemical localization of nitrate reductase in *Escherichia coli*. Biochem. Soc. Trans. **6**:1210–1211.
169. **Graham, A., and D. H. Boxer.** 1980. Implication of α-subunit of *Escherichia coli* nitrate reductase in catalytic activity. Biochem. Soc. Trans. **8**:329–330.
170. **Graham, A., and D. H. Boxer.** 1980. The membrane location of the β-subunit of nitrate reductase from *Escherichia coli*. Biochem. Soc. Trans. **8**:331.
171. **Graham, A., and D. H. Boxer.** 1980. Arrangement of respiratory nitrate reductase in the cytoplasmic membrane of *Escherichia coli*: location of β-subunit. FEBS Lett. **113**:15–20.
172. **Graham, A., and D. H. Boxer.** 1981. The organisation of formate dehydrogenase in the cytoplasmic membrane of *Escherichia coli*. Biochem. J. **195**:627–637.
173. **Graham, A., D. H. Boxer, B. A. Haddock, M. A. Mandrand-Berthelot, and R. W. Jones.** 1980. Immunochemical analysis of the membrane-bound hydrogenase of *Escherichia coli*. FEBS Lett. **113**:167–173.
174. **Graham, A., H. E. Jenkins, N. H. Smith, M. A. Mandrand-Berthelot, B. A. Haddock, and D. H. Boxer.** 1980. The synthesis of formate dehydrogenase and nitrate reductase protein in various *fdh* and *chl* mutants of *Escherichia coli*. FEMS Microbiol. Lett. **7**:145–151.
175. **Graham, A., A. D. Tucker, and N. H. Smith.** 1981. The formate-nitrate respiratory chain of *Escherichia coli*: localization

of proteins by immunoadsorption studies. FEMS Microbiol. Lett. **11**:141–147.
176. **Gray, C. T., and H. Gest.** 1965. Biological formation of molecular hydrogen. Science **148**:186–192.
177. **Gray, C. T., J. W. T. Wimpenny, D. E. Hughes, and M. R. Mossman.** 1966. Regulation of metabolism in facultative bacteria. I. Structural and functional changes in *Escherichia coli* associated with shifts between the aerobic and anaerobic states. Biochim. Biophys. Acta **117**:22–32.
178. **Gray, C. T., J. W. T. Wimpenny, D. E. Hughes, and M. Ranlett.** 1963. A soluble *c*-type cytochrome from anaerobically grown *Escherichia coli* and various Enterobacteriaceae. Biochim. Biophys. Acta **67**:157–160.
179. **Green, G. N., and R. B. Gennis.** 1983. Isolation and characterization of a mutant in *Escherichia coli* lacking the cytochrome *d* terminal oxidase. J. Bacteriol. **154**:1269–1275.
180. **Grundström, T., and B. Jaurin.** 1982. Overlap between *ampC* and *frd* operons on the *Escherichia coli* chromosome. Proc. Natl. Acad. Sci. U.S.A. **79**:1111–1115.
181. **Guest, J. R.** 1977. Menaquinone biosynthesis: mutants of *Escherichia coli* K-12 requiring 2-succinylbenzoate. J. Bacteriol. **130**:1038–1046.
182. **Guest, J. R.** 1981. Partial replacement of succinate dehydrogenase function by phage and plasmid-specified fumarate reductase in *Escherichia coli*. J. Gen. Microbiol. **122**:171–179.
183. **Guest, J. R., and D. J. Shaw.** 1981. Molecular cloning of menaquinone biosynthetic genes of *Escherichia coli* K12. Mol. Gen. Genet. **181**:379–383.
184. **Gutman, M., A. Schejter, and Y. Avi-dor.** 1968. The preparation and properties of the membranal DPNH dehydrogenase of *Escherichia coli*. Biochim. Biophys. Acta **162**:506–517.
185. **Gutowski, S. J., and H. Rosenberg.** 1976. Effects of dicyclohexylcarbodiimide on proton translocation coupled to fumarate reduction in anaerobically grown cells of *Escherichia coli* K12. Biochem. J. **160**:813–816.
186. **Gutowski, S. J., and H. Rosenberg.** 1977. Proton translocation coupled to electron flow from endogenous substrates to fumarate in anaerobically grown *Escherichia coli* K12. Biochem. J. **164**:265–267.
187. **Guynn, R. W., and R. L. Veech.** 1973. The equilibrium constants of the adenosine triphosphate hydrolysis and the adenosine triphosphate-citrate lyase reactions. J. Biol. Chem. **248**:6966–6972.
188. **Hackett, C. S., and C. H. MacGregor.** 1981. Synthesis and degradation of nitrate reductase in *Escherichia coli*. J. Bacteriol. **146**:352–359.
189. **Hackett, N. R., and P. D. Bragg.** 1982. The association of 2 distinct *b* cytochromes with the respiratory nitrate reductase of *Escherichia coli*. FEMS Microbiol. Lett. **13**:213–217.
190. **Hackett, N. R., and P. D. Bragg.** 1983. Membrane cytochromes of *Escherichia coli* grown aerobically and anaerobically with nitrate. J. Bacteriol. **154**:708–718.
191. **Hackett, N. R., and P. D. Bragg.** 1983. Membrane cytochromes of *Escherichia coli chl* mutants. J. Bacteriol. **154**:719–727.
192. **Haddock, B. A.** 1973. The reconstitution of oxidase activity in membranes derived from a 5-aminolaevulinic acid-requiring mutant of *Escherichia coli*. Biochem. J. **136**:877–884.
193. **Haddock, B. A.** 1977. The isolation of phenotypic and genotypic variants for the functional characterization of bacterial oxidative phosphorylation, p. 95–120. *In* B. A. Haddock and W. A. Hamilton (ed.), Microbial energetics. Cambridge University Press, Cambridge.
194. **Haddock, B. A.** 1982. The genetics of electron transport in *Escherichia coli*, p. 459–463. *In* A. N. Martonosi (ed.), Membranes and transport, vol. 1. Plenum Publishing Corp., New York.
195. **Haddock, B. A., and J. A. Downie.** 1974. The reconstitution of functional respiratory chains in membranes from electron transport-deficient mutants of *Escherichia coli* as demonstrated by quenching of atebrin fluorescence. Biochem. J. **142**:703–706.
196. **Haddock, B. A., J. A. Downie, and P. B. Garland.** 1976. Kinetic characterization of the membrane-bound cytochromes of *Escherichia coli* grown under a variety of conditions by using a stopped-flow dual-wavelength spectrophotometer. Biochem. J. **154**:285–294.
197. **Haddock, B. A., J. A. Downie, and H. G. Lawford.** 1974. The function of ubiquinone respiration studied in cytochrome-deficient mutants of *Escherichia coli*. Proc. Soc. Gen. Microbiol. **1**:50.
198. **Haddock, B. A., and C. W. Jones.** 1977. Bacterial respiration. Bacteriol. Rev. **41**:47–99.
199. **Haddock, B. A., and M. W. Kendall-Tobias.** 1975. Functional anaerobic electron transport linked to the reduction of nitrate and fumarate in membranes from *Escherichia coli* as demonstrated by quenching of atebrin fluorescence. Biochem. J. **152**:655–659.
200. **Haddock, B. A., and M. A. Mandrand-Berthelot.** 1982. *Escherichia coli* formate-to-nitrate respiratory chain: genetic analysis. Biochem. Soc. Trans. **10**:478–480.
201. **Haddock, B. A., and H. U. Schairer.** 1973. Electron transport chains of *Escherichia coli*: reconstitution of respiration in a 5-amino leavulinic acid-requiring mutant. Eur. J. Biochem. **35**:34–45.
202. **Hager, L. P., and E. Itagaki.** 1967. The preparation and properties of cytochrome b_{562} from *Escherichia coli*. Methods Enzymol. **10**:373–378.
203. **Haldar, K., P. Y. Olsiewski, C. Walsh, G. J. Kazarowski, A. Bhaduri, and H. R. Kaback.** 1982. Simultaneous reconstitution of *Escherichia coli* membrane vesicles with D-lactic and D-amino acid dehydrogenases. Biochemistry **21**:4590–4596.
204. **Hamilton, J. A., G. B. Cox, F. D. Looney, and F. Gibson.** 1970. Ubisemiquinone in membranes from *Escherichia coli*. Biochem. J. **116**:319–320.
205. **Hanson, R. L., and C. Rose.** 1980. Effects of an insertion mutation in a locus affecting pyridine nucleotide transhydrogenase (*pnt*::Tn*5*) on the growth of *Escherichia coli*. J. Bacteriol. **141**:401–404.
206. **Harrison, D. E. F.** 1976. The regulation of respiration rate in growing bacteria. Adv. Microb. Physiol. **14**:243–313.
207. **Hatefi, H., and Y. M. Galante.** 1980. Isolation of cytochrome b_{560} from Complex II (succinate, ubiquinone oxidoreductase) and its reconstitution with succinate dehydrogenase. J. Biol. Chem. **255**:5530–5537.
208. **Hederstedt, L., E. Holmgren, and L. Rutberg.** 1979. Characterization of a succinate dehydrogenase complex solubilized from the cytoplasmic membrane of *Bacillus subtilis* with the nonionic detergent Triton X-100. J. Bacteriol. **138**:370–376.
209. **Hederstedt, L., and L. Rutberg.** 1981. Succinate dehydrogenase—a comparative review. Microbiol. Rev. **45**:542–555.
210. **Hellingwerf, K. J., J. G. H. Bolscher, and W. N. Konings.** 1981. The electrochemical proton gradient generated by the fumarate reductase system in *Escherichia coli* and its bioenergetic implications. Eur. J. Biochem. **113**:369–374.
211. **Hendler, R. W.** 1977. Automated electrodic potentiometry of potassium ferricyanide and respiratory components. Anal. Chem. **49**:1914–1918.
212. **Hendler, R. W., and A. H. Burgess.** 1972. Respiration and protein synthesis in *Escherichia coli* membrane-envelope fragments. VI. Solubilization and characterization of the electron transport chain. J. Cell Biol. **55**:266–281.
213. **Hendler, R. W., and A. H. Burgess.** 1974. Fractionation of the electron transport chain of *Escherichia coli*. Biochim. Biophys. Acta **357**:215–230.
214. **Hendler, R. W., and N. Nanninga.** 1970. Respiration and protein synthesis in *Escherichia coli* membrane-envelope fragments. III. Electron microscopy and analysis of the cytochromes. J. Cell Biol. **46**:114–129.
215. **Hendler, R. W., and R. I. Schrager.** 1979. Potentiometric analysis of *Escherichia coli* cytochromes in the optical absorbance range of 500 nm to 700 nm. J. Biol. Chem. **254**:11288–11299.
216. **Hendler, R. W., D. N. Towne, and R. I. Shrager.** 1975. Redox properties of *b*-type cytochromes in *Escherichia coli* and rat liver mitochondria and techniques for their analyses. Biochim.

Biophys. Acta **376**:42–62.
217. **Hirsch, C. A., M. Rasminsky, B. D. Davis, and E. C. C. Lin.** 1963. A fumarate reductase in *Escherichia coli* distinct from succinate dehydrogenase. J. Biol. Chem. **238**:3770–3774.
218. **Hong, J. S., and H. R. Kaback.** 1972. Mutants of *Salmonella typhimurium* and *Escherichia coli* pleiotropically defective in active transport. Proc. Natl. Acad. Sci. U.S.A. **69**:3336–3340.
219. **Ingledew, W. J.** 1978. Cytochrome a_1 as an oxidase?, p. 79–87. *In* H. Degn, D. Lloyd, and G. C. Hill (ed.), Functions of alternative terminal oxidases. Pergamon Press, Oxford.
220. **Ingledew, W. J.** 1983. The electron transport chain of *Escherichia coli* grown anaerobically with fumarate as terminal electron acceptor: an electron paramagnetic resonance study. J. Gen. Microbiol. **129**:1651–1659.
221. **Ingledew, W. J., J. C. Cox, R. W. Jones, and P. B. Garland.** 1978. Vectorial oxidoreductions: the ferrous iron oxidase complex of *Thiobacillus ferrooxidans* and the nitrate reductase complex of *Escherichia coli*, p. 334–341. *In* P. L. Dutton, A. Scarpa, and J. S. Leigh (ed.), Frontiers of biological energetics, vol. 1. Academic Press, Inc, New York.
222. **Ingledew, W. J., G. A. Reid, R. K. Poole, H. Blum, and T. Ohnishi.** 1980. The iron-sulphur centres of aerobically-grown *Escherichia coli* K12. An electron paramagnetic resonance study. FEBS Lett. **111**:223–227.
223. **Ishida, A.** 1977. A carbon monoxide-binding hemoprotein formed by heme accumulation in *Escherichia coli*. J. Biochem. **81**:1869–1878.
224. **Ishida, A., and S. Hino.** 1972. Effect of oxygen on cytochrome pattern and heme synthesis in *Escherichia coli*. J. Gen. Appl. Microbiol. **18**:225–237.
225. **Ishida, A., and N. Shiraishi.** 1978. Development of hemoproteins and respiratory activities of *Escherichia coli* grown at high or low aeration. J. Gen. Appl. Microbiol. **24**:139–141.
226. **Ishimoto, M., and O. Shimokawa.** 1978. Reduction of trimethylamine N-oxide by *Escherichia coli* as anaerobic respiration. Z. Allg. Mikrobiol. **18**:173–181.
227. **Itagaki, E., and L. P. Hager.** 1966. Studies on cytochrome b_{562} of *Escherichia coli*. I. Purification and crystallization of cytochrome b_{562}. J. Biol. Chem. **241**:3687–3695.
228. **Itagaki, E., and L. P. Hager.** 1968. The amino acid sequence of cytochrome b_{562} of *Escherichia coli*. Biochem. Biophys. Res. Commun. **32**:1013–1019.
229. **Jackson, R. H., J. A. Cole, and A. Cornish-Bowden.** 1981. The steady-state kinetics of NADH-dependent nitrite reductase from *E. coli* K12. Nitrite and hydroxylamine reduction. Biochem. J. **199**:171–178.
230. **Jackson, R. H., J. A. Cole, and A. Cornish-Bowden.** 1982. The steady-state kinetics of the NADH-dependent nitrite reductase from *Escherichia coli* K12. The reduction of single-electron acceptors. Biochem. J. **203**:505–510.
231. **Jackson, R. H., A. Cornish-Bowden, and J. A. Cole.** 1981. Prosthetic groups of the NADH-dependent nitrite reductase from *Escherichia coli* K12. Biochem. J. **193**:861–867.
232. **Jaworowski, A., H. D. Campbell, M. I. Poulis, and I. G. Young.** 1981. Genetic identification and purification of the respiratory NADH dehydrogenase of *Escherichia coli*. Biochemistry **20**:2041–2047.
233. **Jaworowski, A., G. Mayo, D. C. Shaw, H. D. C. Campbell, and I. G. Young.** 1981. Characterization of the respiratory NADH dehydrogenase of *Escherichia coli* and reconstitution of NADH oxidase in *ndh* mutant membrane vesicles. Biochemistry **20**:3621–3628.
234. **Jenkins, H. E., A. Graham, and B. A. Haddock.** 1979. Characterization of a *chlG* mutant of *Escherichia coli* K12. FEMS Microbiol. Lett. **6**:169–173.
235. **Johnson, J. L.** 1980. The molybdenum cofactor common to nitrate reductase, xanthine dehydrogenase and sulphite oxidase, p. 345–384. *In* M. Coughlan (ed.), Molybdenum and molybdenum containing enzymes. Pergamon Press, Oxford.
236. **Jones, C. W.** 1978. Microbial oxidative phosphorylation. Biochem. Soc. Trans. **6**:361–363.
237. **Jones, C. W.** 1980. Cytochrome patterns in classification and identification including their relevance to the oxidase test. Soc. Appl. Bacteriol. Symp. Ser. **8**:127–138.
238. **Jones, C. W., J. M. Brice, and C. Edwards.** 1977. The effect of respiratory chain composition on the growth efficiencies of aerobic bacteria. Arch. Microbiol. **115**:85–93.
239. **Jones, H., and W. A. Venables.** 1983. Solubilisation of D-amino acid dehydrogenase of *Escherichia coli* K12 and its re-binding to envelope preparations. Biochimie **65**:177–183.
240. **Jones, H., and W. A. Venables.** 1983. Effects of solubilisation on some properties of the membrane-bound respiratory enzyme D-amino acid dehydrogenase of *Escherichia coli*. FEBS Lett. **151**:189–192.
241. **Jones, R. G. W.** 1967. Ubiquinone deficiency in an auxotroph of *Escherichia coli* requiring 4-hydroxybenzoic acid. Biochem. J. **103**:714–719.
242. **Jones, R. W.** 1979. The topography of the membrane-bound hydrogenase of *Escherichia coli* explored by non-physiological electron acceptors. Biochem. Soc. Trans. **7**:724–725.
243. **Jones, R. W.** 1979. Hydrogen-dependent proton translocation by membrane vesicles from *Escherichia coli*. Biochem. Soc. Trans. **7**:1136–1137.
244. **Jones, R. W.** 1980. The role of the membrane-bound hydrogenase in the energy-conserving oxidation of molecular hydrogen by *Escherichia coli*. Biochem. J. **188**:345–350.
245. **Jones, R. W.** 1980. Proton translocation by the membrane-bound formate dehydrogenase of *Escherichia coli*. FEMS Microbiol. Lett. **8**:167–171.
246. **Jones, R. W., and P. B. Garland.** 1977. Sites and specificity of the reaction of bi-pyridylium compounds with anaerobic respiratory enzymes of *Escherichia coli*. Effects of permeability barriers imposed by the cytoplasmic membrane. Biochem. J. **164**:199–211.
247. **Jones, R. W., and P. B. Garland.** 1978. The proton-consuming site of the respiratory nitrate reductase of *Escherichia coli* is on the cytoplasmic aspect of the cytoplasmic membrane. Biochem. Soc. Trans. **6**:416–418.
248. **Jones, R. W., and P. B. Garland.** 1982. The function of ubiquinone and menaquinone in the respiratory chain of *Escherichia coli*, p. 465–476. *In* B. L. Trumpower (ed.), Function of quinones in energy conserving systems. Academic Press, Inc., New York.
249. **Jones, R. W., B. A. Haddock, and P. B. Garland.** 1978. Vectorial organization of proton-translocating oxidoreductions of *Escherichia coli*, p. 71–80. *In* G. F. Azzone, M. Avron, J. C. Metcalfe, E. Quagliariellio and N. Siliprandi (ed.), The proton and calcium pumps. Elsevier/North-Holland Biomedical Press, Amsterdam.
250. **Jones, R. W., W. J. Ingledew, A. Graham, and P. B. Garland.** 1978. Topography of nitrate reductase of the cytoplasmic membrane of *Escherichia coli*. The nitrate-reducing site. Biochem. Soc. Trans. **6**:1287–1289.
251. **Jones, R. W., R. G. Kranz, and R. B. Gennis.** 1982. Immunochemical analysis of the membrane-bound succinate dehydrogenase of *Escherichia coli*. FEBS Lett. **142**:81–87.
252. **Jones, R. W., A. Lamont, and P. B. Garland.** 1980. The mechanism of proton translocation driven by the respiratory nitrate reductase complex of *Escherichia coli*. Biochem. J. **190**:79–94.
253. **Jurtshuk, P., T. J. Mueller, and W. C. Acord.** 1975. Bacterial terminal oxidases. Crit. Rev. Microbiol. **3**:399–468.
254. **Kaback, H. R.** 1974. Transport studies in bacterial membrane vesicles. Science **186**:882–892.
255. **Kaczorowski, G., L. D. Kohn, and H. R. Kaback.** 1978. Purification and properties of D lactate dehydrogenase from *Escherichia coli* ML-308-225. Methods Enzymol. **53**:519–527.
256. **Kaczorowski, G., L. Shaw, M. Fuentes, and C. Walsh.** 1975. Coupling of alanine racemase and *b*-alanine dehydrogenase to active transport of amino acids in *Escherichia coli* B membrane vesicles. J. Biol. Chem. **250**:2855–2865.
257. **Kaczorowski, G., L. Shaw, R. Laura, and C. Walsh.** 1975. Active transport in *Escherichia coli* B membrane vesicles. Differential inactivating effects from the enzymatic oxidation of β-chloro-L-alanine and β-chloro-D-alanine. J. Biol. Chem. **250**:8921–8930.

258. **Kaczorowski, G., and C. Walsh.** 1975. Active transport in *Escherichia coli* B membrane vesicles. Irreversible uncoupling by chloropyruvate. J. Biol. Chem. **250**:8931–8937.
259. **Kamitakahara, J. R., and W. J. Polglase.** 1970. The 503 nanometer pigment of *Escherichia coli*. Biochem. J. **120**:771–775.
260. **Kaprálek, F., E. Jechová, and M. Otavová.** 1982. Two sites of oxygen control in induced synthesis of respiratory nitrate reductase in *Escherichia coli*. J. Bacteriol. **149**:1142–1145.
261. **Karlibian, D., and P. Couchoud.** 1974. Dihydro-orotate oxidase of *Escherichia coli* K12: purification, properties, and relation to the cytoplasmic membrane. Biochim. Biophys. Acta **364**:218–232.
262. **Kauffman, H. F., and B. F. van Gelder.** 1973. The respiratory chain of *Azotobacter vinelandii*. I. Spectral properties of cytochrome *d*. Biochim. Biophys. Acta **305**:260–267.
263. **Kauffman, H. F., B. F. van Gelder, and D. V. Dervartanian.** 1980. Effects of ligands on cytochrome *d* from *Azotobacter vinelandii*. J. Bioenerg. Biomembr. **12**:265–277.
264. **Kay, W. W., and H. L. Kornberg.** 1971. The uptake of C4-dicarboxylic acids by *Escherichia coli*. Eur. J. Biochem. **18**:274–281.
265. **Keilin, D.** 1970. The history of cell respiration and cytochrome, p. 269–288. Cambridge University Press, Cambridge.
266. **Kemp, M. B., B. A. Haddock, and P. B. Garland.** 1975. Synthesis and sidedness of membrane-bound respiratory nitrate reductase (EC 1.7.99.4) in *Escherichia coli* lacking cytochromes. Biochem. J. **148**:329–333.
267. **Kenney, W. C., W. H. Walter, and T. P. Singer.** 1977. Studies on succinate dehydrogenase. XX. Amino acid sequence around the flavin site. J. Biol. Chem. **247**:4510–4513.
268. **Kerr, C. T., and R. W. Miller.** 1968. Dihydroorotate-ubiquinone reductase complex of *Escherichia coli* B. J. Biol. Chem. **243**:2963–2968.
269. **Kim, A. C., and P. D. Bragg.** 1971. Properties of nonheme iron in a cell envelope fraction from *Escherichia coli*. J. Bacteriol. **107**:664–670.
270. **Kim, I. C., and P. D. Bragg.** 1971. Some properties of the succinate dehydrogenase of *Escherichia coli*. Can. J. Biochem. **49**:1098–1104.
271. **Kimura, H., and M. Futai.** 1978. Effects of phospholipids on L lactate dehydrogenase from membranes of *Escherichia coli* activation and stabilization of the enzyme with phospholipids. J. Biol. Chem. **253**:1095–1100.
272. **Kistler, W. S., C. A. Hirsch, N. R. Cozzarelli, and E. C. C. Lin.** 1969. Second pyridine nucleotide-independent L-α-glycerophosphate dehydrogenase in *Escherichia coli* K-12. J. Bacteriol. **100**:1133–1135.
273. **Kistler, W. S., and E. C. C. Lin.** 1972. Anaerobic L-α-glycerophosphate dehydrogenase of *Escherichia coli*: its genetic locus and its physiological role. J. Bacteriol. **108**:1224–1234.
274. **Kistler, W. S., and E. C. C. Lin.** 1972. Purification and properties of the flavine-stimulated anaerobic L-α-glycerophosphate dehydrogenase of *Escherichia coli*. J. Bacteriol. **112**:539–547.
275. **Kita, K., and Y. Anraku.** 1981. Composition and sequence of *b* cytochromes in the respiratory chain of aerobically-grown *Escherichia coli* K12 in the early exponential phase. Biochem. Int. **2**:105–112.
276. **Kita, K., M. Kasahara, and Y. Anraku.** 1982. Formation of a membrane potential by reconstituted liposomes made with cytochrome b_{556}-*o* complex, a terminal oxidase of *Escherichia coli* K12. J. Biol. Chem. **257**:7933–7935.
277. **Kita, K., I. Yamato, and Y. Anraku.** 1978. Purification and properties of cytochrome b_{556} in the respiratory chain of aerobically grown *Escherichia coli* K12. J. Biol. Chem. **253**:8910–8915.
278. **Kito, M., and L. I. Pizer.** 1969. Purification and regulatory properties of the biosynthetic L-glycerol 3-phosphate dehydrogenase from *Escherichia coli*. J. Biol. Chem. **244**:3316–3323.
279. **Kline, E. S., and H. R. Mahler.** 1965. The lactic dehydrogenases of *Escherichia coli*. Ann. N.Y. Acad. Sci. **119**:905–917.
280. **Koch, A. L.** 1976. How bacteria face depression, recession and derepression. Perspect. Biol. Med. **20**:44–63.
281. **Koch, A. L.** 1979. Microbial growth in low concentrations of nutrients, p. 261–279. *In* M. Shilo (ed.), Strategies of microbial life in extreme environments. Dahlen Konferenzen, Berlin.
282. **Koch, A. L., and H. C. Wang.** 1982. How close to the theoretical diffusion limit do bacterial uptake systems function? Arch. Microbiol. **131**:36–42.
283. **Kohn, L. D., and H. R. Kaback.** 1973. Mechanisms of active transport in isolated bacterial membrane vesicles. Part 15. Purification and properties of the membrane bound D-lactate dehydrogenase from *Escherichia coli*. J. Biol. Chem. **248**:7012–7017.
284. **Koland, J. G., M. W. Mather, R. B. Gennis, J. S. White, and L. P. Hager.** 1982. Activation of pyruvate oxidase and interaction of membrane components. p. 83–92. *In* A. N. Martonosi (ed.), Membranes and transport, vol. 1. Plenum Press, New York.
285. **Konings, W. N., and H. R. Kaback.** 1973. Anaerobic transport in *Escherichia coli* membrane vesicles. Proc. Natl. Acad. Sci. U.S.A. **70**:3376–3381.
286. **Konings, W. N., and P. A. M. Michels.** 1980. Electron-transfer-driven soluble translocation across bacterial membranes, p. 33–86. *In* C. J. Knowles (ed.), Diversity of bacterial respiratory systems, vol. 1. CRC Press Inc., Boca Raton, Fla.
287. **Kovatchev, S., W. L. C. Vaz, and H. Eibl.** 1981. Lipid dependence of the membrane-bound D-lactate dehydrogenase of *Escherichia coli*. J. Biol. Chem. **256**:10369–10374.
288. **Kranz, R. G., and R. B. Gennis.** 1982. Isoelectric focusing and crossed immunoelectrophoresis of heme proteins in the *Escherichia coli* cytoplasmic membrane. J. Bacteriol. **150**:36–45.
289. **Kranz, R. G., and R. B. Gennis.** 1983. Immunological characterization of the cytochrome *o* terminal oxidase from *Escherichia coli*. J. Biol. Chem. **258**:10614–10621.
290. **Kristjansson, J. K., and T. C. Hollocher.** 1979. Substrate-binding site for nitrate reductase of *Escherichia coli* is on the inner aspect of the membrane. J. Bacteriol. **137**:1227–1233.
291. **Kröger, A.** 1978. Fumarate as terminal acceptor of phosphorylative electron transport. Biochim. Biophys. Acta **505**:129–145.
292. **Kung, H.-F., and U. Hennings.** 1972. Limiting availability of binding sites for dehydrogenases on the cell membrane of *Escherichia coli*. Proc. Natl. Acad. Sci. U.S.A. **69**:925–929.
293. **Lakchaura, B. D., T. Fassum, and J. Jagger.** 1976. Inactivation of adenosine 5′-triphosphate synthesis and reduced-form nicotinamide adenine dinucleotide dehydrogenase activity in *Escherichia coli* by near-ultraviolet and violet radiations. J. Bacteriol. **125**:111–118.
294. **Lambden, P. R., and J. R. Guest.** 1976. Mutants of *Escherichia coli* K12 unable to use fumarate as an anaerobic electron acceptor. J. Gen. Microbiol. **97**:145–160.
295. **Larson, T. J., M. Ehrmann, and W. Boos.** 1983. Periplasmic glycerophosphate diester phospho diesterase of *Escherichia coli*, a new enzyme of the *glp* regulon. J. Biol. Chem. **258**:5428–5432.
296. **Lawford, H. G., and B. A. Haddock.** 1973. Respiration-driven proton translocation in *Escherichia coli*. Biochem. J. **136**:217–220.
297. **Lemberg, R., and J. Barrett (ed.).** 1973. Cytochromes, p. 217–326. Academic Press, Inc., New York.
298. **Lemire, B. D., J. J. Robinson, R. D. Bradley, D. G. Scraba, and J. H. Weiner.** 1983. Structure of fumarate reductase on the cytoplasmic membrane of *Escherichia coli*. J. Bacteriol. **155**:391–397.
299. **Lemire, B. D., J. J. Robinson, and J. H. Weiner.** 1982. Identification of membrane anchor polypeptides of *Escherichia coli* fumarate reductase. J. Bacteriol. **152**:1126–1131.
300. **Liang, A., and R. L. Houghton.** 1981. Coregulation of oxidized nicotinamide adenine dinucleotide (phosphate) transhydrogenase and glutamate dehydrogenase activities in enteric bacteria during nitrogen limitation. J. Bacteriol. **146**:997–1002.
301. **Lin, E. C. C.** 1976. Glycerol dissimilation and its regulation in bacteria. Annu. Rev. Microbiol. **30**:535–578.
302. **Liu, M. C., H. D. Peck, A. Abu-Jaoude, M. Chippaux, and J. Le Gall.** 1981. A reappraisal of the role of the low potential *c*-type cytochrome (cytochrome c_{552}) in NADH-dependent ni-

trite reduction and its relationship with a co-purified NADH oxidase in *Escherichia coli* K12. FEMS Microbiol. Lett. **10**:333–337.
303. **Ljungdahl, L. G.** 1980. Formate dehydrogenases: role of molybdenum, tungsten and selenium, p. 465–486. *In* M. Coughlan (ed.), Molybdenum and molybdenum-containing enzymes. Pergamon Press, Oxford.
304. **Lloyd, D., R. K. Poole, and S. W. Edwards.** 1982. The cell division cycle. Temporal organization and control of cellular growth and reproduction. Academic Press, London.
305. **Lohmeier, E., D. S. Hagen, P. Dickie, and J. H. Weiner.** 1981. Cloning and expression of the fumarate reductase gene of *Escherichia coli*. Can. J. Biochem. **59**:158–164.
306. **Lovitt, R. W., and J. W. T. Wimpenny.** 1981. Physiological behaviour of *Escherichia coli* grown in opposing gradients of oxidant and reductant in the gradostat. J. Gen. Microbiol. **127**:269–276.
307. **Lund, T., and J. B. Raynor.** 1975. Electron spin resonance of some bacterial respiratory membranes. Bioenergetics **7**:161–166.
308. **Lutkenhaus, J. F., B. A. Moore, M. Masters, and W. D. Donachie.** 1979. Individual proteins are synthesized continuously throughout the *Escherichia coli* cell cycle. J. Bacteriol. **138**:352–360.
309. **MacGregor, C. H.** 1975. Solubilization of *Escherichia coli* nitrate reductase by a membrane-bound protease. J. Bacteriol. **121**:1102–1110.
310. **MacGregor, C. H.** 1976. Biosynthesis of a membrane-bound nitrate reductase in *Escherichia coli*: evidence for a soluble precursor. J. Bacteriol. **126**:122–131.
311. **MacGregor, C. H., and C. W. Bishop.** 1977. Do cytochromes function as oxygen sensors in the regulation of nitrate reductase biosynthesis? J. Bacteriol. **131**:372–373.
312. **MacGregor, C. H., and A. R. Christopher.** 1978. Asymmetric distribution of nitrate reductase subunits in the cytoplasmic membrane of *Escherichia coli*: evidence derived from surface labelling studies and transglutaminase. Arch. Biochem. Biophys. **185**:204–213.
313. **MacGregor, C. H., and G. E. McElhaney.** 1981. New mechanism for post-translocational processing during assembly of a cytoplasmic membrane protein? J. Bacteriol. **148**:551–558.
314. **MacGregor, C. H., and C. A. Schnaitman.** 1971. Alterations in the cytoplasmic membrane proteins of various chlorate-resistant mutants of *Escherichia coli*. J. Bacteriol. **108**:564–570.
315. **MacGregor, C. H., C. A. Schnaitman, D. E. Normansell, and M. G. Hodgins.** 1974. Purification and properties of nitrate reductase from *Escherichia coli* K12. J. Biol. Chem. **249**:5321–5327.
316. **Macy, J., H. Kulla, and G. Gottschalk.** 1976. Hydrogen-dependent anaerobic growth of *Escherichia coli* on L-malate-:succinate formation. J. Bacteriol. **125**:423–428.
317. **Mandrand-Berthelot, M. A., M. Y. K. Wee, and B. A. Haddock.** 1978. An improved method for the identification and characterization of mutants of Escherichia coli defective in formate dehydrogenase activity. FEMS Lett. **4**:37–40.
318. **Maruyama, Y.** 1956. Biochemical aspects of the cell growth of *Escherichia coli* as studied by the method of synchronous culture. J. Bacteriol. **72**:821–826.
319. **Mason, T. G., and G. Richardson.** 1981. *Escherichia coli* and the human gut: some ecological considerations. J. Appl. Bacteriol. **51**:1–6.
320. **Mather, M., R. Blake, J. Koland, H. Schrock, P. Russell, T. O'Brien, L. P. Hager, and R. B. Gennis.** 1982. *Escherichia coli* pyruvate oxidase. Interaction of a peripheral membrane protein with lipids. Biophys. J. **37**:87–88.
321. **Mather, M., L. M. Schopfer, V. Massey, and R. B. Gennis.** 1982. Studies of the flavin adenine dinucleotide binding region in *Escherichia coli* pyruvate oxidase. J. Biol. Chem. **257**:12887–12892.
322. **Mathews, F. S., P. H. Bethge, and E. W. Czerwinski.** 1979. The structure of cytochrome b_{562} from *Escherichia coli* at 2.5 Å resolution. J. Biol. Chem. **254**:1699–1706.
323. **Matsushita, K., L. Patel, R. B. Gennis, and H. R. Kaback.** 1983. Reconstitution of active transport in proteoliposomes containing cytochrome *o* oxidase and *lac* carrier protein purified from *Escherichia coli*. Proc. Natl. Acad. Sci. U.S.A. **80**:4889–4893.
324. **Mavis, R. D., and P. R. Vagelos.** 1972. The effect of phospholipid fatty acid composition on membranous enzymes in *Escherichia coli*. J. Biol. Chem. **247**:652–659.
325. **McRee, D. E., and D. C. Richardson.** 1982. Preliminary X-ray diffraction studies on the hemoprotein subunit of *Escherichia coli* sulphite reductase. J. Mol. Biol. **154**:179–180.
326. **Meister, A.** 1982. Limits for decomposition of spectra into single bands. J. Theor. Biol. **94**:541–553.
327. **Meyer, D. J.** 1973. Interaction of cytochrome oxidases aa_3, and *d* with nitrite. Nature (London) New Biol. **245**:276–277.
328. **Meyer, D. J., and C. W. Jones.** 1973. Oxidative phosphorylation in bacteria which contain different cytochrome oxidases. Eur. J. Biochem. **36**:144–151.
329. **Miki, K., and E. C. C. Lin.** 1973. Enzyme complex which couples glycerol-3-phosphate dehydrogenation to fumarate reductase in *Escherichia coli*. J. Bacteriol. **114**:767–771.
330. **Miki, K., and E. C. C. Lin.** 1975. Anaerobic energy yielding reaction associated with transhydrogenation from glycerol-3-phosphate to fumarate by an *Escherichia coli* system. J. Bacteriol. **124**:1282–1287.
331. **Miki, K., and E. C. C. Lin.** 1975. Electron transport chain from glycerol-3-phosphate to nitrate in *Escherichia coli*. J. Bacteriol. **124**:1288–1294.
332. **Miki, K., T. J. Silhavy, and K. J. Andrews.** 1978. Resolution of *glpA* and *glpT* loci into separate operons in *Escherichia coli* K-12 strains. J. Bacteriol. **138**:268–269.
333. **Miki, K., and T. H. Wilson.** 1978. Proton translocation associated with anaerobic transhydrogenation from glycerol-3-phosphate to fumarate in *Escherichia coli*. Biochem. Biophys. Res. Commun. **83**:1570–1575.
334. **Miller, J. B., and N. K. Amy.** 1983. Molybdenum cofactor in chlorate-resistant and nitrate reductase-deficient insertion mutants of *Escherichia coli*. J. Bacteriol. **155**:793–801.
335. **Miller, M. J., and R. B. Gennis.** 1983. The purification and characterization of the cytochrome *d* terminal oxidase complex of the *Escherichia coli* aerobic respiratory chain. J. Biol. Chem. **258**:9159–9165.
336. **Misri, R., and R. K. Poole.** 1983. An apparatus for the continuous and simultaneous monitoring of oxygen and solute uptake by growing microbial cultures. Application to synchronous and asynchronous cultures of *Escherichia coli*. J. Microbiol. Methods **1**:181–190.
337. **Mitchell, P.** 1966. Chemiosmotic coupling in oxidative and photosynthetic phosphorylation. Glynn Research, Bodmin, Cornwall, U.K.
338. **Mitchell, P., and J. Moyle.** 1979. Respiratory-chain protonmotive stoichiometry. Biochem. Soc. Trans. **7**:887–894.
339. **Møller, V.** 1954. Diagnostic use of the Braun KCN test within the Enterobacteriaceae. Acta Pathol. Microbiol. Scand. **34**:115–116.
340. **Moss, F.** 1952. The influence of oxygen tension on respiration and cytochrome a_2 formation of *Escherichia coli*. Aust. J. Exp. Biol. Med. Sci. **30**:531–540.
341. **Motteram, P. A. S., J. E. G. McCarthy, S. J. Ferguson, J. B. Jackson, and J. A. Cole.** 1981. Energy conservation during the formate-dependent reduction of nitrite by *Escherichia coli*. FEMS Microbiol. Lett. **12**:317–320.
342. **Myer, Y. P., and P. A. Bullock.** 1978. Cytochrome b_{562} from *Escherichia coli*: conformational configurational and spin-state characterization. Biochemistry **17**:3723–3729.
343. **Narindrasorasak, S., A. H. Goldie, and B. D. Sanwal.** 1979. Characteristics and regulation of a phospholipid-activated malate oxidase from *Escherichia coli*. J. Biol. Chem. **254**:1540–1545.
344. **Newton, N. A., G. B. Cox, and F. Gibson.** 1971. The function of menaquinone (vitamin K12) in *Escherichia coli* K12. Biochim. Biophys. Acta **244**:155–156.
345. **Nicholas, D. J. D., P. W. Wilson, W. Heinen, G. Palmer, and H. Beinert.** 1982. Use of electron paramagnetic resonance

spectroscopy in investigations of functional metal components in micro-organisms. Nature (London) **196**:433–436.
346. **Nicholls, D. G.** 1982. Bioenergetics. An introduction to the chemiosmotic theory. Academic Press, London.
347. **Nishimura, Y., I. K. P. Tan, Y. Ohgami, K. Kohgami, and T. Kamihara.** 1983. Induction of membrane-bound L-lactate dehydrogenase in *Escherichia coli* under conditions of nitrate respiration, fumarate reduction and trimethylamine-N-oxide reduction. FEMS Microbiol. Lett. **17**:283–286.
348. **Nosoh, Y., and M. Itoh.** 1965. The 503 mu pigment in bacteria and yeast. Plant Cell Physiol. **6**:771–774.
349. **O'Brien, T. A., R. Blake, and R. B. Gennis.** 1977. Regulation by lipids of cofactor binding to a peripheral membrane enzyme: binding of thiamin pyrophosphate to pyruvate oxidase. Biochemistry **16**:3105–3109.
350. **O'Brien, T. A., H. L. Schrock, P. Russell, R. Blake, and R. B. Gennis.** 1976. Preparation of *Escherichia coli* pyruvate oxidase utilizing a thiamine pyrophosphate affinity column. Biochim. Biophys. Acta **452**:13–29.
351. **O'Brien, T. A., E. Shelton, M. Mather, and R. B. Gennis.** 1982. Conformational studies of *Escherichia coli* pyruvate oxidase. Biochim. Biophys. Acta **705**:321–329.
352. **Ohki, M.** 1972. Correlation between metabolism of phosphatidyl glycerol and membrane synthesis in *Escherichia coli*. J. Mol. Biol. **68**:249–264.
353. **Ohnishi, T.** 1979. Mitochondrial iron sulphur flavo-dehydrogenases, p. 1–87. *In* R. A. Capaldi (ed.), Membrane proteins in energy transduction. Marcel Dekker, New York.
354. **Ohnishi, T., J. Lim, D. B. Winter, and T. E. King.** 1976. Thermodynamic and EPR characteristics of a HiPIP-type iron-sulphur centre in the succinate dehydrogenase of the respiratory chain. J. Biol. Chem. **251**:2105–2109.
355. **Ohnishi, T., J. C. Salerno, D. B. Winter, J. Lim, C.-A.Yu, L. Yu, and T. E. King.** 1976. Thermodynamic and EPR characteristics of two ferredoxin-type iron-sulphur centers in the succinate-ubiquinone reductase segment of the respiratory chain. J. Biol. Chem. **251**:2094–2104.
356. **Olden, K., and W. P. Hempfling.** 1973. The 503-nm pigment of *Escherichia coli* B: characterization and nutritional conditions affecting its accumulation. J. Bacteriol. **113**:914–921.
357. **Olsiewski, P. J., G. J. Kaczorowski, and C. Walsh.** 1980. Purification and properties of D amino-acid dehydrogenase, an inducible membrane-bound iron-sulfur flavoenzyme from *Escherichia coli* B. J. Biol. Chem. **255**:4487–4494.
358. **Olsiewski, P. J., G. J. Kaczorowski, C. T. Walsh, and H. R. Kaback.** 1981. Reconstitution of *Escherichia coli* membrane vesicles with D amino-acid dehydrogenase. Biochemistry **20**:6272–6279.
359. **Orth, V., M. Chippaux, and M. C. Pascal.** 1980. A mutant defective in electron transfer to nitrate in *Escherichia coli* K12. J. Gen. Microbiol. **117**:257–262.
360. **Ota, A., T. Yamanaka, and K. Okunuki.** 1964. Oxidative phosphorylation coupled with nitrate respiration. II. Phosphorylation coupled with anaerobic nitrate reduction in a cell-free extract of *Escherichia coli*. J. Biochem. (Tokyo) **55**:131–135.
361. **Owen, P., and C. Condon.** 1982. The succinate dehydrogenase of *Escherichia coli*: subunit composition of the Triton X-100 solubilized antigen. FEMS Microbiol. Lett. **14**:223–227.
362. **Owen, P., and H. R. Kaback.** 1978. Molecular structure of membrane vesicles from *Escherichia coli*. Proc. Natl. Acad. Sci. U.S.A. **78**:3148–3152.
363. **Owen, P., and H. R. Kaback.** 1979. Immunochemical analysis of membrane vesicles from *Escherichia coli*. Biochemistry **18**:1413–1422.
364. **Owen, P., and H. R. Kaback.** 1979. Antigenic architecture of membrane vesicles from *Escherichia coli*. Biochemistry **18**:1422–1426.
365. **Owen, P., H. R. Kaback, and K. A. Graeme-Cook.** 1980. Identification of antigen 19/27 as dihydrolipoyl dehydrogenase and its probable involvement in ubiquinone-mediated NADH-dependent transport phenomena in membrane vesicles of *Escherichia coli*. FEMS Microbiol. Lett. **7**:345–349.
366. **Owen, P., G. J. Kaczorowski, and H. R. Kaback.** 1980. Resolution and identification of iron-containing antigens in membrane vesicles from *Escherichia coli*. Biochemistry **19**:596–600.
367. **Padan, E., D. Zilberstein, and H. Rottenberg.** 1976. The proton electrochemical gradient in *E. coli* cells. Eur. J. Biochem. **63**:533–541.
368. **Pascal, M. C., F. Casse, M. Chippaux, and M. Lepelletier.** 1975. Genetic analysis of mutants of *Escherichia coli* K12 and *Salmonella typhimurium* LT2 deficient in hydrogenase activity. Mol. Gen. Genet. **141**:173–179.
369. **Pateman, J. A., D. J. Cove, B. M. Rever, and D. B. Roberts.** 1964. A common cofactor for nitrate reductase and xanthine dehydrogenase which also regulates the synthesis of nitrate reductase. Nature (London) **201**:58–60.
370. **Peck, H. D., Jr., and H. Gest.** 1957. Formic dehydrogenase and the hydrogenlyase enzyme complex in coli-aerogenes bacteria. J. Bacteriol. **73**:706–721.
371. **Pinsett, J.** 1954. The need for selenite and molybdate in the formation of formic dehydrogenase by members of the *coli-aerogenes* group of bacteria. Biochem. J. **57**:10–16.
372. **Polglase, W. J., W. T. Pun, and J. Whithaar.** 1965. Lipoquinones of *Escherichia coli*. Biochim. Biophys. Acta **118**:425–426.
373. **Poole, R. K.** 1977. The influence of growth substrate and capacity for oxidative phosphorylation on respiratory oscillations in synchronous cultures of *Escherichia coli* K12. J. Gen. Microbiol. **99**:369–377.
374. **Poole, R. K.** 1977. Development of respiratory activity during the cell cycle of *Schizosaccharomyces pombe* 972 h^-: respiratory oscillations and heat dissipation in cultures synchronized with 2'-deoxyadenosine. J. Gen. Microbiol. **103**:19–27.
375. **Poole, R. K.** 1980. Temporal diversity of bacterial respiratory systems. Membrane and respiratory development during the cell cycle, p. 87–114. *In* C. J. Knowles (ed.), Diversity of bacterial respiratory systems. CRC Press Inc., Boca Raton, Fla.
376. **Poole, R. K.** 1982. The oxygen reactions of bacterial cytochrome oxidases. Trends Biochem. Sci. **7**:32–34.
377. **Poole, R. K.** 1983. Bacterial cytochrome oxidases. A structurally and functionally diverse group of electron-transfer proteins. Biochim. Biophys. Acta **726**:205–243.
378. **Poole, R. K.** 1984. Is respiratory metabolism in the prokaryotic cell cycle manifestly coupled to a clock?, p. 193–207. *In* L. N. Edmunds (ed.), Cell cycle clocks. Marcel Dekker, New York.
379. **Poole, R. K., B. S. Baines, J. A. M. Hubbard, M. N. Hughes, and N. J. Campbell.** 1982. Resonance Raman spectroscopy of an oxygenated intermediate species of cytochrome oxidase *d* from *Escherichia coli*. FEBS Lett. **150**:147–150.
380. **Poole, R. K., H. Blum, R. I. Scott, A. Collinge, and T. Ohnishi.** 1980. The orientation of cytochromes in membrane multilayers prepared from aerobically grown *Escherichia coli* K12. J. Gen. Microbiol. **119**:145–154.
381. **Poole, R. K., and B. Chance.** 1981. The reaction of cytochrome *o* in *Escherichia coli* K12 with oxygen. Evidence for a spectrally and kinetically distinct cytochrome *o* in cells from oxygen-limited culture. J. Gen. Microbiol. **126**:277–287.
382. **Poole, R. K., and B. A. Haddock.** 1974. Energy-linked reduction of nicotinamide adenine dinucleotide in membranes derived from normal and various respiratory-deficient mutant strains of *Escherichia coli* K12. Biochem. J. **144**:77–85.
383. **Poole, R. K., and B. A. Haddock.** 1975. Effects of sulphate-limited growth in continuous culture on the electron-transport chain and energy conservation in *Escherichia coli* K12. Biochem. J. **152**:537–546.
384. **Poole, R. K., C. Kumar, I. Salmon, and B. Chance.** 1983. The 650 nm chromophore in *Escherichia coli* is an oxygenated compound, not the oxidized form of cytochrome oxidase *d*: an hypothesis. J. Gen. Microbiol. **129**:1335–1344.
385. **Poole, R. K., and I. Salmon.** 1978. The pool sizes of adenine nucleotides in exponentially growing, stationary phase and 2'-deoxy-adenosine-synchronous cultures of *Schizosaccharomyces pombe* 972 h^-. J. Gen. Microbiol. **106**:153–164.
386. **Poole, R. K., I. Salmon, and B. Chance.** 1983. The reaction with oxygen of cytochrome oxidase (cytochrome *d*) in *Escherichia coli* K12: optical studies of intermediate species and

cytochrome *b* oxidation at sub-zero temperatures. J. Gen. Microbiol. **129**:1345–1355.
387. **Poole, R. K., R. I. Scott, and H. Blum.** 1981. Respiratory biogenesis during the cell cycle of aerobically-grown *Escherichia coli* K12. The accumulation of iron-sulphur clusters and their orientation in the membrane. J. Gen. Microbiol. **124**:181–185.
388. **Poole, R. K., R. I. Scott, and B. Chance.** 1980. Low-temperature spectral and kinetic properties of cytochromes in *Escherichia coli* K12 grown at lowered oxygen tension. Biochim. Biophys. Acta **591**:471–483.
389. **Poole, R. K., R. I. Scott, and B. Chance.** 1981. The light-reversible binding of carbon monoxide to cytochrome a_1 in *Escherichia coli* K12. J. Gen. Microbiol. **125**:431–438.
390. **Poole, R. K., A. Sivaram, I. Salmon, and B. Chance.** 1982. Photolysis at very low temperatures of CO-liganded cytochrome oxidase (cytochrome *d*) in oxygen-limited *Escherichia coli*. FEBS Lett. **141**:237–241.
391. **Poole, R. K., J. E. Van Wielink, B. S. Baines, W. N. M. Reijnders, I. Salmon, and L. F. Oltmann.** 1983. The membrane-bound cytochromes of an aerobically grown, extremely thermophilic bacterium, PS3: characterization by spectral deconvolution coupled with potentiometric analysis. J. Gen. Microbiol. **129**:2163–2173.
392. **Poole, R. K., A. J. Waring, and B. Chance.** 1979. Evidence for a functional oxygen-bound intermediate in the reaction of *Escherichia coli* cytochrome *o* with oxygen. FEBS Lett. **101**:56–58.
393. **Poole, R. K., A. J. Waring, and B. Chance.** 1979. The reaction of cytochrome *o* in *Escherichia coli* with oxygen. Low temperature kinetics and spectral studies. Biochem. J. **184**:379–389.
394. **Pope, N. R., and J. A. Cole.** 1982. Generation of a membrane potential by one of two independent pathways for nitrite reduction by *Escherichia coli*. J. Gen. Microbiol. **128**:219–222.
395. **Porter, N., J. W. Drozd, and J. D. Linton.** 1983. The effects of cyanide on the growth and respiration of *Enterobacter aerogenes* in continuous culture. J. Gen. Microbiol. **129**:7–16.
396. **Porter, N., and C. J. Knowles.** 1979. Cyanide-resistant growth in *Citrobacter freundii* and other Enterobacteriaceae. FEMS Microbiol. Lett. **5**:323–326.
397. **Poulis, M. I., D. C. Shaw, H. D. Campbell, and I. G. Young.** 1981. *In vitro* synthesis of the respiratory NADH dehydrogenase of *Escherichia coli*. Biochemistry **20**:4178–4185.
398. **Poulson, R., K. J. Whitlow, and W. J. Polglase.** 1976. Catabolite repression of protoporphyrin IX biosynthesis in *Escherichia coli* K12. FEMS Lett. **62**:351–353.
399. **Pratt, E. A., L. W. M. Fung, J. A. Flowers, and C. Ho.** 1979. Membrane-bound D lactate dehydrogenase from *Escherichia coli*: purification and properties. Biochemistry **18**:312–316.
400. **Pratt, E. A., J. A. Jones, P. F. Cottam, S. R. Dowd, and C. Ho.** 1983. A biochemical study of the reconstitution of D-lactate dehydrogenase-deficient membrane vesicles using fluorine-labelled components. Biochim. Biophys. Acta **729**:167–175.
401. **Pudek, M. R., and P. D. Bragg.** 1974. Inhibition by cyanide of the respiratory chain oxidases of *Escherichia coli*. Arch. Biochem. Biophys. **164**:682–693.
402. **Pudek, M. R., and P. D. Bragg.** 1975. Reaction of cyanide with cytochrome *d* in respiratory particles from exponential phase *Escherichia coli*. FEBS Lett. **50**:111–113.
403. **Pudek, M. R., and P. D. Bragg.** 1976. Trapping of an intermediate in the oxidation-reduction cycle of cytochrome *d* in *Escherichia coli*. FEBS Lett. **62**:330–333.
404. **Pudek, M. R., and P. D. Bragg.** 1976. Redox potentials of the cytochromes in the respiratory chain of aerobically-grown *Escherichia coli*. Arch. Biochem. Biophys. **174**:546–552.
405. **Puig, J., and E. Azoulay.** 1967. Etude genetique et biochimique des mutants resistant du $C10_3$- (genes *chlA, chlB, chlC*). C. R. Acad. Sci. Ser. D **264**:1916–1918.
406. **Rainnie, D. J., and P. D. Bragg.** 1973. The effect of iron deficiency on respiration and energy coupling in *Escherichia coli*. J. Gen. Microbiol. **77**:339–349.
407. **Raj, T., P. Russell, W. H. Flygare, and R. B. Gennis.** 1977. Quasi-elastic light scattering studies on pyruvate oxidase. Biochim. Biophys. Acta **481**:42–49.
408. **Ramos, S., and H. R. Kaback.** 1977. The relationship between the electrochemical proton gradient and active transport in *Escherichia coli* membrane vesicles. Biochemistry **16**:854–859.
409. **Raunio, R. P., L. D'Ari Strauss, and W. T. Jenkins.** 1973. D-Alanine oxidase from *Escherichia coli*: participation in the oxidation of L-alanine. J. Bacteriol. **115**:567–573.
410. **Raunio, R. P., and W. T. Jenkins.** 1973. D-Alanine oxidase from *Escherichia coli*: localization and induction by L-alanine. J. Bacteriol. **115**:560–566.
411. **Recny, M. A., and L. P. Hager.** 1982. Reconstitution of native *Escherichia coli* pyruvate oxidase from apoenzyme monomers and FAD. J. Biol. Chem. **257**:12878–12886.
412. **Reddy, T. L. P., and R. W. Hendler.** 1978. Reconstitution of *Escherichia coli* succinoxidase from soluble components. J. Biol. Chem. **253**:7972–7979.
413. **Reeves, J. P.** 1971. Transient pH changes during D-lactate oxidation by membrane vesicles. Biochem. Biophys. Res. Commun. **45**:931–936.
414. **Reeves, J. P., J. S. Hong, and H. R. Kaback.** 1973. Reconstitution of D-lactate-dependent transport in membrane vesicles from a D-lactate dehydrogenase mutant of *Escherichia coli*. Proc. Natl. Acad. Sci. U.S.A. **70**:1917–1921.
415. **Reid, G. A., B. A. Haddock, and W. J. Ingledew.** 1981. Assembly of functional *b*-type cytochromes in membranes from a 5-aminolaevulinic acid-requiring mutant of *Escherichia coli*. FEBS Lett. **131**:346–351.
416. **Reid, G. A., and W. J. Ingledew.** 1979. Characterization and phenotypic control of the cytochrome content of *Escherichia coli*. Biochem. J. **182**:465–472.
417. **Reid, G. A., and W. J. Ingledew.** 1980. The purification of a respiratory oxidase complex from *Escherichia coli*. FEBS Lett. **109**:1–4.
418. **Rice, C. W., and W. P. Hempfling.** 1978. Oxygen-limited continuous culture and respiratory energy conservation in *Escherichia coli*. J. Bacteriol. **134**:115–124.
419. **Rich, P. R.** 1982. The organization of the quinone pool. Biochem. Soc. Trans. **10**:482–484.
420. **Riviere, C., G. Giordano, J. Pommier, and E. Azoulay.** 1975. Membrane reconstitution in *chl*-r mutants of *Escherichia coli* K12. VIII. Purification and properties of the F_A factor, the product of the *chlB* gene. Biochim. Biophys. Acta **389**:219–235.
421. **Robinson, J. J., and J. H. Weiner.** 1980. The effect of amphipaths on the flavin-linked aerobic glycerol-3-phosphate dehydrogenase from *Escherichia coli*. Can. J. Biochem. **58**:1172–1178.
422. **Robinson, J. J., and J. H. Weiner.** 1981. The effect of anions on fumarate reductase isolated from the cytoplasmic membrane of *Escherichia coli*. Biochem. J. **199**:473–477.
423. **Robinson, J. J., and J. H. Weiner.** 1982. Molecular properties of fumarate reductase isolated from the cytoplasmic membrane of *Escherichia coli*. Can. J. Biochem. **60**:811–816.
424. **Rosenberg, H., G. B. Cox, J. D. Butlin, and S. J. Gutowski.** 1975. Metabolite transport in mutants of *Escherichia coli* K12 defective in electron transport and coupled phosphorylation. Biochem. J. **146**:417–423.
425. **Ruch, F. E., E. C. C. Lin, J. D. Kowit, C. T. Tang, and A. L. Goldberg.** 1980. In vivo inactivation of glycerol dehydrogenase in *Klebsiella aerogenes*: properties of active and inactivated proteins. J. Bacteriol. **141**:1077–1085.
426. **Ruiz-Herrera, J., and A. Alvarez.** 1972. A physiological study of formate dehydrogenase, formate oxidase and hydrogen lyase from *Escherichia coli* K12. Antonie Van Leeuwenhoek J. Microbiol. Serol. **38**:479–491.
427. **Ruiz-Herrera, J., A. Alvarez, and I. Figueroa.** 1972. Solubilization and properties of formate dehydrogenases from the membrane of *Escherichia coli*. Biochim. Biophys. Acta **289**:254–261.
428. **Ruiz-Herrera, J., and J. A. De Moss.** 1969. Nitrate reductase complex of *Escherichia coli* K-12: participation of specific formate dehydrogenase and cytochrome b_1 components in

nitrate reduction. J. Bacteriol. **99**:720–729.
429. **Ruiz-Herrera, J., and L. G. Garcia.** 1972. Regulation of succinate dehydrogenase in *Escherichia coli*. J. Gen. Microbiol. **7**:29–35.
430. **Ruiz-Herrera, J., M. K. Showe, and J. A. de Moss.** 1969. Nitrate reductase complex of *Escherichia coli* K-12: isolation and characterization of mutants unable to reduce nitrate. J. Bacteriol. **97**:1291–1297.
431. **Russell, P., H. L. Schrock, and R. B. Gennis.** 1977. Lipid activation and protease activation of pyruvate oxidase: evidence suggesting a common site of interaction on the protein. J. Biol. Chem. **252**:7883–7887.
432. **Sakaguchi, M., and A. Kawai.** 1977. Electron donors and carriers for the reduction of trimethylanine N-oxide in *Escherichia coli*. Bull. Jpn. Sci. Fish. **43**:437–442.
433. **Sakaguchi, M., and A. Kawai.** 1978. The participation of cytochromes in the reduction of trimethylanine *N* oxide by *Escherichia coli*. Bull. Jpn. Soc. Sci. Fish. **44**:511–516.
434. **Santos, E., H.-F. Kung, I. G. Young, and R. Kaback.** 1982. *In vitro* synthesis of the membrane-bound D-lactate dehydrogenase of *Escherichia coli*. Biochemistry **21**:2085–2091.
435. **Sasarman, A., M. Surdeanu, and T. Horodniceanu.** 1968. Locus determining the synthesis of δ-aminolevulinic acid in *Escherichia coli*. J. Bacteriol. **96**:1882–1884.
436. **Savage, D. C.** 1977. Microbial ecology of the gastrointestinal tract. Annu. Rev. Microbiol. **31**:107–133.
437. **Scarpulla, R. C., and R. L. Soffer.** 1978. Membrane-bound proline dehydrogenase from *Escherichia coli*: solubilization, purification and characterization. J. Biol. Chem. **253**:5997–6001.
438. **Schrock, H. L., and R. B. Gennis.** 1980. Specific ligand enhancement of the affinity of *Escherichia coli* pyruvate oxidase for dipalmitoyl phosphatidylcholine. Biochim. Biophys. Acta **614**:215–220.
439. **Schryvers, A., E. Lohmeier, and J. H. Weiner.** 1978. Chemical and functional properties of the native and reconstituted forms of the membrane-bound, aerobic glycerol-3-phosphate dehydrogenase of *Escherichia coli*. J. Biol. Chem. **253**:783–788.
440. **Schryvers, A., and J. H. Weiner.** 1981. The anaerobic sn-glycerol-3-phosphate dehydrogenase of *Escherichia coli*. Purification and characterization. J. Biol. Chem. **256**:9959–9966.
441. **Scott, R., R. K. Poole, and B. Chance.** 1981. Respiratory biogenesis during the cell cycle of aerobically-grown *Escherichia coli* K12. The accumulation and ligand binding of cytochrome *o*. J. Gen. Microbiol. **122**:255–261.
442. **Scott, R. I., and R. K. Poole.** 1982. A re-examination of the cytochromes of *Escherichia coli* using fourth-order finite difference analysis: their characterization under different growth conditions and accumulation during the cell cycle. J. Gen. Microbiol. **128**:1685–1696.
443. **Shaw, D. J., and J. R. Guest.** 1981. Molecular cloning of the *fnr* gene of *Escherichia coli* K12. Mol. Gen. Genet. **181**:95–100.
444. **Shaw, D. J., and J. R. Guest.** 1982. Amplification and product identification of the *fnr* gene of *Escherichia coli*. J. Gen. Microbiol. **128**:2221–2228.
445. **Shaw, D. J., E. C. Robinson, R. Meganathan, R. Bentley, and J. R. Guest.** 1983. Recombinant plasmids containing menaquinone biosynthetic genes of *Escherichia coli*. FEMS Microbiol. Lett. **17**:63–67.
446. **Shaw-Goldstein, L. A., R. B. Gennis, and C. Walsh.** 1978. Identification, localization and function of the thiamine pyrophosphate and FAD dependent pyruvate oxidase in isolated membrane vesicles of *Escherichia coli* B. Biochemistry **17**:5605–5613.
447. **Shipp, W. S.** 1972. Cytochromes of *Escherichia coli*. Arch. Biochem. Biophys. **150**:459–472.
448. **Shipp, W. S., M. Piotrowski, and A. E. Friedman.** 1972. Apparent cytochrome gene dose effects in F-*rac* and F-*gal* heterogenases of *Escherichia coli*. Arch. Biochem. Biophys. **150**:473–481.
449. **Short, S. A., H. R. Kaback, T. Hawkins, and L. D. Kohn.** 1975. Immunochemical properties of the membrane-bound D lactate dehydrogenase from *Escherichia coli*. J. Biol. Chem. **250**:4285–4290.
450. **Short, S. A., H. R. Kaback, and L. D. Kohn.** 1974. D-lactate dehydrogenase binding in *Escherichia coli* DLD membrane vesicles reconstituted for active transport. Proc. Natl. Acad. Sci. U.S.A. **71**:1461–1465.
451. **Short, S. A., H. R. Kaback, and L. D. Kohn.** 1975. Localization of D lactate dehydrogenase in native and reconstituted *Escherichia coli* membrane vesicles. J. Biol. Chem. **250**:4291–4296.
452. **Siegel, L. M., and P. S. Davis.** 1974. Reduced nicotinamide adenine dinucleotide phosphate-sulfite reductase of Enterobacteria. IV. The *Escherichia coli* hemoflavoprotein: subunit structure and dissociation into hemoprotein and flavoprotein components. J. Biol. Chem. **249**:1587–1598.
453. **Simoni, R. D., and M. K. Shallenberger.** 1972. Coupling of energy to active transport of amino acids in *Escherichia coli*. Proc. Natl. Acad. Sci. U.S.A. **69**:2663–2667.
454. **Singh, A. P., and P. D. Bragg.** 1974. Energization of phenylalanine transport and energy-dependent transhydrogenase by ATP in cytochrome-deficient *Escherichia coli* K12. Biochem. Biophys. Res. Commun. **57**:1200–1206.
455. **Singh, A. P., and P. D. Bragg.** 1975. Reduced nicotinamide adenine dinucleotide-dependent reduction of fumarate coupled to membrane energization in a cytochrome-deficient mutant of *Escherichia coli* K12. Biochim. Biophys. Acta **396**:229–241.
456. **Singh, A. P., and P. D. Bragg.** 1976. Anaerobic transport of amino acids coupled to the glycerol-3-phosphate-fumarate oxidoreductase system in a cytochrome-deficient mutant of *Escherichia coli*. Biochim. Biophys. Acta **423**:450–461.
457. **Singh, A. P., and P. D. Bragg.** 1976. Transport of α-methyl glucoside in a cytochrome-deficient mutant of *Escherichia coli* K12. FEBS Lett. **64**:169–172.
458. **Smith, M. W., and F. C. Neidhardt.** 1983. Proteins induced by anaerobiosis in *Escherichia coli*. J. Bacteriol. **154**:336–343.
459. **Smith, M. W., and F. C. Neidhardt.** 1983. Proteins induced by aerobiosis in *Escherichia coli*. J. Bacteriol. **154**:344–350.
460. **Smith, P. H., and R. E. Hungate.** 1958. Isolation and characterization of a *Methanobacterium ruminantium* n. sp. J. Bacteriol. **75**:713–718.
461. **Smyth, C. J., J. Siegel, M. R. I. Salton, and P. Owen.** 1978. Immunochemical analysis of inner and outer membranes of *Escherichia coli* by crossed immunoelectrophoresis. J. Bacteriol. **133**:306–319.
462. **Spencer, M. E., and J. R. Guest.** 1973. Isolation and properties of fumarate reductase mutants of *Escherichia coli*. J. Bacteriol. **114**:563–570.
463. **Spencer, M. E., and J. R. Guest.** 1974. Proteins of the inner membrane of *Escherichia coli*: identification of succinate dehydrogenase by polyacrylamide gel electrophoresis with *sdh* amber mutants. J. Bacteriol. **117**:947–953.
464. **Spencer, M. E., and J. R. Guest.** 1982. Molecular cloning of four tricarboxylic acid cycle genes of *Escherichia coli*. J. Bacteriol. **151**:542–552.
465. **Stewart, V.** 1982. Requirement of *fnr* and *narL* functions for nitrate reductase expression in *Escherichia coli* K-12. J. Bacteriol. **151**:1320–1325.
466. **Stewart, V., and C. H. MacGregor.** 1982. Nitrate reductase in *Escherichia coli* K-12: involvement of *chlC*, *chlE*, and *chlG* loci. J. Bacteriol. **151**:788–799.
467. **Stouthamer, A. H., and C. W. Bettenhausen.** 1981. Influence of 2,4-dinitrophenol on the maximum specific growth rate of chemostat cultures of *Paracoccus denitrificans*. FEMS Microbiol. Lett. **10**:33–35.
468. **Stroobant, P., and H. R. Kaback.** 1979. Reconstitution of ubiquinone-linked functions in membrane vesicles from a double quinone mutant of *Escherichia coli*. Biochemistry **18**:226–231.
469. **Takagi, M., and M. Ishimoto.** 1983. *Escherichia coli* mutants defective in trimetylamine N-oxide reductase. FEMS Microbiol. Lett. **17**:247–250.
470. **Takagi, M., T. Tsuchiya, and M. Ishimoto.** 1981. Proton translocation coupled to trimethylamine N-oxide reduction in

anaerobically grown *Escherichia coli*. J. Bacteriol. **148**:762–768.
471. **Tanaka, Y., Y. Anraku, and M. Futai.** 1976. *Escherichia coli* membrane D-lactate dehydrogenase, isolation of the enzyme in aggregated form and its activation by Triton X-100 and phospholipids. J. Biochem. (Tokyo) **80**:821–830.
472. **Tang, C. T., E. J. St. Martin, R. G. Forage, and E. C. C. Lin.** 1982. The development of a strain of *Escherichia coli* that employs a dehydrogenase for the dissimilation of glycerol, p. 425–438. *In* V. Krunphanzl, B. Sikyra, and Z. Vanek (ed.), Overproduction of microbial products. Academic Press, London.
473. **Tarmy, E. M., and N. O. Kaplan.** 1968. Chemical characterization of D-lactate dehydrogenase from *Escherichia coli* B. J. Biol. Chem. **243**:2579–2586.
474. **Tarmy, E. M., and N. O. Kaplan.** 1968. Kinetics of *Escherichia coli* B D-lactate dehydrogenase and evidence for pyruvate-controlled change in conformation. J. Biol. Chem. **243**:2587–2596.
475. **Tarr, H. L. A.** 1954. Microbiological deterioration of fish *post mortem* and its detection and control. Bacteriol. Rev. **18**:1–15.
476. **Taylor, W. H., and M. L. Taylor.** 1964. Enzymes of the pyrimidine pathway in *Escherichia coli*. II. Intracellular localization and properties of dihydroorotic dehydrogenase. J. Bacteriol. **88**:105–110.
477. **Terriere, C., G. Giordano, C.-L. Medani, O. H. Boxer, B. A. Haddock, and E. Azoulay.** 1981. Precursor forms of formate dehydrogenase in *chlA* and *chlB* mutants of *Escherichia coli*. FEMS Microbial. Lett. **11**:287–293.
478. **Thomson, A. J.** 1977. Ligand binding properties of the haem group. Nature (London) **265**:15–16.
479. **Thomson, J. W., and B. M. Shapiro.** 1981. The respiratory chain NADH dehydrogenase of *Escherichia coli*. Isolation of an NADH:quinone oxidoreductase from membranes and comparison with membrane-bound NADH:dichlorophenolindophenol oxidoreductase. J. Biol. Chem. **256**:3077–3084.
480. **Tomsett, A. B., and R. H. Garrett.** 1981. The isolation and characterization of mutants defective in nitrate assimilation in *Neurospora crassa*. Genetics **95**:649–660.
481. **Trutko, S. M., N. P. Golovchenko, and V. K. Akhimenko.** 1978. Changes in the electron transport chain in *Escherichia coli* as a function of the conditions of culturing and phase of growth. Microbiologiya **47**:1–5.
482. **Tsuchiya, T., A. Misawa, Y. Miyake, K. Yamasaki, and S. Niiya.** 1982. Solubilization and reconstitution of membrane energy-transducing systems of *Escherichia coli*. FEBS Lett. **142**:231–234.
483. **Van der Plas, J., K. J. Hellingwerf, H. G. Seijen, J. R. Guest, J. H. Weiner, and W. N. Konings.** 1983. Identification and localization of enzymes of the fumarate reductase and nitrate respiration systems of *Escherichia coli* by crossed immunoelectrophoresis. J. Bacteriol. **153**:1027–1037.
484. **Van Wielink, J. E., L. F. Oltmann, F. J. Leeuwerik, J. A. de Hollander, and A. H. Stouthamer.** 1982. A method for *in situ* characterisation of *b*- and *c*-type cytochromes in *Escherichia coli* and in complex III from beef heart mitochondria by combined spectrum deconvolution and potentiometric analysis. Biochim. Biophys. Acta **681**:177–190.
485. **Van Wielink, J. E., W. N. M. Reijnders, L. F. Oltmann, and A. H. Southamer.** 1983. The characterization of the membrane-bound *b*- and *c*-type cytochromes of differently grown *Escherichia coli* cells by means of coupled potentiometric analysis and spectrum deconvolution. FEMS Microbiol. Lett. **18**:167–172.
486. **Venables, W. A., and J. R. Guest.** 1968. Transduction of nitrate reductase loci of *Escherichia coli* by phage P1 and λ. Mol. Gen. Genet. **103**:127–140.
487. **Vincent, S. P.** 1979. Oxidation-reduction potentials of molybdenum and iron-sulphur centres in nitrate reductase from *Escherichia coli*. Biochem. J. **177**:757–759.
488. **Vincent, S. P., and R. C. Bray.** 1978. Electron-paramagnetic-resonance studies on nitrate reductase from *Escherichia coli* K12. Biochem. J. **171**:639–647.
489. **Voellmy, R. W., and A. L. Goldberg.** 1981. ATP-stimulated endoprotease is associated with the cell membrane of *Escherichia coli*. Nature (London) **290**:419–421.
490. **Wallace, B. J., and I. G. Young.** 1977. Aerobic respiration in mutants of *Escherichia coli* accumulating quinone analogues of ubiquinones. Biochim. Biophys. Acta **461**:75–83.
491. **Wallace, B. J., and I. G. Young.** 1977. Role of quinones in electron transport to oxygen and nitrate in *Escherichia coli*. Studies with a *ubiA*$^-$ *menA*$^-$ double quinone mutant. Biochim. Biophys. Acta **461**:84–100.
492. **Wang, E., and C. Walsh.** 1978. Suicide substrates for the alanine racemase of *Escherichia coli* B. Biochemistry **17**:1313–1321.
493. **Weiner, J. H.** 1974. The localization of glycerol-3-phosphate dehydrogenase in *Escherichia coli*. J. Membr. Biol. **15**:1–14.
494. **Weiner, J. H., and P. Dickie.** 1979. Fumarate reductase of *Escherichia coli*. Elucidation of the covalent-flavin component. J. Biol. Chem. **154**:8590–8593.
495. **Weiner, J. H., and L. A. Heppel.** Purification of the membrane-bound and pyridine nucleotide independent L glycerol-3-phosphate dehydrogenase from *Escherichia coli*. Biochim. Biophys. Res. Commun. **47**:1360–1365.
496. **Wild, J., and T. Klopotowski.** 1981. D-amino acid dehydrogenase of *Escherichia coli* K12: positive selection of mutants defective in enzyme activity and localization of the structural gene. Mol. Gen. Genet. **181**:373–378.
497. **Wimpenny, J. W. T., and J. A. Cole.** 1967. The regulation of metabolism in facultative bacteria. III. The effect of nitrate. Biochim. Biophys. Acta **148**:233–242.
498. **Wimpenny, J. W. T., M. Ranlett, and C. T. Gray.** 1963. Repression and derepression of cytochrome *c* biosynthesis in *Escherichia coli*. Biochim. Biophys. Acta **73**:170–172.
499. **Xavier, A. V., E. W. Czerwinski, P. H. Bethge, and F. S. Mathews.** 1978. Identification of the haem ligands of cytochrome b_{562} by X-ray and NMR methods. Nature (London) **295**:245–247.
500. **Yamamoto, I., and M. Ishimoto.** 1977. Anaerobic growth of *Escherichia coli* on formate by reduction of nitrate, fumarate and trimethylanine N-oxide. Z. Allg. Mikrobiol. **17**:235–242.
501. **Yamamoto, I., and M. Ishimoto.** 1978. Hydrogen-dependent growth of *Escherichia coli* in anaerobic respiration and the presence of hydrogenases with different functions. J. Biochem. **84**:673–679.
502. **Yamamoto, I., and M. Ishimoto.** 1981. Oxidation of lactate in comparison with that of glucose in nitrate respiration of *Escherichia coli*. J. Gen. Appl. Microbiol. **27**:11–20.
503. **Yamato, I., A. Futai, Y. Anraku, and Y. Nonomura.** 1978. Cytoplasmic membrane vesicles of *Escherichia coli*. II. Orientation of the vesicles studied by localization of enzymes. J. Biochem. **83**:117–128.
504. **Yoch, D. C., and R. I. Carithers.** 1979. Bacterial iron-sulfur proteins. Microbiol. Rev. **43**:384–421.
505. **Young, I. G.** 1975. Biosynthesis of bacterial meanquinones. Menaquinone mutants of *Escherichia coli*. Biochemistry **14**:399–405.
506. **Young, I. G., A. Jaworowski, and H. I. Poulis.** 1978. Amplification of the respiratory NADH dehydrogenase of *Escherichia coli* by gene cloning. Gene **4**:25–36.
507. **Young, I. G., A. Jaworowski, and M. Poulis.** 1982. Cloning of the gene for the respiratory D-lactate dehydrogenase of *Escherichia coli*. Biochemistry **21**:2092–2095.
508. **Young, I. G., B. L. Rogers, H. D. Campbell, A. Jaworowski, and D. C. Shaw.** 1981. Nucleotide sequence coding for the respiratory NADH dehydrogenase of *Escherichia coli*. Eur. J. Biochem. **116**:165–170.
509. **Young, I. G., and B. J. Wallace.** 1976. Mutations affecting the reduced nicotinamide adenine dinucleotide dehydrogenase complex of *Escherichia coli*. Biochim. Biophys. Acta **449**:376–385.
510. **Zahl, K. J., C. Rose, and R. L. Hanson.** 1978. Isolation and partial characterization of a mutant of *Escherichia coli* lacking pyridine nucleotide transhydrogenase. Arch. Biochem. Biophys. **190**:598–602.